# Fluorescence Probes for Cellular Thiol and Disulfide Detection: Sythesis and Biophysical Characterization

Timothy Jonhera
*Marquette University*

# FLUORESCENCE PROBES FOR CELLULAR THIOL AND DISULFIDE DETECTION: SYTHESIS AND BIOPHYSICAL CHARACTERIZATION

By

Timothy Jonhera, B.Sc

A Dissertation submitted to the Faculty of the Graduate School,
Marquette University,
in Partial Fulfillment of the Requirements for the Degree of Doctor of Philosophy

Milwaukee, Wisconsin

December 2011

ABSTRACT
FLUORESCENCE PROBES FOR CELLULAR THIOL AND DISULFIDE DETECTION: SYTHESIS AND BIOPHYSICAL CHARACTERIZATION

Timothy Jonhera, B.Sc.

Marquette University, 2011

The total concentration of cellular thiols is about 30 mM, and use of current fluorescent chemical probes to quantitate these thiols inside cells is impractical. We recently reported fluorescent dithio probes (donor-S-S-acceptor, DSSA) with unusually low reduction potential (- 0.6 V) that can detect changes in intracellular thiols and cross membranes of bacterial and mammalian cells, but they could not quantify thiol redox state. Here we report a new variant of the DSSA series, which has hydroxy coumarin (Ex: 320 nm, Em: 460 nm) as donor and fluorescein (Ex: 485 nm, Em: 520 nm) as acceptor. The probe was characterized *in vitro* by titration with glutathione in a physiologically relevant range and monitoring changes in fluorescence emission from both Coumarin and Fluorescein, upon reduction of the disulfide bond that joins this donor-acceptor FRET pair. The ratio of fluorescence emission band intensity, changes upon reduction with glutathione, and because of the probe's low reduction potential, permits quantitative measurement of glutathione levels in the 1 – 10 mM range. This is the first demonstration of ratiometric (FRET-based) thiol level measurement and will be enabling for quantitative assessment of thiol redox state (GSG/GSSG) inside cells. Preliminary studies in *E.Coli* are also presented. We also report an improved version of our previously reported fluorescent-dithio probes for detecting cellular thiols, referred to as PMR-CYS-FITC, where PMR is p-methyl red (aka dabcyl), a fluorescein quencher. Unlike most thiol-reactive probes, PMR-CYS-FITC can also detect certain disulfides, making it useful for 'disulfide proteomics'. PMR-CYS-FITC was used to identify new disulfide-containing protein(s) in the zebrafish chorion, with potential role(s) in protecting the embryo during development. Confocal microscopy of the embryo, followed by in-gel staining and imaging of proteins, then tandem MS, led to our discovery of two novel disulfide-containing proteins in the fish chorion, lipovitellin and C-reactive protein (CRP). CRP is a well-known biomarker for infection or inflammation (associated with oxidative stress) in humans, so discovery of CRP in the zebrafish has relevance for its use as a model organism. *In vitro* biophysical characterization of this probe provides further explanations for the differential reactivity of disulfides, and enhanced fluorescence for some fluorescein-protein mixed disulfides.

# ACKNOWLEDGMENTS

Timothy Jonhera, B.Sc

I would like to thank my wife Lorena, my daughter Kirstin Ruvarashe, my friends and God. I would like to thank my teachers, my faculty, my committee and especially my advisor Dr Sem. I would like to thank the Graduate School and all of the Marquette University administration. I thank Dr. Henry Tomasiewicz, Dr. Merker P Merilyn, Bongard D Robert and Lindemer Brian for assistance with some of the zebrafish and BPAEC fluorescence imaging.

# TABLE OF CONTENTS

## LIST OF FIGURES

# CHAPTER 1

# INTRODUCTION

# 1. GENERAL INTRODUCTION

Cellular thiol containing compounds and proteins play an important role in redox signaling and control. They play a central role in combating oxidative stress and maintaining redox state in both eukaryotes (-0.23V) and prokaryotes (-0.27V). Oxidative stress is a large rise in the cellular reduction potential from the perspective of cellular thiols (Ex. GSH/GSSG). Oxidative stress plays a central role in the cellular response to environmental insults. Health problems which are associated with oxidative stress and changes in cellular thiol levels and oxidation state include heat shock[2], heavy metal exposure[3], dietary factors[4], shear stress[5], high glucose[6], lipids and lipid products[4], oxidative/nitrosative stress[5], hormones, cancer[6], and HIV[7], as well as in arthritis, Alzheimer's disease, stroke and Parkinson's disease [8-13]. The cell protects against oxidative stress with various enzymes, including catalase, superoxide dismutase and glutathione peroxidase. $H_2O_2$ produced by superoxide dismutase is converted to water by glutathione peroxidase (**Fig.1**). Inappropriate oxidation of protein thiols is one of the most damaging outcomes of oxidative stress in cells. Thi oxidation is predominantly of cysteines to cystines, although the methionine thio ether can be oxidized to a sulfoxide then to a sulfone. Cysteine residues play a key role in maintaining protein tertiary structure and in catalysis [17, 18], but improper formation of disulfide bonds will inactivate proteins. Indeed, the cytosol of both eukaryotes and prokaryotes is a reducing environment[19], where cysteines would normally be present as thiols rather than disulfides. This *thiol redox state* is maintained by GSH[20], which is able to reduce protein disulfides (PSSP) in an enzyme catalyzed reaction (**Fig.1**).

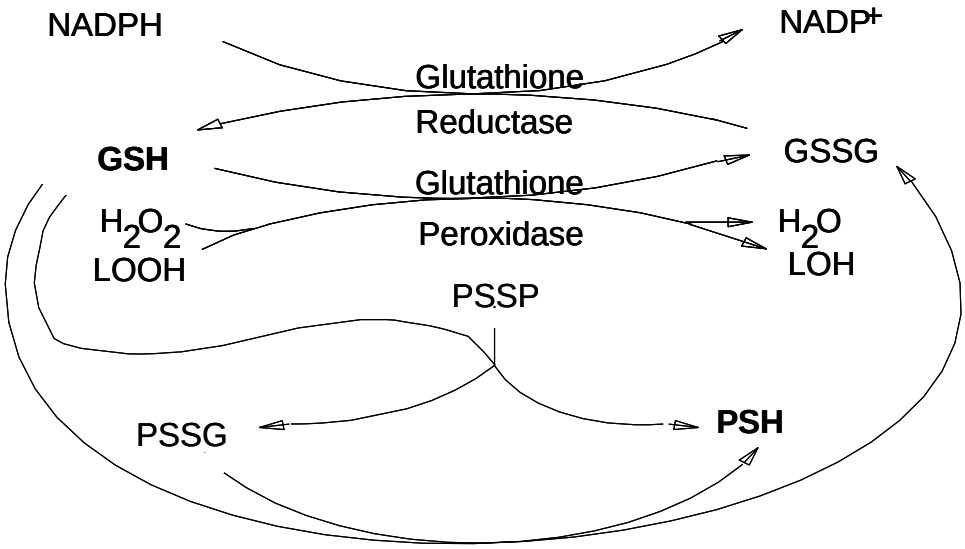


The extent of variability of thiol redox state within different cellular microenvironments is not well understood due lack of *in vivo* fluorescent probes that can penetrate cell walls and selectively label thiols without causing oxidative or other cellular damage

### 1.1 Measuring ROS

Among the most widely used probes to assess *oxidative stress* in living cells is 2,7-dichlorodihydro-fluorescein diacetate (DCFH/DA) [21]. However, this reagent provides only an indirect, relatively non-specific and qualitative measure of ROS (reactive oxygen species); so, its validity as an accurate probe of oxidative stress is currently controversial[24, 25, 26, 27, 28]. Recently, there has been a concern about the use of DCFH to assess oxidative stress, because it is actually able to catalyze the production of ROS - so it is "subject to the serious artifact that it produces what it is purported to measure" [29]. Another widely used technique for studying intracellular ROS is electron paramagnetic resonance (EPR) [30, 31], although this technique suffers from lack of sensitivity and is not readily available to most scientists. While levels of ROS are an important measure of oxidative stress (assuming they can be accurately measured), our research is focused on a complementary and commonly used metric of oxidative stress, the relative concentration of reduced and oxidized glutathione (**GSH/GSSG**) and protein thiols (**PSH/PSSP**).

### 1.2 Measuring GSH/GSSG in vitro

Since cells protect against oxidative stress with GSH (**Fig.1**), measurement of GSH/GSSG ratios are an important complement to any measurements of ROS. GSH is normally present in cells at 1-10 mM concentration, with a GSH/GSSG ratio of ~200:1 [20, 32]. However, exactly how GSH and PSH (protein thiols) vary in cells under oxidative stress (ex. $H_2O_2$ exposure) and GSH depletion (ex. treatment with BSO: buthionine

sulfoximine [33]) is not known accurately, due to the absence of a reliable probe for *in situ* (within the living cell) detection of thiols. Unfortunately, most current methods to measure GSH require tissue destruction and cell lysis, followed by purification and biochemical assay [33, 34] - procedures which may compromise recovery or promote artifactual GSH oxidation. Furthermore, it is difficult to measure GSH/GSSG ratios in different organelles, other than by cumbersome separation of sub-cellular structures followed by biochemical assay. The latter approach has been used to assess *thiol redox state* potentials (based only on GSH/GSSG) in *E. coli* as well as in the eukaryotic endoplasmic reticulum and cytosol [19]. An improved strategy would be to use a minimally invasive *in situ* probe of cellular thiol redox state.

### 1.3 Measuring CSH/CSSC and PSH/PSSP

Ultimately, what matters most in a cell is not just the GSH/GSSG ratio, but the redox state of the various protein thiols (PSH/PSSP), since the primary cellular function of GSH (besides conjugating electrophiles) is to maintain the proper redox state of protein cysteine residues through thioredoxin and glutaredoxin catalyzed disulfide reduction (**Fig. 1**). For this reason, there has been recent interest in assessing the "Thiol-Disulfide State" across the entire *thiol-proteome*[35]. Since GSH regulates the thiol redox state across the *thiol-proteome* via reversible equilibria, the GSH/GSSG ratio largely determines the thiol redox state for all cellular thiols (CSH/CSSC, where CSH = PSH + GSH) [34]. Our dithio probes react with most thiols [1], including both PSH (protein-SH) and GSH. And, the extent of probe reduction (fluorescence) will be responsive to CSH/CSSC

ratios, thereby permitting quantification and or labeling of this ratio (Chapters 2 and 3). Noteworthy is that measurements of CSH levels in cells may be dominated by PSH, since protein thiols are estimated to be present at ~20-40 mM, compared to 1-10 mM for GSH [34]. Thus, our aggregate measurements of total cellular thiol redox state (CSH/CSSC) will provide a useful measure of oxidative stress.

### 1.4 Current Probes for Labeling Cellular Thiols

Probes do exist (ex. maleimide, iodoacetamide and methyl bromide-conjugated bodipy) to covalently label cellular thiols with fluorescent tags, but they are fairly nonspecific for nucleophilic groups, and are typically used for labeling thiols in cellular extracts [35, 36, 37]. Unfortunately, these probes will perturb cellular thiol redox state because they react irreversibly with protein thiols, and would therefore shift the CSSC => CSH equilibrium. Bromobimanes[38, 39] have also been used to fluorescently label cellular thiols, but their high redox potential would likewise disrupt cellular thiol redox state. Importantly, *none of these reagents provide a quantitative measure of the CSH/CSSC ratio***.** One strategy for measuring cellular thiol redox state is using a green fluorescent protein (GFP) redox indicator [40]. But, a strategy which requires genetic alteration of a cell is too cumbersome for routine use. Our thiol probes could provide the first quantitative measurements of CSH/CSSC ratios in native cells.

## 1.5 Design Constraints for Dithio Probes

The dithio fluorescent probes being developed herein could provide a highly sensitive and direct measurement of thiol redox state in intact cells. Different versions of the probes are being developed, with the intention of optimizing them to: (a) have low redox potential (about - 0.6 V), (b) cross cell walls, (c) be selective for thiols, (d) react reversibly to permit dynamic reporting on thiol redox status, (e) be insensitive to pH variations in the cell, and (f) provide measures of free thiol redox state based on fluorescence or FRET (ratiometric) output. The FRET assay can be done either quantitatively or as a qualitative fluorescence imaging study of relative thiol concentration in different sub-cellular locations. Preliminary probes have been developed, and shown to be transported across cell walls in various cell types: *E. coli* (Chapters 2 and 3), bovine endothelial lung cells, zebrafish embryos and mouse neuronal cells. In some cases, they have been shown to detect changes in oxidative stress.

## 1.6 Proteomic Approach to the Identification of Oxidized Proteins (PSSP*)*

Besides aggregate measures of how the CSH/CSSC ratio changes under conditions of oxidative stress, it is informative to know exactly which proteins are most affected by the oxidative stress (i.e. had thiols oxidized to disulfides). In previous studies, this had been accomplished using selective isotope labeling of thiols, followed by mass spectrometry to identify individual proteins that have become oxidized (ex. diagonal 2D PAGE); $^{14}$C NEM (N-ethyl maleimide) labeling[40,41]strategy being developed herein will

use our fluorescent probes to label protein thiols (chapter 2). This is intended as a complement to our *in vivo* redox measurements (not as an improvement on related methods) to identify specific proteins affected by oxidative stress using similar reagents to those that were used to measure the CSH/CSSC ratios. This application of our probes involves: exposure of cells to probes, fluorescent imaging of cells, cell lysis, 1D or 2D gel electrophoresis, and tandem MS-based identification of proteins that change, in comparing with or without pre-exposure to oxidative stress.

### 1.5 Fluorescence quenching

Quenching refers to a decrease in the intensity of fluorescence and can be due to a variety of processes. In collissional quenching, an excited fluorophore is deactivated and returned to the ground state during a diffusive encounter with another molecule (quencher)[43].

The decrease in intensity is described by the Stern- Volmer equation:

$$\frac{F_0}{F} = 1 + K[Q] = 1 + k_q\tau[Q] \quad \textbf{(1)}$$

Where : K= Stern-Volmer quenching constant; $\tau =$ fluorescence lifetime; F= final intensity (after quenching); $F_0$= initial intensity ; $k_q$=bimolecular quenching ; [Q]= quencher concentration.

The mechanism of quenching depends on the fluorophore-quencher pair. Quenching can be due to a variety of other processes besides collisional quenching. It can be due to formation of a nonfluorescent complex between a fluorophore and a quencher. In this case quenching occurs in the ground state and does not rely on diffusion or molecular

collisions. This type of quenching is refered to as static quenching[43]. Some other trivial processes, such as nonmolecular  mechanisms like attenuation of the incident light by the fluorophore itself or other absorbing species, can result in fluorescence quenching. Quenching and dequenching of a fluorophore provides evidence of molecular interactions and since the intensity of fluorescence or fluorescence quantum yield is also sensitive to environment, fluorescence quenching can find utility in probing micro-environmental conditions.

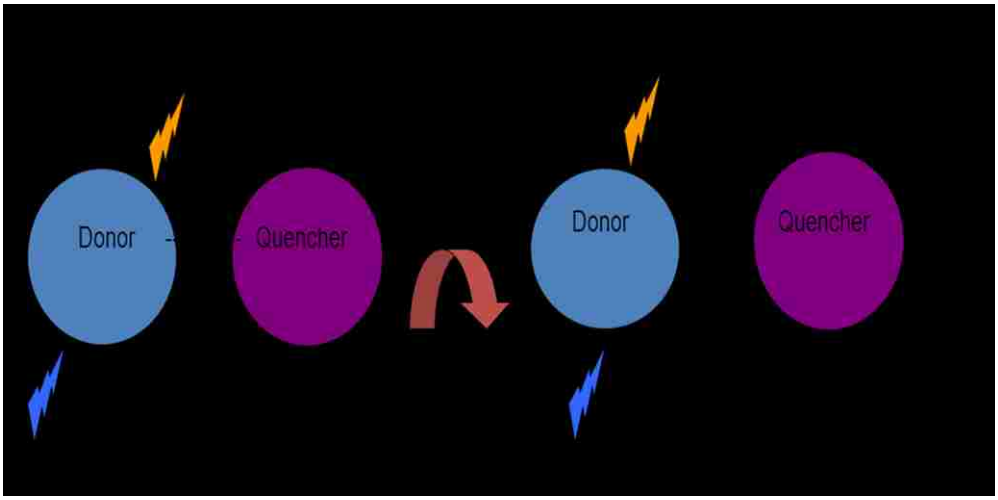
Donor
Quencher
Donor
Quencher

**1.8 Fluorescence Resonance Energy Transfer (FRET)**

FRET describes an energy transfer process between two chromophores (donor and acceptor). For FRET to occur between donor and acceptor chromophores, they must possess strong electronic transitions, and there should be substantial overlap of the donor emission spectrum with the acceptor absorption. If the donor and the acceptor are close enough in space and properly oriented, energy can be transferred, from the donor to the acceptor, resulting in quenching of the donor emission and sensitization of the acceptor emission spectra.

When light excites a fluorophore at an appropriate wavelength (in the range 250-500 nm), it transitions from the ground state ($S_0$) to a higher vibrational level ($S_1$, $S_2$, $S_3$, etc)[42]. This quickly decays to the lowest vibrational level of the $S_1$ state and then decays slowly to one of the $S_0$ states (Fig.3) as described by the Jablonski diagram.

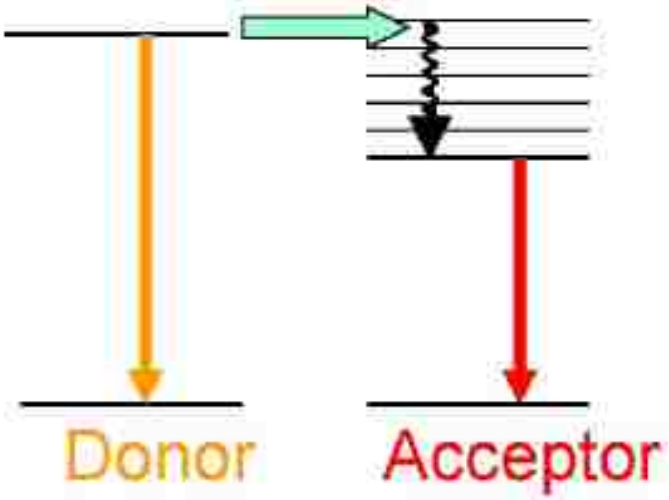


**Fig 3**: Diagram illustrationg energy transfer during FRET

The efficiency of the energy transfer during FRET depends on the distance between the donor and acceptor, according to the Förster equation. The Förster distance ($R_0$) the distance at which the FRET efficiency (E) is 50 %, as illustrated in Fig 4 below.

The Förster radius itself can be defined more explicitly, in the following manner:

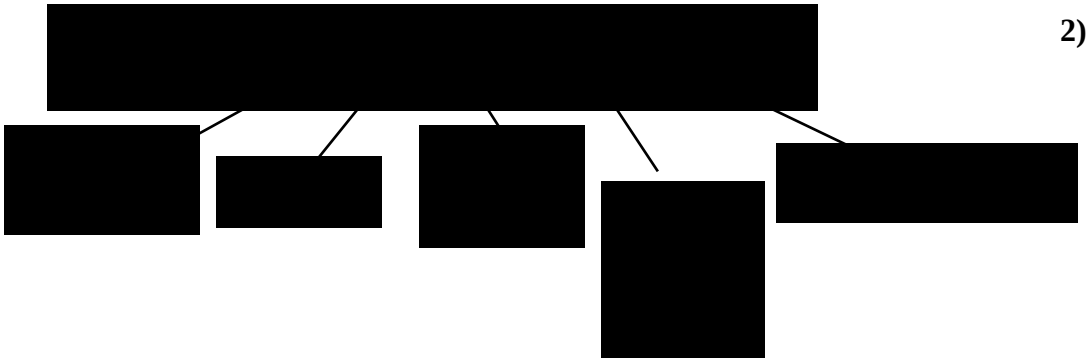

**2)**

Equation 2 shows that FRET efficiency also depends on the overlap of the donor and acceptor spectral bands and the relative orientation of the dipoles of the donor and acceptor. The sensitivity of FRET to separation distance between donor and acceptor can be utilized as a molecular ruler (in distances between $1 \pm 0.5 \times R_0$).

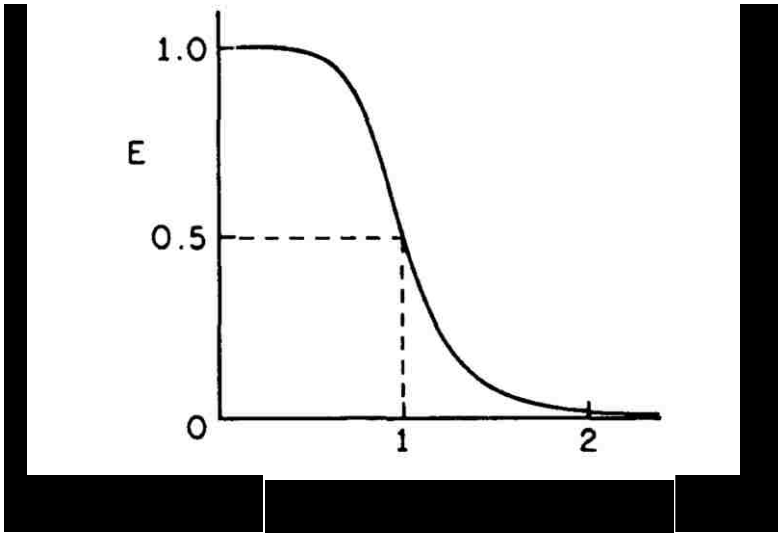

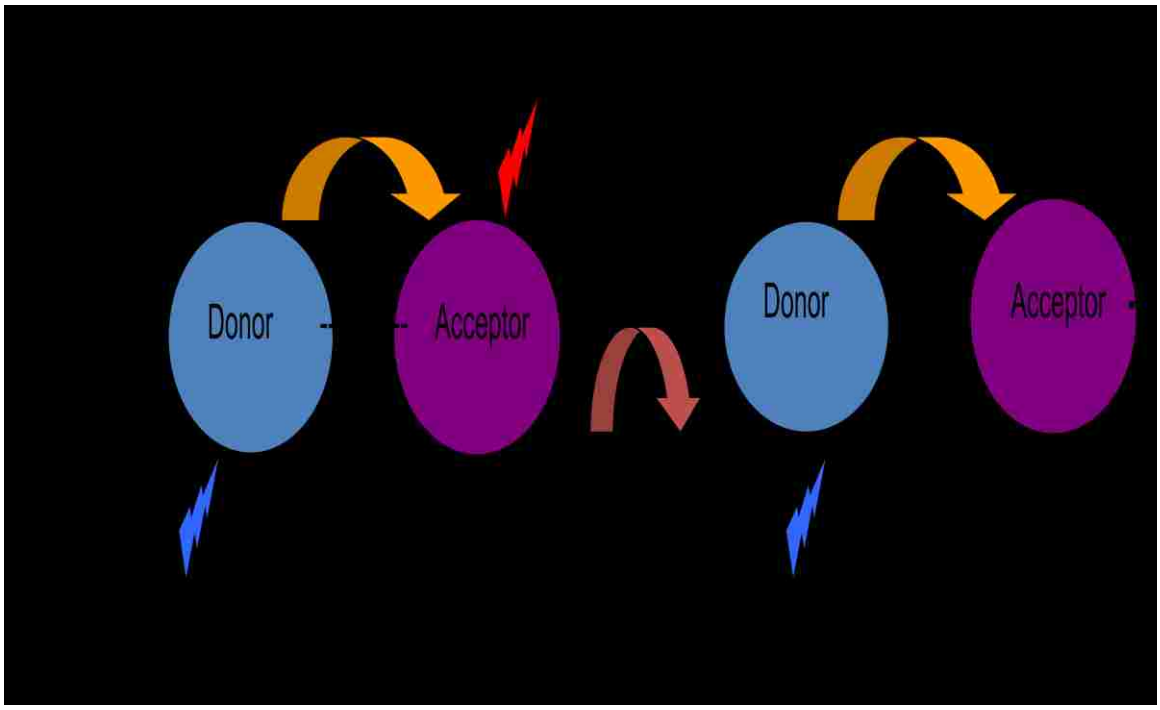
Donor
Acceptor
Donor
Acceptor

# CHAPTER 2

## Dithio probes for cellular imaging and proteomic analysis of reactive disulfides: Discovery of zebrafish chorion proteins with a potential role in lipid transport

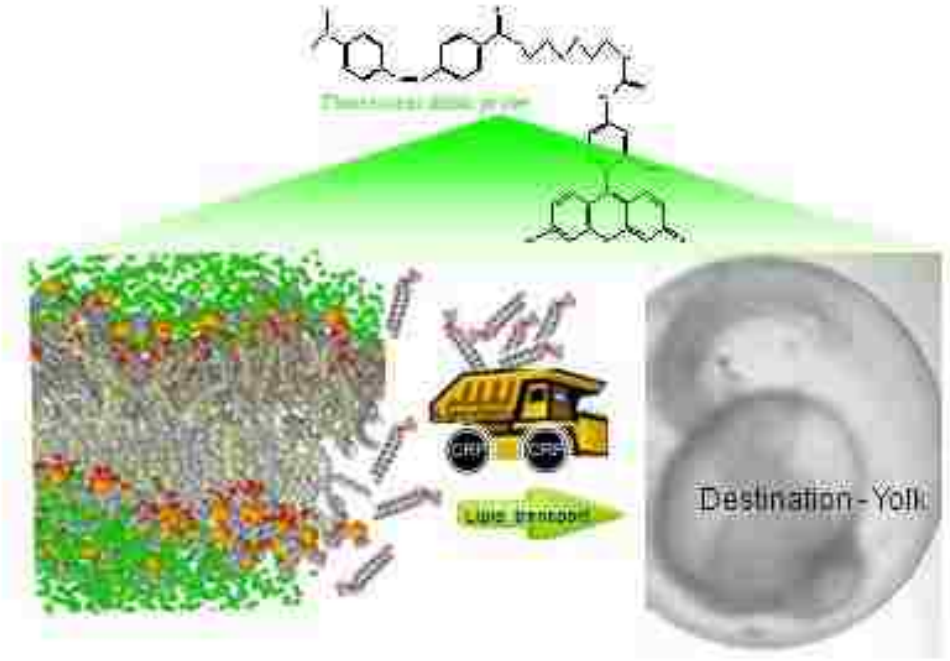

## 2.0 PREAMBLE

While thiol reactions might serve as biomarkers to identify a disease state or a perturbation to normal cellular function, such oxidative events (ex. formation of sulfenic acids[17] and RSNO's) are also thought to be part of normal cellular regulatory cascades, such as T-cell activation[18,19]. Clearly, there is a need for chemical probes to permit live-cell imaging, as well as proteomic analysis, of these various events. To this end, fluorescent probes have been reported to monitor peroxides[20-22a], sulfenic acids[17] and thiols [23-27]. Likewise, proteomic methods have been developed to detect reactive thiols[22b,28,29] and disulfides[29]. But, disulfide detection is indirect and cumbersome, by first alkylating thiols, then reducing disulfides and detecting the newly freed thiols. While there has been no previous report of disulfide imaging in cells, the DSSQ probe presented herein (**Fig. 6a**) will enable such studies. Furthermore, while previous thiol imaging probes have been nonselective for protein thiols (PSH) and glutathione (GSH) or have focused on GSH, the probes presented herein are selective for protein disulfides (PSSP) and thiols (PSH), over GSSG.

The cytosol of both prokaryotes and eukaryotes is a reducing environment[30]. In eukaryotes the reduced GSH form can be as high as ~33 000-fold excess over the oxidized from (GSSG)[31]. In contrast, the endoplasmic reticulum of eukaryotic cells is oxidizing ($E^{o'}$ = -0.18 V)[32] as is the periplasmic space in *E. coli*[33]. Accordingly, these environments would be rich in protein disulfides. Protein disulfide exchange reactions are

catalyzed by the thioredoxins, with the best-characterized thiol-disulfide exchange pathway being the Dsb system of *E. coli*. The Dsb enzymes represent a prototype for a large family of enzymes, referred to as thiol-disulfide oxidoreductases (TDORs). Thioredoxins and TDORs catalyze disulfide exchange reactions, and play an important role in proper formation of disulfides as part of protein folding. In *E. coli*, DsbA (disulfide bond protein A) exists in the periplasmic space in its oxidized form, and is kept in an oxidized state by the membrane-bound DsbB. Also in the periplasm are disulfide isomerases DsbC and DsbG, which are reduced by DsbD. While this is a well-studied thiol-disulfide exchange pathway in *E. coli*, much of the function of these enzymes – including how these pathways interact – is not yet fully understood[34,35]. Analogous thiol-disulfide exchange systems are present in both Gram positive and Gram negative bacteria[34].

Another important function of thiol-disulfide exchange reactions is in facilitating viral infection of mammalian cells. Protein disulfide isomerases are also present on the surface of mammalian cells[36], and disulfide exchange reactions play a key role in HIV entry into cells[37,38]. For example, locking thioredoxin (which is secreted by T-cells) and CD4 thiols in a reduced state prevents viral entry into the cell. Similarly, inhibition of thiol-disulfide exchange prevents entry of hepatitis B virus into cells[39]. So, thiol-disulfide exchange reactions occur predominantly at the interface between cells, both eukaryotic and prokaryotic, and their environments. This generalization can be extended to multicellular systems, or at least to the development of multicellualr systems, in terms of the chorion that protects a developing embryo. The chorion shelters the developing embryo from the environment, and is referred to as the zona pellucida in mammalian

eggs, or the vitelline envelop in fish eggs[40]. A well-studied chorion is that of drosophila, where vitelline membrane proteins are produced in stages 8-10 of eggshell development. As the chorion develops, the vitelline proproteins become proteolytically cleaved, and are incorporated into the vitelline membrane layer in a process that includes disulfide cross-linking[41a]. Moving from drosophila to a vertebrate model system, it was shown by mass spectrometry/proteomics that there is similar vitelline processing in forming the chorion (vitelline envelop, VE) in trout, and that the VE proteins contain six disulfides; homologous proteins are present in mammals as well[44b]. These VE proteins polymerize into long fibrils[44c] in the chorion, presumably via disulfide cross-linking. Clearly, the importance of thiol-disulfide disulfide exchange reactions in cell biology ranges from bacterial cell walls, to mammalian plasma membranes, to the extracellular shell that protects a developing embryo. Essentially, they occur at the interface of single cells, or developing multicellular organisms, and the environment. The fluorescent dithio probe presented herein permits the imaging and proteomic analysis of these disulfides.

## 2.1 Donor Quencher probe for Thiol and Disulfide Detection

Development and use of a fluorescent dithio probe to study disulfides requires a detailed understanding of the properties and reactivity of disulfides, in part because the probe itself is disulfide based, but also because the proteins it is being used to image participate in disulfide exchange reactions. Extensive studies of thioredoxin disulfides, and TDOR disulfides (including the Dsb family) have identified an important CXXC motif, and have highlighted the importance of proximity (effective concentration) in

catalysis[42, 43], as well as the role of intervening residues XX. It has also been observed that there are often tryptophans at the -1 (proximal) and -4 (distal) position, relative to this motif. Indeed, it has been noted that cleavage of the disulfide in DsbA of *E. coli* results in decreased fluorescence of the tryptophan, due to removal of the tryptophan/disulfide quenching effect [44]. Clearly, this aromatic-disulfide interactions results in quenching, and one might such expect aromatic-disulfide interactions to also affect the stability of the disulfide bond (thereby affecting redox potential). The presence of this type of donor/acceptor (HOMO/LUMO) interaction might be expected to stabilize a complex as well. Evidence that this is the case is provided by a model system that was structurally characterized by Iwamoto et al.[45], where a molecular tweezers was synthesized that contained two flexible aromatic ring systems, and a cleavable disulfide bond. Production of the disulfide induces a movement (attraction) of the aromatic rings towards the disulfide, as shown in **Figure 6b**. We propose that, in general, disulfides have an affinity for aromatic systems, and that when the disulfide/aromatic interaction is present, it results in quenching; the latter has been established for tryptophan/disulfide interactions[47]. Indeed, we believe that the recent report by Lu et al.[46] that aromatic/aromatic interactions in heat shock transcription factor 1 are driving disulfide bond formation, and producing quenching of tryptophan fluorescence (**Fig. 6c**), are better described as aromatic/dithio interactions that stabilize the disulfide bond, and subsequently produce tryptophan quenching.

The DSSQ probe presented herein (**Fig. 6a**) builds on the above concept of aromatic/disulfide interactions, and capitalizes on the fact that aromatic interactions are less favorable in in mixed disulfides with glutathione or certain proteins (**Fig. 6d**). But,

they *can* occur in mixed disulfides with proteins that have aromatic amino acids in their active sites (**Fig. 6d**), such as the thioredoxins, TDOR's, and other proteins involved in thiol-disulfide exchange reactions. While the "Q" half of DSSQ could be anything as long as the fluorescent donor "D" remains quenched, even glutathione or transport peptides (ex. tat) or targeting groups (ex. phosphonium head groups)[22a], our initial design included a colored group (para-methyl red; PMR) because it permits easy visualization of all labeled proteins (Protein-SS-Q), to complement fluorescence imaging of fluorescein-tagged proteins (P-SS-D).

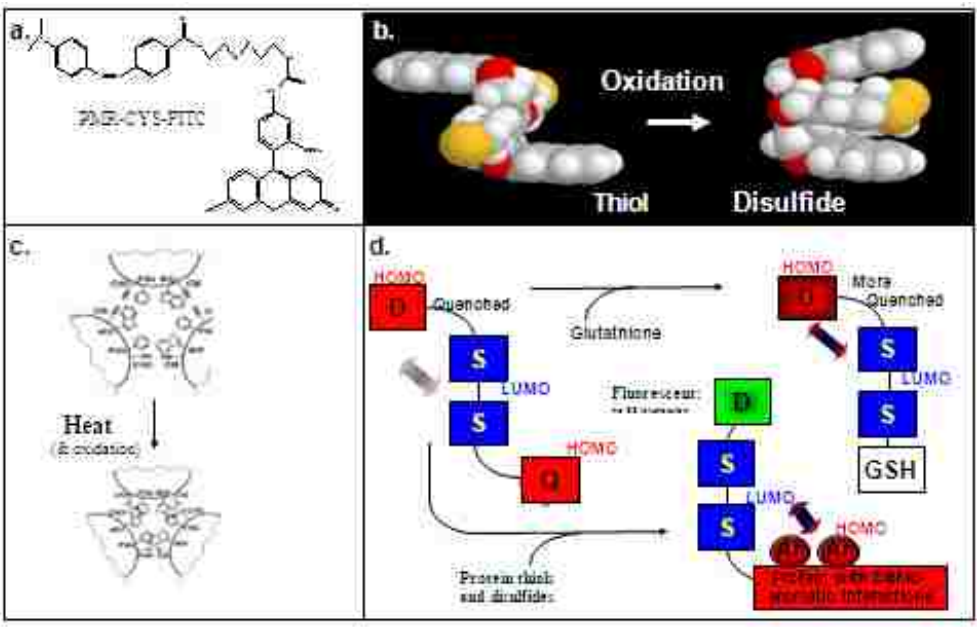


[redacted]

### 2.2.1 RESULTS

### 2.2.2 Reduction of DSSQ (PMR-CYS-FITC) by reduced glutathione (GSH)

GSH in its physiologically relevant concentration range of 0 mM to 10 mM, and beyond (to 16 mM), was reacted with a very low DSSQ concentration (5 µM), which is representative of what might be present in a cell. The reaction kinetics were monitored by collecting emission spectra for the fluorescent donor, fluorescein (excitation at 492 nm, emission at 520 nm), at various time points (**Fig. 7**). Kinetic data were fitted using the fluorescein emission intensity (**F**) as a function of time (**t**), and fitting to equation (3):

$$\mathbf{F = F_0 + F(1 - e^{-kt})} \qquad \mathbf{(3)}$$

where $\mathbf{F = F_{max} - F_0}$, the fluorescence change due to reaction ($F_{max}$ is fluorescence when reaction The control experiment with fluorescen was performed to explore the possibility of complex formation between GSH or GSSG and fluorescein, as well as to compare quenching effects of the glutathione thiol vs. disulfide, fluorescence of free fluorescein was monitored as a function of [GSH] or [GSSG] in **Fig .7**. The results show that there was no quenching of fluorescein with increase in [GSH] or [GSSG], suggesting, quenching of fluorescein is due to HOMO/LUMO intramolecular attactraction and not intermolecular.

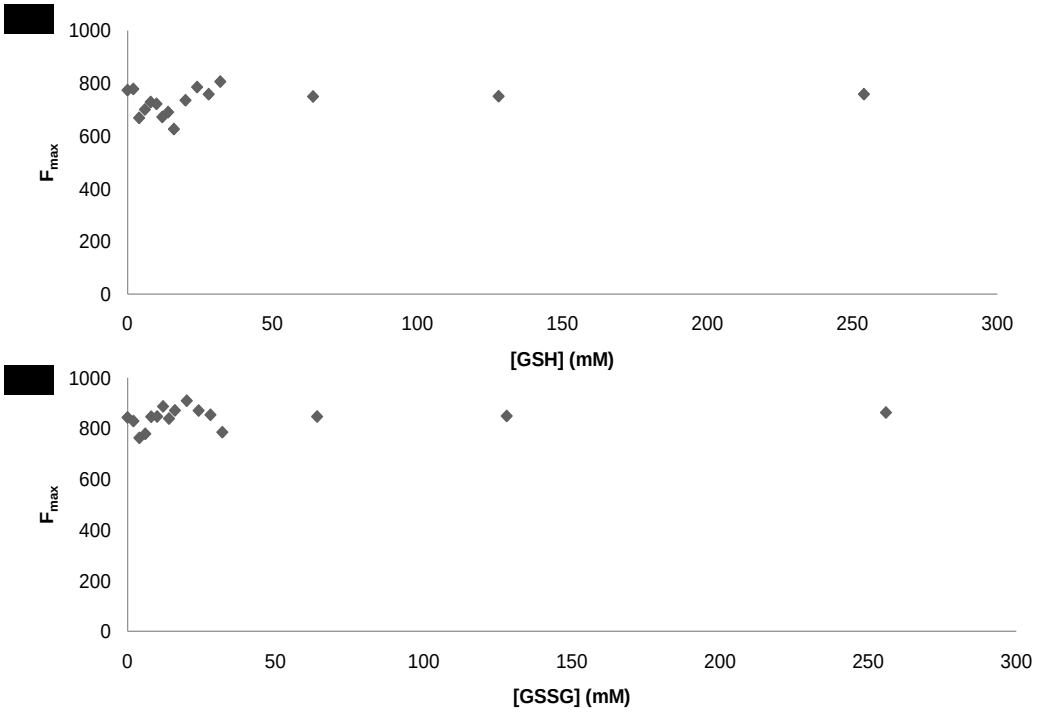
1000
800
600
400
200
0
$F_{max}$
0
50
100
150
200
250
300
[GSH] (mM)
1000
800
600
400
200
0
$F_{max}$
0
50
100
150
200
250
300
[GSSG] (mM)

[redacted]

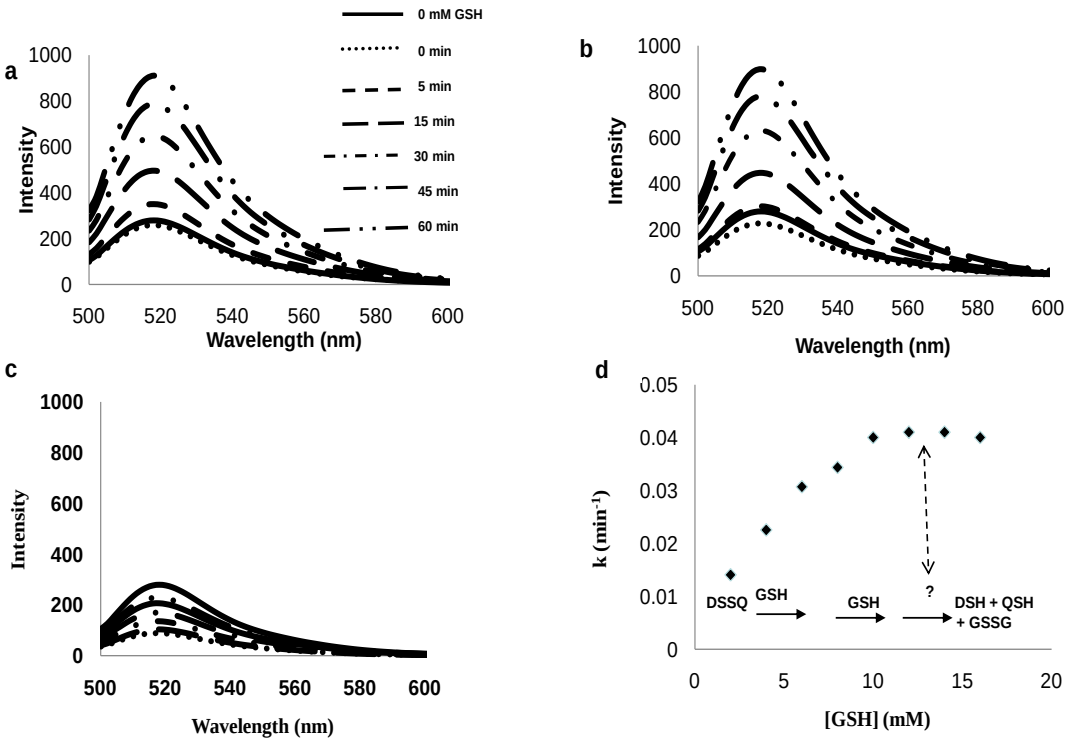
a
0 mM GSH
0 min
5 min
15 min
30 min
45 min
60 min
Intensity
Wavelength (nm)
b
Intensity
Wavelength (nm)
c
Intensity
Wavelength (nm)
d
k (min-1)
DSSQ
GSH
GSH
?
DSH + QSH
+ GSSG
[GSH] (mM)

[redacted]

### 2.2.2 Calculation of HOMO and LUMO molecular orbitals and energies in DSSQ (PMR- cys-FITC)

We speculate that there is an electronic donor/acceptor (HOMO/LUMO) attraction between electron deficient disulfides and electron rich aromatic ring systems, which causes them to be attracted to each other, and also leads to quenching via nonradiative energy transfer, if one of these aromatic rings systems is fluorescent. To explore this hypothesis, semiempirical quantum mechanical calculations (AM1, as implemented in Spartan) were performed on PMR-cys-FITC, with highest occupied molecular orbital (HOMO), second highest occupied molecular orbital (HOMO-1) and the lowest unoccupied molecular orbital (LUMO) shown in **Fig 9b**. As expected, the LUMO is on the electrophilic disulfide, while the HOMO is on fluorescein, with energies of -2.19 eV and -8.36 eV, respectively. The HOMO-1 is on para-methyl red, but any interaction between the LUMO of the disulfide and the HOMO-1 on fluorescein would be in competition with the more favored electronic interaction between the disulfide and para-methyl red. Accordingly, the disulfide quenching of fluorescein might be somewhat less that it would be if para-methyl red were replaced with glutathione, as is shown in **Fig 9c**. In this case the HOMO is on fluorescein (energy = -8.73 eV) and the LUMO is again on the disulfide (energy = -2.14 eV), but now there is no competition for interaction between fluorescein and the disulfide, so one would expect more effective quenching. Especially relevant for labeling of protein thiols is the expectation that if a HOMO on a protein aromatic residue can be located more proximal to the disulfide than is the case in **Fig 9b**, there would be an even more effective interaction with the disulfide, thereby causing a more dramatic increase in fluorescence from fluorescein. To illustrate this

potential for strong aromatic/disulfide attraction, AM1 calculations were also performed on the dithio/molecular tweezers system reported by Iwamoto *et al*.[45]. One can see the close interaction between the dithio LUMO (energy = -1.50 eV) and the aromatic ring HOMO (energy = -8.66 eV) orbitals, in the structure that was crystallized (**Fig. 9d**).

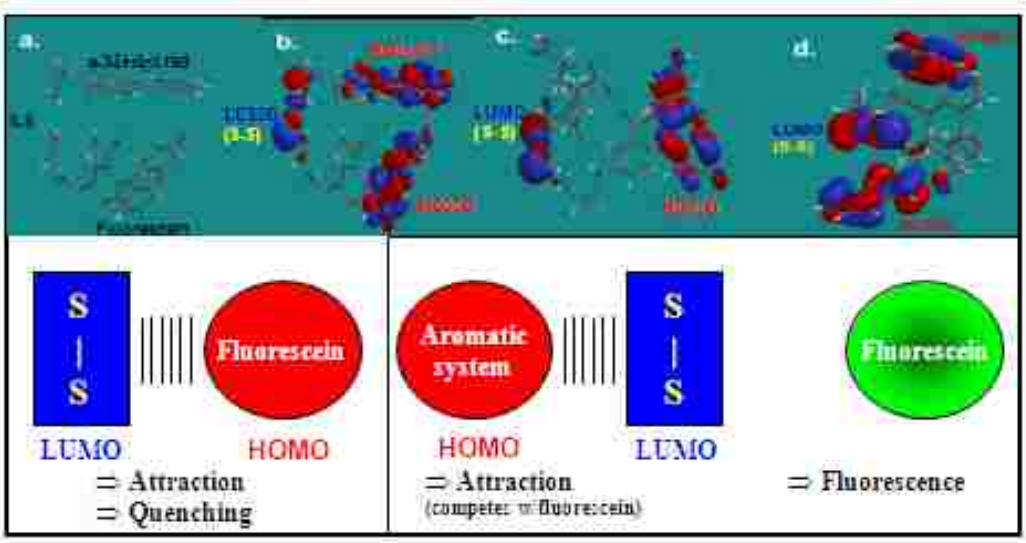


[redacted]

### 2.2.3 pH dependence of fluorescence spectrum

If one is to use the DSSQ probe presented herein, it is important to be aware of its performance under different conditions, especially pH. Indeed, a known limitation of fluorescein is its pH dependence. For this reason, we plan to make derivatives of DSSQ using donors other than fluorescein that lack this pH dependent behavior (ex. Alex 488). In terms of potential limitations of the present DSSQ probe, it is known that fluorescein can exist in seven prototropic forms: cationic xanthene, neutral xanthene, zwitterion, quinoid, monoanion (carboxylic), monoanion (phenolic), and dianion. It is hard to distinguish each form in solution, as the neutral form of fluorescein is a mixture of the lactone (70%), zwitterionic (15%), and quinoid (15%) forms. It is known that the quinoid and monoanionic forms have similar absorption spectra. The emission spectra of the monoanionic and quinoid forms are also identified and shown to be similar but not identical. The quinoid and monoanionic forms, which are predominant at pH above pH 6.3, have similar fluorescence properties. This is the reason why derivatives of fluorescein (FITC; fluorescein isothiocyanate) are often used for fluorescence applications done close to physiological pH. The changes in fluorescence properties of fluorescein as pH is lowered below 7.0 (due to existence of these other forms) include a decrease in intensity of the 520 nm emission band, and an increase in intensity of emission bands between 420 nm and 470 nm, which often appear as two distinct peaks. As most studies, including those reported herein, are done in a physiologically relevant pH range (pH ~7.4), the above-mentioned pH effects are not problematic. To explore these pH effects, as well as any problems associated with aggregation or solubility, DSSQ emission spectra were measured

at different concentrations and in different buffers: pH 8.2 (100 mM Tris), pH 7.4 (100 mM HEPES), pH 7.0 (100 mM HEPES) and pH 5.0 (100 mM acetate). The fluorescence spectra in **Fig. 10** indicate that fluorescence only begins to decrease at pH below 7.6, with a small decrease observed at 7.0 and a dramatic decrease observed at pH 5.0. Emission spectra of DSSQ at pH 7.6 and pH 8.2 are consistent with fluorescein being present predominantly as a mixture of the quinoid and monoanionic forms. At pH 7-8, there appears to be no aggregation, at up to 4 µM, but probe is not soluble much beyond 4 µM. At lower pH probe is more soluble (**Fig 10a**), but this is of little value as it is less fluorescent. Solubility might be higher in solutions that contain surfactants or proteins – for example, we note that solubility as high as 50 µM can be achieved in certain cell culture media. Note that the fluorescence being measured in **Fig 7a** is residual (unquenched) fluorescence from fluorescein, but it provides useful information about solubility of the probe, and the state of the fluorescein ring system.

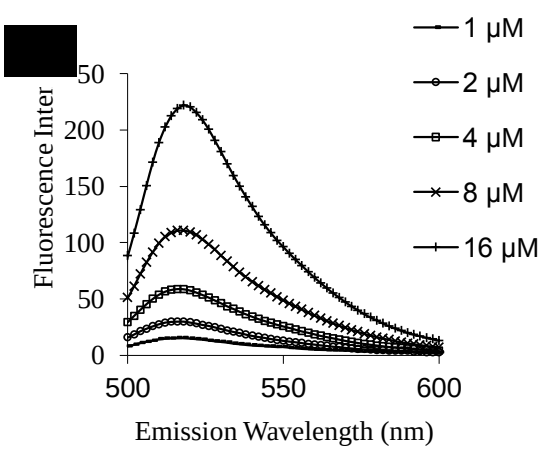
1 μM
2 μM
4 μM
8 μM
16 μM
Fluorescence Inter
50
200
150
100
50
0
500
550
600
Emission Wavelength (nm)

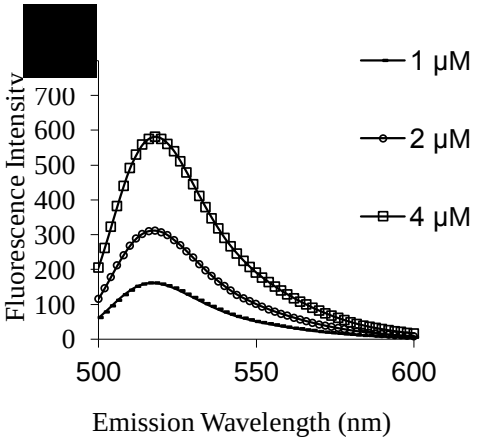
1 μM
2 μM
4 μM
Fluorescence Intensity
700
600
500
400
300
200
100
0
500
550
600
Emission Wavelength (nm)

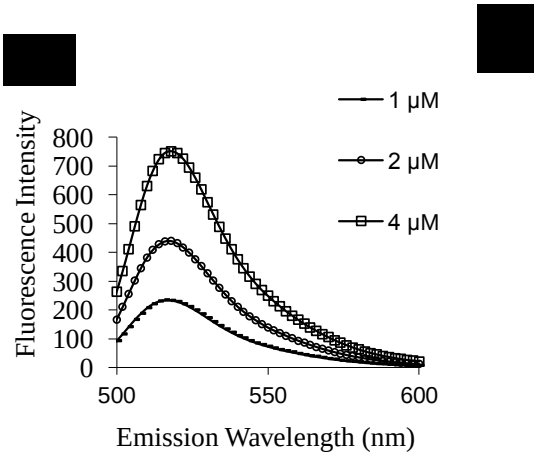
1 μM
2 μM
4 μM
Fluorescence Intensity
800
700
600
500
400
300
200
100
0
500
550
600
Emission Wavelength (nm)

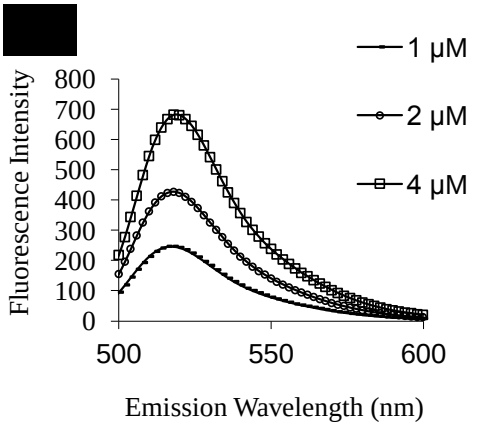
1 μM
2 μM
4 μM
Fluorescence Intensity
800
700
600
500
400
300
200
100
0
500
550
600
Emission Wavelength (nm)

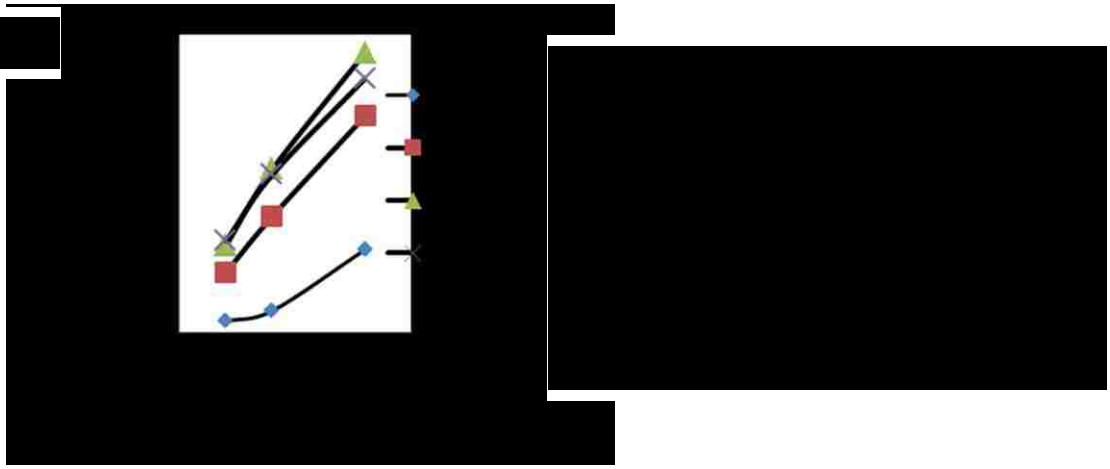

### 2.2.4 Studies in *E. coli* and in zebrafish embryos

Preliminary in cell studies of thiols using DSSQ (PMR-CYS-FITC) were done in bacteria, comparing wild type *E. coli* (BL21 DE3 strain) to the Origami *E. coli* strain. The Origami strain of *E. coli* is deficient in glutathione reductase and thioredoxin reductase, so should have protein thiols and glutathione present in their oxidized state (PSSP; GSSG), with minimal levels of the reduced state (GSH; PSH) present[64]. Incubation of cells with 10 or 50 μM probe, followed by washing and fluorescence reading, indicates that there is much more fluorescence signal in the wild type strain (**Fig. 11**). This is because the DSSQ probe reacts with the more abundant GSH and PSH to produce fluorescent signal. Reaction with GSSG produces no signal, and reaction with PSSP would only be expected with a small subset of highly reactive proteins. Cleary, fluorescence signal coming from reaction with GSH and PSH is dominant when considering the whole *E. coli* cell. It appears that a 30-60 minute incubation time with probe is adequate, although longer incubations produce marginal increases in fluorescence signal. We reported similar uptake studies previously, using a different version of this probe that had more background signal[1].

DSSQ probe was also used to fluorescently image developing zebrafish embryo. Incubation with probe, as well as microinjection into the yolk, produced the same type of fluorescent image, with signal predominantly in the chorion. This means that the probe cannot penetrate into the embryo to image thiols (GSH and PSH), even though we have shown that such probes can penetrate cultured bovine endothelial lung cells (**Fig.17**) and mouse neuronal cells. But, probe seems to react significantly with proteins in the chorion,

producing a strong fluorescent signal. This signal was observed similarly, with or without pre-exposure to iodoacetamide, so is likely coming from disulfide exchange reactions, rather than reaction with thiols (**Fig. 12b**). As noted, disulfide exchange with GSSG produces no fluorescence signal, and the expectation is that in general, protein disulfides will not produce fluorescent signal either, unless the mixed disulfide that forms is in an active site that sequesters the disulfide with aromatic groups (as in **Fig. 6b** and in **Fig. 6d**). To determine the type of protein that is reacting with DSSQ, to confirm that it does indeed possess such a "reactive disulfide", mass spectrometry-based identification was used (next section).

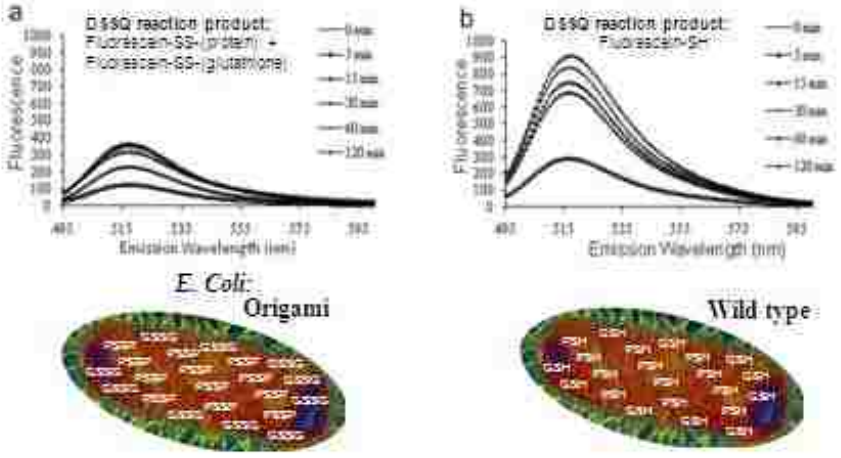
a
DSSQ reaction product:
Fluorescein-SS-(protein) +
Fluorescein-SS-(glutathione)
Fluorescence
Emission Wavelength (nm)
b
DSSQ reaction product:
Fluorescein-SH
Fluorescence
Emission Wavelength (nm)
E. Coli:
Origami
Wild type

[redacted]

### 2.2.5 Proteomics studies

To identify the protein(s) producing fluorescent signals in **Fig 12b**, chorion was mechanically removed from the embryos at 1 day post fertilization, after treatment with probe as described in the previous section. The chorion (free of embryo and yolk) was collected for subsequent proteomic analysis. An advantage of having the para-methyl red (PMR) group as the "Q" substituent on the DSSQ probe is that labeled proteins can be visualized easily, as can be seen in the bright field image of the chorion material that was collected (**Fig. 12c**). That is, it behaves like a histological stain that will produce visible signal for labeled proteins, irrespective of whether the fluorescein label (which should also be present) is quenched or unquenched. That is, one expects a mixture of protein-SS-fluorescein and protein-SS-PMR, but the red color of PMR provides a convenient feature for tracking labeled protein during purification. Chorion proteins were then seperated on an SDS PAGE gel, and stained with either Coomassie brilliant blue, or by fluorescent imaging of the DSSQ probe, since protein was pretreated with DSSQ without denaturation (**Fig. 13**). The two fluorescent bands at ~20 kDa were identified as being proteins of interest (note: the very intense band should be ignored – it is from probe itself). To confirm that these fluorescent bands were from the protein that produced fluorescent signal in the chorion, this same analysis was repeated, using an acid workup (TCA) of the chorion that had been DSSQ labeled, to prevent additional disulfide exchange that might lead to loss of DSSQ probe. Again, fluorescent bands were observed in the same region. Comparison of coomassie and fluorescein signal indicates that only a subset of chorion proteins reacts with the DSSQ probe. These bands, which we refer to as

band H (High molecular weight) and band L (Low molecular weight), were extracted from the coomassie stained gel, trypsinized, and sequenced using tandem mass spectrometry. Mass spectral analysis of peptide fragments (**Fig. 14**) identified several peptides which, after searching the zebrafish proteome database, allowed identification of band H (High molecular weight) as being from the zebrafish homolog of human C-reactive protein (CRP), with sequence:

GCLKSVGLSGKTLLFPIATDTSYVKLSPRKPLSLSAFTLCMRVATELPAKREIILFA
YRTPDDDELNVWREKDGRFSVYIQSSKDAAFFRLHPLSTFQTHLCVTWESATGL
TAFWVDGQRSLHQVYRKGYSIRPGGTVLLGQDPDSYVGSFNAAQSFVGEITDLQ
MWDYVLSGTQIKAVYLNQDDRVKGNVFNWNTIKYDVTGNVLVVPDN

Band L (Low molecular weight) was identified as being from the zebrafish homolog of human lipovitellin, with sequence:

MRAVVLALTLALVASQQNKLVPEFAHDKTYVYKYEALLLSGIVQEGLAKAGIQI
KSKVLLSAATENTFLLKFVDPLFYEYAGTWPKDQVFPATKLNSALAAQLQTPIKF
EYANGVVGKVFAPAGVSPSVLNLYRGILNILQLNFKKTQNIYELQEAGAQGVCK
TQYVISEDPKADRI

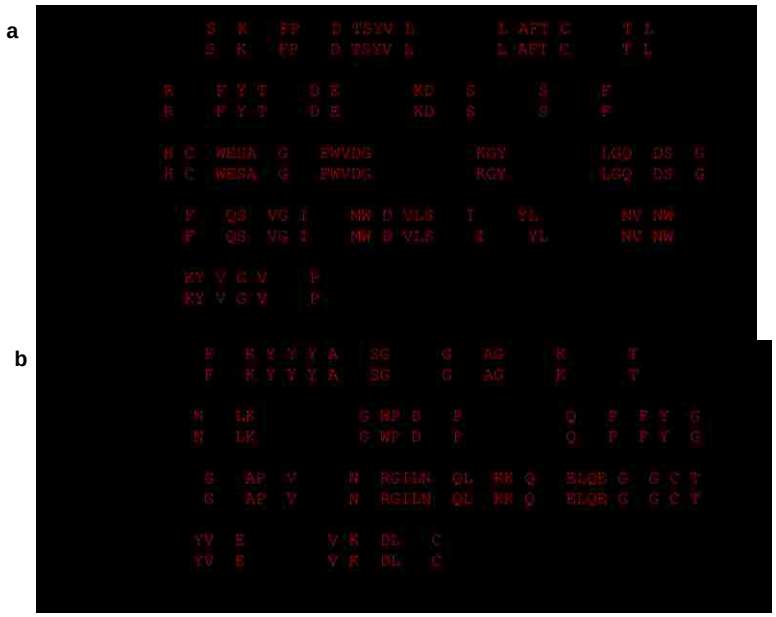


These sequences were submitted for homology modeling via the SWISS-MODEL server (swissmodel.expasy.org), to construct homology models. The zebrafish CRP and lipovitellin have > 30% sequence identity to homologs (**as seen in the figure above**) with crystal structures that can serve as templates in building the homology models: human CRP structure with 3.0 Å resolution (pdb code 1 GNH)[47] and silver lamprey (*Ichthyomyzon unicuspis*) lipovitellin structure with 1.90 Å resolution (pdb code 1lsh)[51]. When sequence identity is higher than 30%, homology models tend to be quite accurate. The homology models of zebrafish lipovitellin and CRP are shown in **Figs. 13 b** and **13 c**, respectively. Both proteins have only two cysteines, and they are located in close

proximity, which suggests they exist as disulfides: Cys145/Cys171 in lipovitellin; Cys38/Cys100 in CRP (**Figs. 13b** and **13c** respectively). Furthermore, both have histidine residues proximal to the reactive disulfide (His170 in lipovitellin; His98 in CRP), and CRP has additional aromatic residues – including Tyr178 that is in Van der Waals contact with His98, and is also located on what appears to be a helical flap that covers the disulfide (perhaps moving out of the way, upon disulfide exchange). That is, Tyr178 may play a role in positioning His98, thereby tuning the redox properties of the disulfide. Importantly, the basic nitrogen of His98 is in Van der Waals contact distance (3.8 Å) with the disulfide sulfur, which would lead to an extremely strong HOMO/LUMO interaction, deactivating the disulfide to attach by thiols, while stabilizing the disulfide. Accordingly, a mixed disulfide with the DSSQ probe would be expected to be quite stable, so would produce a highly fluorescent fluorescein, as the disulfide would no longer be quenching the fluorescein (as in **Fig. 6d**).

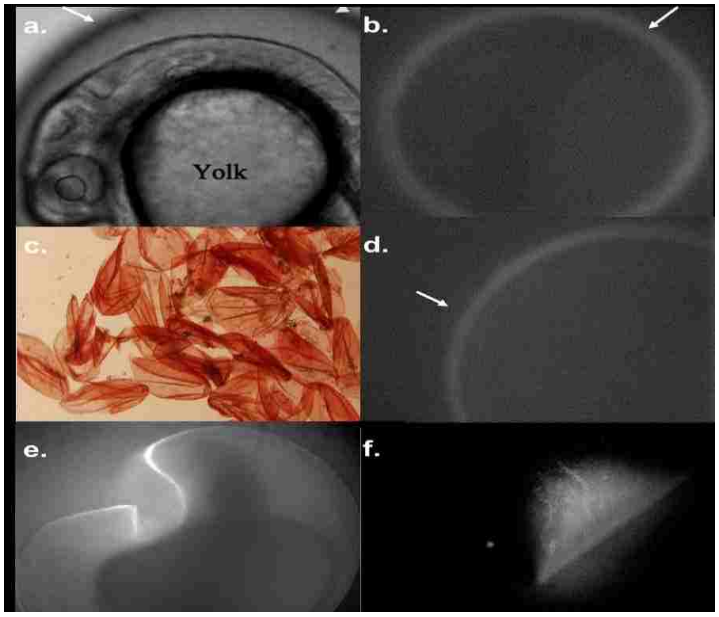


**Fig 12:** Intact zebra fish embryo (**a**, **b**) and Zebrafish chorion (**c**) at 1 day post fertilization , after treatment with 50 µM DSSQ probe. **a** and **b** are bright field fluorescence images of intact embryo with arrow identifying fluorescence labeling of intact chorion. **c** bright field image of chorion (removed from embryo). **d**. Signal was observed similarly, with pre-exposure to iodoacetamide. Figs **e** and **f** support our hypothesis that Zebra fish CRP and lipovitellin may work in concert in response to tissue in humans. In all cases Ex. 490 nm, Em. 520 nm.

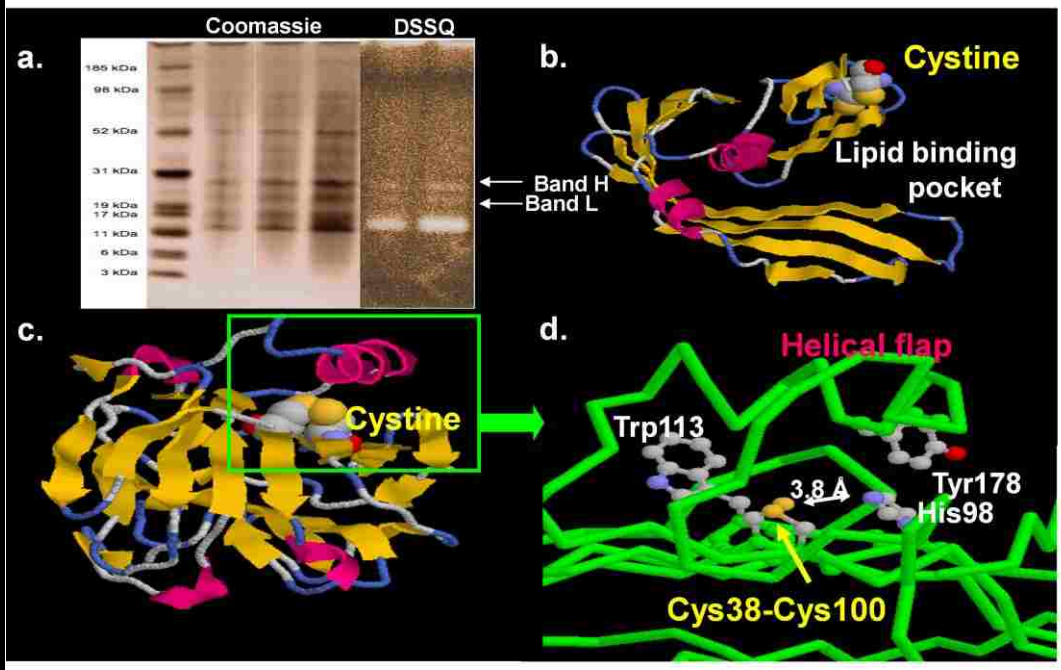
a.
Coomassie
DSSQ
185 kDa
98 kDa
52 kDa
31 kDa
19 kDa
17 kDa
11 kDa
6 kDa
3 kDa
Band H
Band L
b.
Cystine
Lipid binding pocket
c.
Cystine
d.
Helical flap
Trp113
3.8 Å
Tyr178
His98
Cys38-Cys100

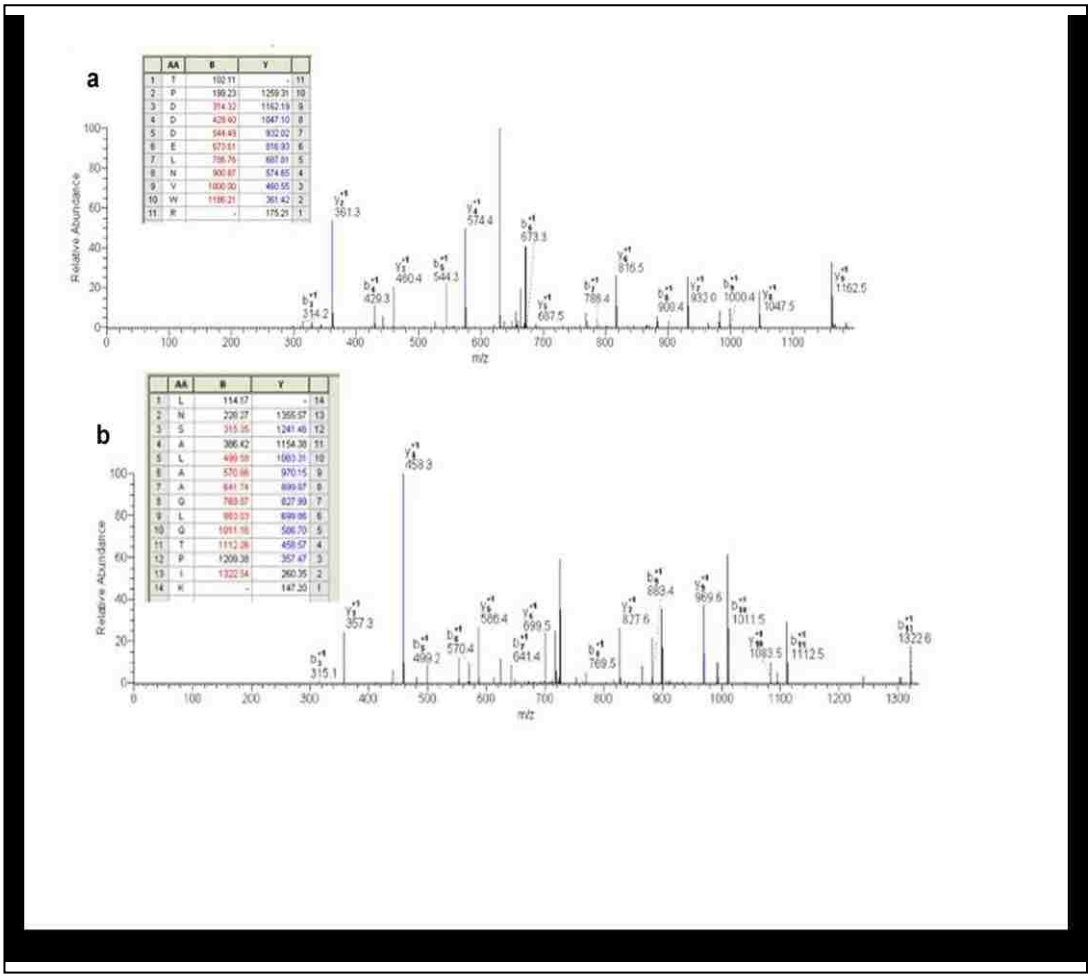


**Fig 14**: Mass spectral fragmentation data for a sample peptide from: (a) Band H (CRP) and (b) Band L (Lipovitellin).

### 2.3.6 Studies with bovine lung cell (BPAEC) and rabbit muscle glyceraldehyde phosphate dehydrogenase (GAPDH)

Fluorescent probe labeling of bovine pulmonary arterial endothelial lung cell (BPAEC) proteins and rabbit muscle glyceraldehyde phosphate dehydogenase (GAPDH) using PMR-Cys-FITC were performed. Cells were lysed by boiling in a non-reducing SDS loading buffer, centrifuged, supernatants loaded and gel run. Both normal BPAEC and the ones pretreated with NEM to block free thiols were run (**Fig. 16a**). The same experiment was performed using coomassie brilliant blue stain (**Fig. 16b**). Note the disappearance of a protein band (illustrated with an arrow in panel **a)** in NEM treated cells. NEM blocks free thiols. The same observations were not seen with coomassie labeled proteins. Similar experiments were also performed on rabbit muscle glyceraldehyde phosphate dehydrogenase (GAPDH), a glycolytic enzyme with an active site cysteine, Cys149, on an SDS-PAGE gel under reducing conditions (**Fig. 16c** and **d**). All the gels were treated with dye for 2 hrs. Experiments prove that PMR-CYS-FITC can label protein thiols. Fluorescence microscopy imaging of BPAEC demonstrates the cell permeability of fluorescent dithio probe (DSSQ). Bovine pulmonary artery endothelial cells (BPAEC) were treated with 50 μM of PMR-CYS-FITC for 30 minutes. Ex. 490 nm, Em. 520 nm). **Figure 17**, shows that DSSQ can label mitochondria in these cells. Multiple z-slideswere obtained to produce a 3 dimensional image of the cell, with labeled mitochondria.

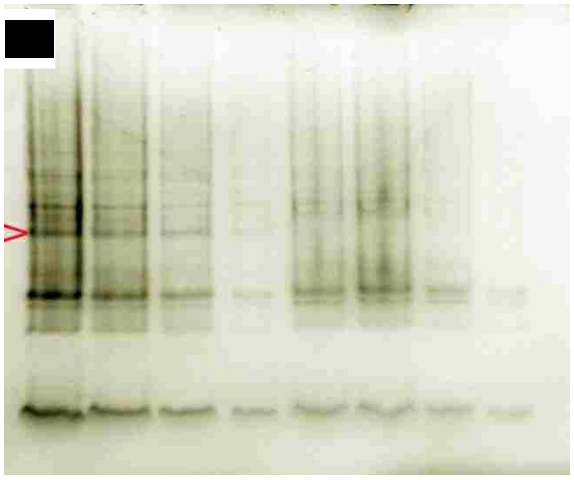

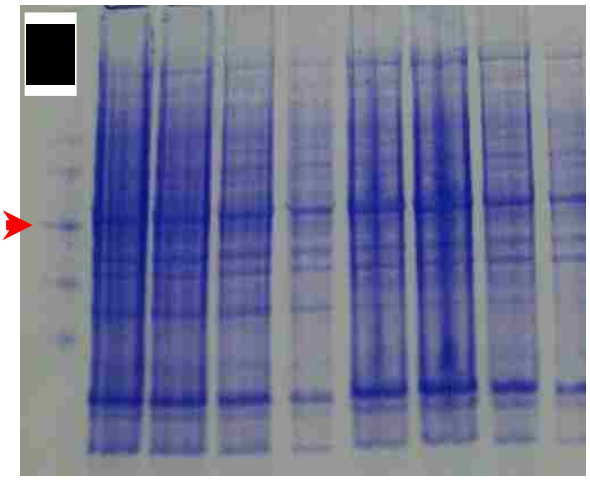

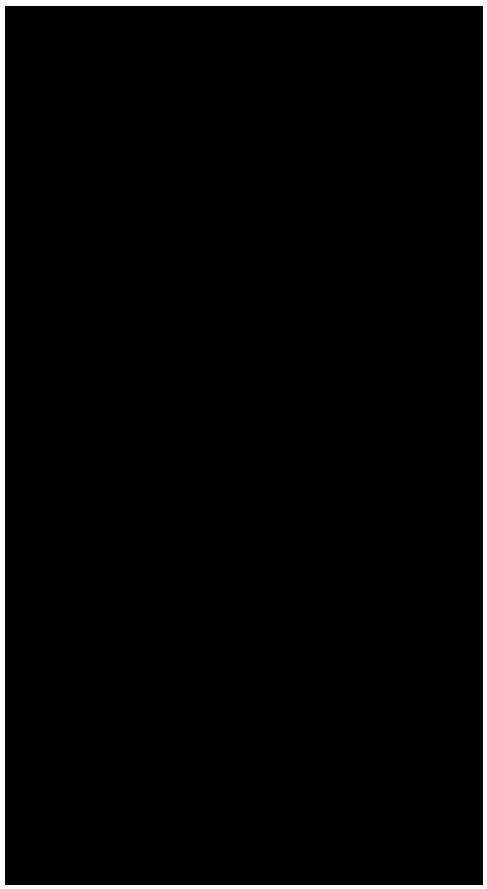

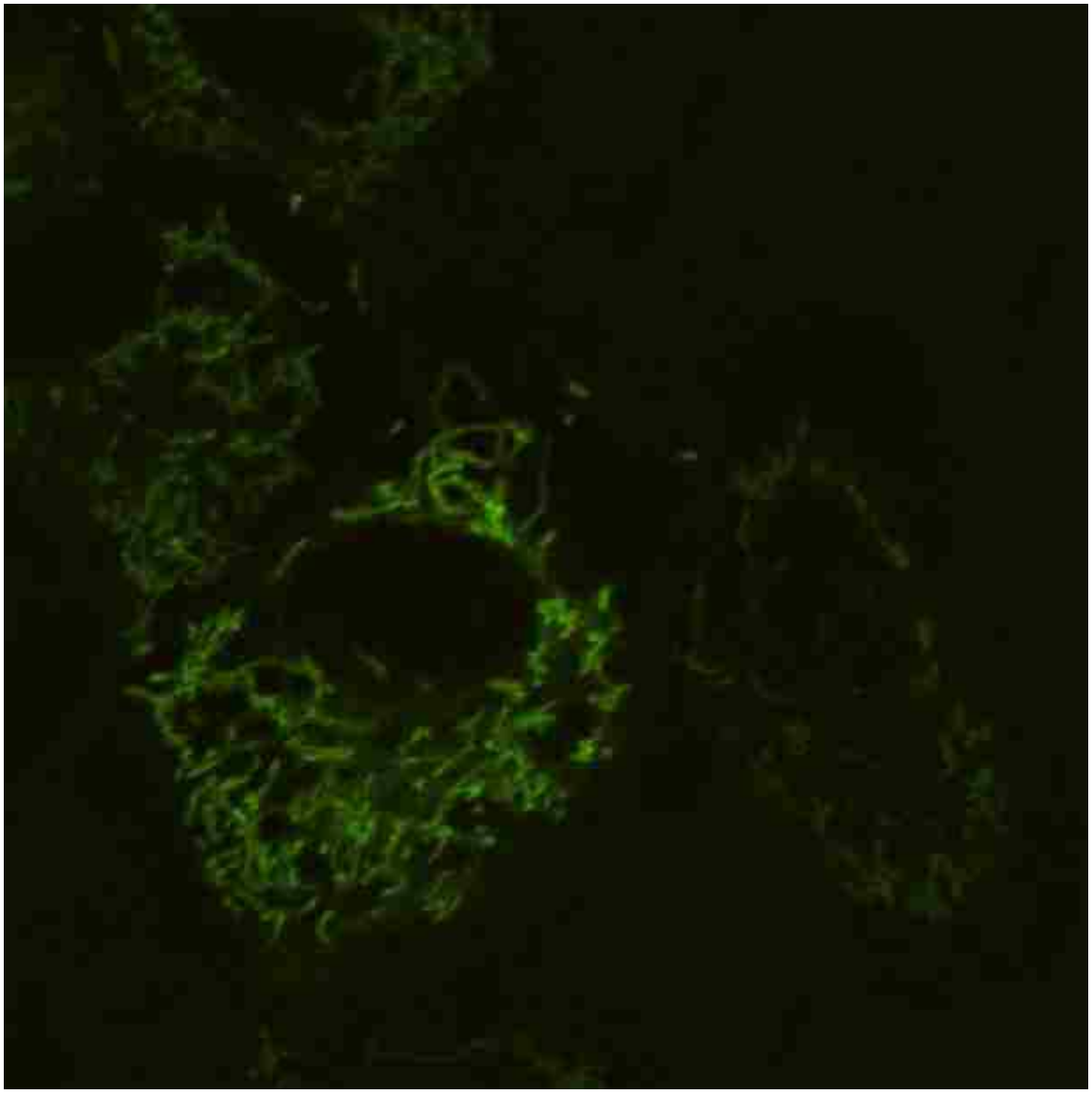

**Fig 17:** DSSQ can label mitochondria in BPAC cells. Multiple z-slides were obtained to produce a 3 dimensional image of the cells, showing labeled mitochondria.

## 2.3. DISCUSSION

We first introduced the concept of fluorescent dithio probes for detecting millimolar concentrations of thiols in cells, using fluorescein tethered to rhodamine[1]. The probe presented herein, DSSQ (**Fig. 6a**) is an improvement, where dabcyl (para-methyl red), a known quencher of fluorescein, has been tetherd via a cleavable disulfide to fluorescein. The unusually low reduction potential (-0.54 V) of these probes facilitates their use at micromolar or lower concentrations (as would be present in cells) to detect changes in millimolar concentrations of thiols. While a number of probes have been reported with much greater sensitivity [27] even able to detect pM thiols [26], the concentration of thiols present in a cell are typically not lower than 1 mM, and GSH levels often vary from 1-10 mM. Because of the low reduction potential of the fluorescent dithio probes, they can detect changes in this range. That is, if GSH levels in a cell change from 1 to 10 mM, and there is only μM concentration of probe present – one can expect to see a significant change in fluorescence. This would not be the case with probes that are more reactive, and more sensitive, as they would be fully reacted and give the same fluorescence level whether thiols are present at 1 or 10 mM. So, an advantage of the low reduction potential of the dithio probes is that they are responsive to changes in thiol levels in a biologically relevant range, which makes them complementary to the various other probes that are available that are more sensitive, but less responsive to *changes* in this range. But why are fluorescent dithio probes so difficult to reduce, and what is the nature of the reaction(s) that they undergo?

Three key concepts have emerged in our attempt to answer the above questions: (i) disulfides are electron poor and tend to interact with electron rich systems, such as aromatic rings (a LUMO/HOMO interaction), (ii) this interaction can lead to quenching if one of the aromatic ring systems is a fluorophore, and (iii) if two Lewis bases (HOMOs) are competing for interaction with the same disulfide (LUMO), the stronger base could weaken the interaction of the disulfide with the weaker or less well-positioned base. The first point is elegantly demonstrated by a molecular tweezers model system, where conversion of a tethered thiol pair to a disulfide actually drives movement of aromatic rings, so that they can interact with the disulfide (**Fig. 6b**). We performed AM1 calculations on this tweezers system, which demonstrates that indeed there is a HOMO/LUMO interaction between the electron rich aromatic rings (HOMO) and the electron deficient disulfide (LUMO) (**Fig. 9d**). An analogous version of this effect may be operative in proteins as well, such as in heat shock transcription factor 1 (**Fig. 6c**), where formation of a disulfide in a heat response requires the presence of aromatic rings (verified by mutagenesis), which is most likely because of the stabilization they provide for the disulfide. In this system, the heat-induced disulfide/aromatic interaction also resulted in quenching of fluorescence. This leads to the second key concept, that disulfide interactions with fluorophors leads to quenching. This is a well-established phenomenon for dithio interactions with tryptophan [46], and is another key concept in the design of our DSSQ probes (**Fig, 6d**). That is, the disulfide can quench fluorescein, as long as it is not involved in a stronger interaction with another Lewis base. This leads to the third key concept – that the disulfide can interact, as an electron deficient Lewis acid (LUMO) with more than one electron rich Lewis base (HOMO), and that this competing interaction can

be used as shown in **Fig. 6d**. That is, the HOMO/LUMO interaction between fluorescein/dithio leads to quenching (**Fig. 9c**), but if there are other electron rich donors that can interact with the disulfide, this weakens the interaction with and quenching of fluorescein (**Fig. 9b**). This competition for interaction with the disulfide is summarized schematically in **Fig. 9**, and in the context of the DSSQ probe, in **Fig. 6d**. Accordingly, one would expect a mixed disulfide with a protein might leave the fluorescein highly quenched by the disulfide, unless that protein had aromatic groups in the active site proximal to the disulfide, which are able to interact more strongly with the disulfide than fluorescein (as shown in **Fig. 6d**). We refer to such proteins as having a "reactive disulfide", because the disulfide product that is produced is highly stabilized, and we believe this type of stabilizing electronic donor/acceptor interaction with disulfides may be prevalent in nature. In any case, potential "reactive disulfides" could be imaged and labeled with fluorescent dithio probes such as the DSSQ probe presented herein.

The reaction between glutathione and PMR-CYS-FITC (DSSQ) is a multi-step process. The first step must result in the formation of a quenched mixed disulfide D*SSG (the other product, the mixed disulfide with para-methyl red, is of little concern, as fluorescein is what is being detected). In the presence of excess glutathione, the reaction goes to completion, giving rise to the increase in fluorescence emission due to formation of unquenched $DS^-$, as shown by the following reaction:

What is it about glutathione that makes it better able to quench fluorescein than a known fluorescein quencher, para-methyl red? To answer this question, various analogs of glutathione were prepared, with different nucleophilic positions blocked, but in all cases reaction occurred largely as with native glutathione. A reasonable interpretation may then be that it is not what glutathione can do that matters, but rather what it can't do; glutathione is not able to compete for electronic interactions with the disulfide (compare **Fig. 9b** and **Fig. 9c**). As is demonstrated schematically in **Fig. 6d**, the lack of a HOMO/LUMO interaction between glutathione and the disulfide frees the disulfide to now interact exclusively with the fluorescein, thereby quenching it more effectively. Recognizing the nature and importance of this disulfide-based quenching effect, and the kinetics of reaction described by equation and **Fig. 8**, is crucial to the proper interpretation of results in cells, using the DSSQ probe. That is, the reaction of GSH or protein thiols (**Fig. 8**) will produce an increase in fluorescence, due to the second step in equation. The first step  produce**s** step produces no fluorescence change. One predicts from this that, in a cell, the DSSQ probe would not react with most disulfides (which are typically not present at >2 mM), and would certainly not react with GSSG. But, the DSSQ probe might react in an oxidizing sub-compartment or membrane environment (rich on PSSP) with certain "reactive disulfides", if a disulfide could be produced that was more stabilized than even DSSQ, with electron rich groups in proximity to the disulfide, as illustrated in **Fig. 6d**. These disulfides we would categorize as being "reactive", because they participate in disulfide exchange reactions with an already-stable disulfide (DSSQ). Whether such "reactive disulfides" have a role in biological processes has never been explored, because there has not yet been a tool to do so, in a proteome-

wide manner. Given the importance of disulfide exchange and thiol-disulfide exchange reactions in biology, including in the infection process, in the formation of the chorion/egg shell around a developing embryo, and various other processes that occur in membranes, a probe that can selectively target "reactive disulfides" could be used to image and identify proteins, and determine if there is functional importance for such reactivity. In summary, while the DSSQ probe can be used to image GSH and PSH in the cytosol, and other reducing environments, it may have an additional use in imaging and identifying a subset of react disulfide-containing proteins that may be present in oxidizing environments.

To explore the first of the two previously described applications of the DSSQ probe, we attempted to measure protein and glutathione (PSH + GSH) levels in normal *E. coli*, versus a mutant strain that is deficient in reduced thiols. The Origami strain of *E. coli* is a K-12 derivative that has mutations in both the thioredoxin reductase (trxB) and glutathione reductase (gor) genes, which greatly enhances disulfide bond formation in the cytoplasm. Consistent with our previous work using a related probe [1], the DSSQ probe can detect the higher levels of thiols, both GSH and PSH, that are present in the wild type strain, compared to the Origami strain. This is observed using a pre-incubation of cells with 50 μM probe (**Fig. 8**). This confirms that the DSSQ probe can penetrate the cell wall to reach the reducing cytosolic environment of *E. coli*, to detect changes in thiol redox state.

The second application for DSSQ probes is to identify proteins with "reactive disulfides". Again, the probe is not typically expected to react with disulfides in biologically relevant concentrations (< 1 mM), unless they are unusually reactive disulfides; that is, if a more stable mixed disulfide is produced. Incubation of zebrafish embryos with DSSQ, or microinjection, produces intense fluorescence only in the protective chorion (i.e. eggshell) layer that envelops the developing embryo. Interestingly, the extent of fluorescence is the same irrespective of whether embryos are pretreated with iodoacetamide (**Fig. 12b**) or not (**Fig. 12d**), consistent with DSSQ probe reacting with disulfides rather than thiols. The proteins responsible for this fluorescence signal were separated using SDS PAGE (**Fig. 13a**), then bands were extracted and proteins identified using tandem mass spectrometry (**Fig. 14**). This disulfide proteomic approach led to our discovery of two novel reactive disulfide-containing proteins in the zebrafish chorion: lipovitellin and C-reactive protein (CRP). CRP is a well-known biomarker, which is part of the acute phase response to injury/tissue damage, infection and inflammation (associated with oxidative stress) in humans [47,48] . CRP levels have also been reported to increase in trout, as part of its acute phase response[47].Lipovitellin is the major protein found in the egg yolk of egg laying animals – and plays a role in storage of trace minerals, as well as lipid transport [49]. The recent crystal structure of the lamprey lipovitellin shows electron density for 7 phospholipids, and multiple hydrocarbon tails, bound in the active site cleft [49]. Homology models of lipovitellin (**Fig. 13**) and CRP (**Fig. 13**) were constructed based on their high level of sequence identity (>30%) when compared with proteins of known 3-dimensional structure: human CRP, and lamprey lipovitellin. Neither protein model has free or exposed thiols, but each has a disulfide.

Therefore, the DSSQ probe has been able to image, and has assisted in disulfide-based proteomics identification of these unusually reactive disulfides (recall that GSSG does not react with our probe at > 2 mM, yet CRP and lipovitellin are reacting at much lower concentrations).

Inspection of the two structures reveals that both have a histidine imidazole in proximity to the disulfide (**Fig. 13**). In fact, the basic imidazole nitrogen of CRP (**Fig. 13d**) is in Van der Waals contact with one thiol of the disulfide (directed to the LUMO), which would be expected to provide stabilization of the disulfide. Likewise, there are additional aromatic groups in the vicinity of the disulfide in CRP (**Fig. 13d**), including Trp113 and Tyr178 that appears to play a role in orienting the basic imidazole of His98. It seems likely therefore, that a mixed disulfide with the DSSQ probe (CRP-SS-fluorescein) would have a disulfide that is highly stabilized by aromatic (and imidazole nitrogen) interactions, that provide at least as much disulfide stabilization as existed in the original DSSQ probe. Is there biological relevance to a disulfide that produces a highly stabilized mixed disulfide, and is therefore prone to undergo disulfide exchange? This is difficult to answer, as there has been little study of such disulfide exchange cascades, but it is known that thiol-disulfide exchange reactions in membranes do play a role viral infection (membrane fusion)[38], and in formation of the egg shell. Importantly, there have been reports that CRP may work in concert with lipid transport proteins (LDL) in humans this led us to a hypothesis as to what the function of these two proteins may be, in the chorion of zebrafish.

Vitellogenesis is the process where yolk is formed in the oocyte from nutrients in the body. As part of this process, lipovitellin (a cleavage product of vitellogeninin) is transported via receptor –mediated endocytosis in an oocyte [47,50,51]. This lipid transport process is analogous to the LDL/LDL Receptors lipid transport system in humans [50], but functions to transport hepatic lipids and minerals to the ovaries [58]. Indeed, lipivitellin shares sequence homology with apolipoprotein B, which plays a role in forming low-density lipoproteins [50,53]Vitellogenin binds to vitellogenin receptor on the surface of oocytes, where it is transported via receptor mediated endocytosis, ultimately to the yolk, where it is stored as a nutrient for the developing embryo. Lipovitellin also transports lipids to the oocyte. Could it be playing a similar function in the zebrafish chorion, transporting lipids to the yolk – either in response to damage to the chorion, or to salvage lipid nutrients as the chorion degrades, typically after 24 hours post fertilization? Of particular interest, since zebrafish CRP and lipovitellin have reactive disulfides, is the fact that vitellogenin receptors in mammals (which are in the LDL receptor family [54] contain cysteine rich ligand binding repeats, that may play a role in vitellogeninin/vitellogenin receptor interactions, and receptor mediated endocytosis; this is analogous to LDL/LDL receptor interactions [54].

So what then might be the role of CRP in zebrafish, and is it associated with lipovitellin in any way? In a recent review by Pepys and Hirschfield [55], it was noted that there has been growing interest in the role of CRP in cardiovascular disease. They note elevated CRP levels are associated with cardiovascular disease [55,56]. Furthermore, treatment with statin drugs, that lower cholesterol and LDL levels, leads to decreased levels of CRP as well [57]. While it has been known for over 50 years that CRP binds to

plasma lipids (ex. phosphatidyl choline), it was a relatively recent discovery that CRP, in either an aggregated or native form, can bind to LDL [58, 59, 60]. The fact that CRP has been reported to interact with LDL leads us to propose that a CRP/lipovitellin interaction may play a role in lipid transport in zebrafish, perhaps transporting lipid from the chorion to the yolk. One might speculate that the purpose of this is to salvage the lipid from the chorion, as a nutrient for the developing embryo, just as vitellogeninin transports protein and lipid to the yolk in mammalian oocytes [50, 51]. This would suggest that zebrafish could be used as a model system to provide a better understanding of the lipid transport process in humans as well. Given the ubiquitous appearance of CRP in the circulation in humans, associated with tissue damage, infection, inflammation, and various other maladies that involve cellular damage, it is tempting to speculate that a CRP/lipovitellin lipid transport may be at play whenever cellular damage has occurred, and there is a need to salvage lipid material. That is, perhaps a damaged or degrading chorion can serve as a model for tissue damage in humans. Are elevated levels of CRP in humans related to the fact that CRP had a role to play in cleaning up lipid after cellular damage? Is the zebrafish chorion a model for this phenomenon? Is the fact that these proteins have reactive disulfides central to their ability to intiate lipd transport from the chorion, just as thiol-disulfide exchange plays a central role in receptor mediated endocytosis or in viral infection? In this regard, it is noteworthy that we observed an interesting clustering or aggregation effect (**Fig. 12e** and **12f**), where spots of intense fluorescence were observed after labeling with DSSQ in the chorion, when there was physical damage to the chorion. Future studies are being directed to exploring the role of CRP and lipovitellin in lipid damage in the chorion, and to address the many new questions raised by these studies.

## 2.4. SUMMARY

In summary, DSSQ probes are useful for measuring changes to levels of thiols, both GSH and PSH, in cells. Beyond thiol detection, they can also be used to image oxidizing environments, such as the chorion (egg shell) of developing embryos. But, not all disulfides will react with the DSSQ probe in a thermodynamically favorable reaction to produce fluorescent signal – only those that produce a highly stabilized mixed disulfide product, characterized by proximal Lewis bases (ex. aromatic rings; the basic imidazole nitrogen of histidine), are expected to react. Such reactive disulfides could have biologically important functions. For example, zebrafish CRP and lipovitellin have reactive disulfides, which may play a role in their proposed ability to transport lipid. Finally, our studies have led to a proposed function for CRP and lipovitellin in zebrafish, with implications for functional homologs of these proteins in humans.

## 2.5. METHODS

Oxidized and reduced glutathione were obtained from CALBIOCHEM. 7-hydroxycoumarin-3-carboxylic acid was obtained from INDOFINE. All biochemical reagents were obtained from Sigma, and all synthetic reagents were obtained from Aldrich. *Escherichia coli* Origami(DE3)pLysS cells as a glycerol stock, and BL21(DE3)pLysS competent cells were obtained from Novagen.

### *In vitro* fluorescence studies of thiol/disulfide reactivity

The buffers used in the pH study were HEPES (pH 7.0, pH 7.6), Tris (pH 8.2) and acetate (pH 5). Fluorescence studies *in vitro* were performed on a BMG Polarstar Galaxy fluorescence plate reader or a Jasco FP-6500 spectrofluorometer. Absorbance studies were done on a HP 8452a diode array spectrophotometer. Reactivity with different thiols/disulfides were quantified by measuring the changes in fluorescence at 520 nm (485 nm excitation) over time in the plate reader using 5 µM DSSQ probe.

### Synthesis of the DSSQ probe

1 mmol of 4-dimethylaminoazobenzene-4’-carboxylic acid (commercially known as p-methyl red) was dissolved in 20 mL of 4:1 acetonitrile/chloroform mixture, to which 1 mmol of BOP reagent (benzotriazol-1-(yloxy)tris (dimethylamino)phosphonium

hexafluorophosphate) and 20 mmol triethyl amine were added and stirred for fifteen minutes. 3 mmol of cystamine in 3 mL acetonitrile was added slowly and progress of reaction is monitored by TLC for every five minutes. The reaction is complete in about an hour and reaction mixture was concentrated. The amide was purified by silica gel (230–400 mesh) column chromatography using 20% methanol in chloroform (yield = 32%). MALDI was used to distinguish between monomer (N-[2-(2-Amino-ethyldisulfanyl)-ethyl]-4-(4-dimethylamino-phenylazo)-benzamide, MW: 403.15) and dimer ( Bis(4-(4-Dimethylamino-phenylazo)-N-(2-mercapto-ethyl)-benzamide, MW: 654.26) and only monomer was used for next step. The 0.1 mmol of resulting amine was reacted with 0.12 mmol fluorescein 5-isothiocyanate (FITC) in acetone at room temperature for 16 h. The final DSSQ (5-[3-(2-{2-[4-(4-Dimethylamino-phenylazo)-benzoylamino]-ethyldisulfanyl}-ethyl)-thioureido]-2-(6-hydroxy-3-oxo-3H-xanthen-9-yl)-benzoic acid, MW: 792.1832 probe was purified by silica gel (230–400 mesh) column chromatography using 30% methanol in chloroform and then by preparative thin-layer chromatography (TLC, percentage yield = 18%). All of the above reactions were done in the dark, and all compounds were characterized by $^{1}$H NMR, [$^{1}$H, $^{1}$H] COSY, and MALDI.

$^{1}$H NMR: 10.3 (bs, 1H, acid proton), 8.8 (s, 1H), 8.45 (bs, 1H, phenolic proton), 8.2 (s, 1H), 8.0 (d, 2H), 7.8 (d, 3H), 7.65 (bs, 1H), 7.1 (d, 1H), 6.8 (d, 2H), 6.65 (d, 2H), 6.4 (bs, 4H), 3.8 (bt, 2H, NH-$CH_2$), 3.55 (bt, 2H, NH-$\underline{CH_2}$), 3.35 (bs, 3H, $\underline{NH}$), 3.05 (s, 6H, $N(CH_3)_2$), 2.9 (bt, 2H, S-$CH_2$), 2.45 (bt, 2H, S-$CH_2$, this peak is merged with DMSO-$d_6$ proton peak). MALDI (793. 3417, $M+1^{]+\cdot}$)

**Determination of DSSQ reduction potential**

In order to determine $E^{o'}$ values, it was necessary to determine fluorescence for the fully reduced DSSQ probe ($F_{max}$). $F_{max}$ could be obtained by titrating 5 µM probe with increasing DTT at pH 7.0 (100 mM HEPES). The $F_{max}$ value of 10940 obtained from the DTT titration was used for $E^{o'}$ calculations for DSSQ. Equilibrium fluorescence values ($F_i$) were measured at each concentration of DTT reductant, and these data were used along with the $F_{max}$ value and the $E^{o'}$ of DTT to calculate $E^{o'}$ for DSSQ. For these reduction measurements, and for the general measurement of thiol levels, the fraction of probe that remains in the oxidized state after equilibration with a reductant (such as DTT) is given by:

$$X = [DSSQ]/([DSSQ] + [DS]) = (F_{max} - F_i)/(F_{max} - F_0) \quad (\mathbf{5})$$

where $F_{max}$ is the fluorescence (Ex = 485 nm, Em = 520 nm) for fully reduced probe (DS), $F_0$ (= 1492) is the fluorescence for fully oxidized probe (DSSQ) and $F_i$ is the fluorescence at some concentration of reductant. From X, an equilibrium constant for DSSQ reduction can be calculated according to:

$$K_{eq} = \frac{[R_{Ox}][DS][QS]}{[R_{Red}]^n[DSSQ]} = \frac{([DSSQ]_0(1 - X))^3}{[DSSQ]_0(X)([R]_0 - n[DSSQ]_0(1-X))^n} \quad (\mathbf{6})$$

For a dithiol reductant like DTT, n = 1. For a mono-thiol reductant like GSH, n = 2. R is reductant, $[R]_0$ is initial concentration of reductant, and $[DSSQ]_0$ is initial concentration of

probe. From $K_{eq}$ and the reduction potential for DTT (-0.33 V ), the DSSQ reduction potential can be calculated according to:

$$E^{o'}_{DSSQ-1} = E^{o'}_{DTT} + RT/nF \ln (K_{eq}) = -0.33V + (0.0592/2) \log (K_{eq}) \quad (7)$$

where R is the gas constant, T is the temperature in Kelvin, F is Faraday's constant and n is the number of electrons transferred.

### *E. coli* uptake studies

*E. coli* (BL21(DE3)pLysS) cells were grown in 10 mL LB broth overnight, then transferred to 250 mL LB broth and stirred at 37$^{o}$C until $OD^{600}$ = 0.6-0.7 was reached. For dose-response studies, cells were exposed to various concentrations of DSSQ probe for 60 minutes, 1 mL aliquots were taken and centrifuged then washed with 4 x 1 mL 100 mM HEPES buffer (pH 7.4), and fluorescence read (Ex = 485 nm; Em = 520 nm) on the Jasco spectrofluorometer. For studies of the kinetics of DSSQ uptake into *E. coli* BL21 cells (**Fig. 8**), the $OD^{600}$ = 0.6-0.7 culture was partitioned into three equal fractions. One fraction was kept as a blank and the two DSSQ probes were added to the other two fractions. In this study the DSSQ probe concentration were 50μM and 10 μM, and the carrier (DMSO) was kept at <0.5%. The cell culture was stirred for 2 hours and 1 mL samples were collected at different time intervals. The samples were centrifuged for 5 min at 13,000 rpm and the supernatant was decanted. The cell pellet was resuspended in 1 mL 100 mM HEPES buffer (pH 7.4), vortexed for 5 sec and centrifuged for 5 min at 13,000 rpm and the supernatant was decanted. This washing was done three times to ensure complete removal of any DSSQ probe bound on the surface of the cells. Finally, just

before the fluorescence reading, the pelleted cells were resuspended in 100 mM HEPES buffer (pH 7.4) and fluorescence from the suspended cells was recorded. On average, the time between cell pelleting and fluorescence reading was kept constant at 2 h. All the results presented in this study were the average of five replicates and the standard deviations were less than 10%. Appropriate blanks with cultured cells were used, to minimize error from light scattering. This whole process was repeated with Origami cells and the standard deviations for these replicates were also less than 10%.

**Zebrafish studies**

Zebrafish embryos were grown and maintained at the NIEHS Marine and Freshwater Biomedical Sciences Center using standard protocols , described elsewhere[1],in accord with accepted procedures of humane animal care. At 1 day-post-fertilization, embryos were exposed externally to 50 μM DSSQ probe for 1.5 hr. Incubations were with 50 μM DSSQ in 1% DMSO in Danieau's buffer (58 mM NaCl, 0.7 mM KCl, 0.4 mM $MgSO_4$, 0.6 mM $Ca(NO_3)_2$ and 0.5 mM Hepes, pH 7.6). Fluorescence images were obtained with an Olympus IX70 microscope (Ex = 489 nm). Images were processed using MetaMorphR software (Molecular Devices Corporation, Sunnyvale California). For thiol labeling ( **Fig.13**),chorion (1.8 ml) was treated with 0.2 ml cold 100% (w/v) TCA, and incubated on ice for 30 mins, then centrifuged. The pellet was washed with cold 10 % TCA then 5 % TCA. The pellet was resuspended in 40 μL of denaturing buffer comprised of Tris (0.2 M, pH 8.5), urea (6 M), EDTA (10 mM) and 0.5 % (w/v) SDS, also with 0.1 M iodoacetamide (IAM). After 10 mins of IAM labeling (room temp) of the remaining

free thiols, reaction was stopped by adding an equal volume of cold 20 % TCA, and recentrifuged. The pellet was washed as described above. The proteins were disolved in 0.5% SDS, 10 mM EDTA, 6 M urea, 0.2 M Tris, 0. M AIM and pH 8.5, 1 %LDS buffer. The chorion and embryo were heated to at 70 $^{o}$C for 10 min, centrifuged at 13000 rcf for two and supernatant was loaded on NUPAGE 4-12 % Bis-Tris gel.

**Zebrafish proteomic studies**

For DSSQ labeling of zebrafish proteins (**Fig. 5**), chorions were manually removed and treated with 0.2 mL cold 100% (w/v) TCA and incubated on ice for 30 mins, then centrifuged. The pellet was washed with cold 10% TCA and then again with 5% TCA. The pellet was then resuspended in 40 µL of denaturing buffer comprised of Tris (0.2 M, pH 8.5), urea (6 M), EDTA (10 mM), 0.5 % (w/v) SDS, and 0.1 M iodoacetamide (IAM). After 10 min of IAM labeling (room temp) of the remaining free thiols, reaction was stopped by adding an equal volume of cold 20 % TCA, and recentrifuged. The pellet was pellet was frozen until use (and resuspending in loading buffer). Resuspended chorion proteins were heated to at 70$^{o}$C for 10 min, centrifuged and supernatant was loaded on a NuPAGE® 4-12 % Bis-Tris gel. Chorion protein bands (BandH and BandL) were cut from the gel. Gel pieces were then transferred to Eppendorf tubes in 1 ml of 40% methanol, 7% acetic acid, then incubated for 30 minutes, and then washed twice with water for 30 min while sonicating. In a like manner, gel pieces were washed an additional two times in 50% acetonitrile, and again twice in 50% acetonitrile in 50 mM ammonium bicarbonate, pH 8.0. The gel pieces were then dried with a speed vac. To each was then added 200 µl

of 20 mM ammonium bicarbonate, pH 8.0, containing 1 µg trypsin (Promega). After incubating overnight at 37$^{o}$C, the digested proteins were extracted twice with 70% acetonitrile in 0.1% formic acid and dried. Each dried sample was suspended in 20 µl of 6M guanidine-HCl, 1mM DTT and 5 mM potassium phosphate (pH 6.5). After sonication, peptides were extracted using a $C_{18}$ ZipTip (Millipore). Extracted peptides were collected into an insert in a vial to be used for mass spectrometry, and dried in the inserts. To each dried sample was added 5 µl of 0.1% formic acid in MS water containing 5% acetonitrile. Samples were then ready for mass spectrometry analysis. Nano-HPLC-mass spectrometry was performed on a Thermo-Fisher LTQ mass spectrometer coupled to a Surveyor HPLC system, with an Aquasil C18 PicoFrit capillary column (75 µm x 10 cm) from New Objective. The MS/MS data were collected and searched against the appropriate subset of the Uniprot database.

**BPAEC fluorescence studies**

Bovine pulmonary arterial endothelial cells (BPAEC) were isolated from segments of calf pulmonary artery obtained from a local slaughterhouse and were cultured to confluence in gelatin coated tissue culture plates. For fluorescence microscopy imaging, the cells were cultured and used within passages 4-20. Lactate dehydrogenase (LDH) activity in the medium and cells were determined to establish cell viability (there was <5% total cellular LDH release into the medium). For fluorescence microscopy, the cells were incubated in Hanks Balanced Salt Solution containing 10 mM of HEPES buffer (HBSS) containing the DSSQ treatment. For in-gel imaging, pelleted cells were lysed by boiling in a non-reducing SDS loading buffer, and incubated with 50 µM DSSQ after a 15 min pre-treatment +/- 20 mM NEM .

# CHAPTER 3

## COUMARIN – FLUORESCEIN- BASED PROBE FOR REAL TIME QUANTITATION OF THIOL LEVELS IN CELLS

### 3. FRET Probe - OH-Coumarin diCystamine-FITC (OH-Coum-Cys-FITC)

**Fig 18**: New FRET-based dithio probe (DSSA). Excitation of coumarin at 320 nm gives emission from coumarin (460 nm) and fluorescein (520 nm).

FRET measurements can be used as a means to probe for micro-environment and thiol redox statein cells due to, and changes in donor –acceptor distances in a disulfide-linked probe, upon reductive cleavage. By monitoring changes in intensities of the donor and acceptor when exposed to different thiol reductants, various cellular environments can be probed. Here we report a new variant of the donor-SS-acceptor (DSSA) series of probes (**Fig.18**). Specifically we report the synthesis and development of OH-Coum-Cys-FITC (hydroxy-coumarin-cystamine-FITC), a FRET based probe for quantitation of thiols inside cells. It is characterized by measuring reduction with thiols at different GSH concentrations and different ratios of GSH/GSSG. The probe is comprised of hydroxy coumarin (Ex: 320 nm, Em: 460 nm) as donor and fluorescein (Ex: 485 nm, Em: 520 nm) as acceptor.

## 3.1 RESULTS AND DISCUSSION

### 3.11 Reduction of OH-Coum-Cys-FITC (DSSA) by reduced glutathione (GSH)

GSH in its physiologically relevant concentration range of 2 mM to 16 mM was exposed to a very low DSSA concentration (5 μM). The reactions were monitored by following spectral changes for both the donor coumarin and acceptor fluorescein peaks and the results are shown in Fig 19. An enhanced initial fluorescein emission is observed due to non- radiative transfer of energy from the donor (coumarin) to the acceptor fluorescein. This occurs whenever two molecules (acceptor and donor) whose absorption (acceptor) and emission (donor) spectra overlap are placed in close proximity. The

efficiency of this energy transfer depends on the distance between donor and acceptor, the degree of spectral overlap of the donor and acceptor spectra, and the relative orientation of the dipoles of the donor and acceptor. This phenomena is refered to as FRET as illustrated in **Fig 5**. FRET results in quenching of emission of the donor. In OH-Coum-Cys-FITC (DSSA), the donor emission (between 390-485 nm) is quenched due to non-radiative energy transfer to the acceptor (excitation=485 nm). Reduced glutathione (GSH) can cleave the –S-S- cystamine linker resulting in loss of FRET. This –S-S- bond cleavage by GSH frees coumarin from fluorescein and thereby increases the fluorescence yield of the donor, hence the increase in coumarin emission with time seen in Fig. 18. As expected. Coumarin emission was also observed to increase with increasing GSH concentration (**Fig 19**). The increase in fluorescein emission (450 nm) is probably due to the presense of a fluorescein absorption band around 330 nm, overlaps with the excitation band of the donor (325 nm). These competing factors can result in an increase in emission from both donor and acceptor, as observed in **Fig 19**. However, this is not a problem, since ratios of the coumarin/fluorescein emission peaks are used in data analysis.

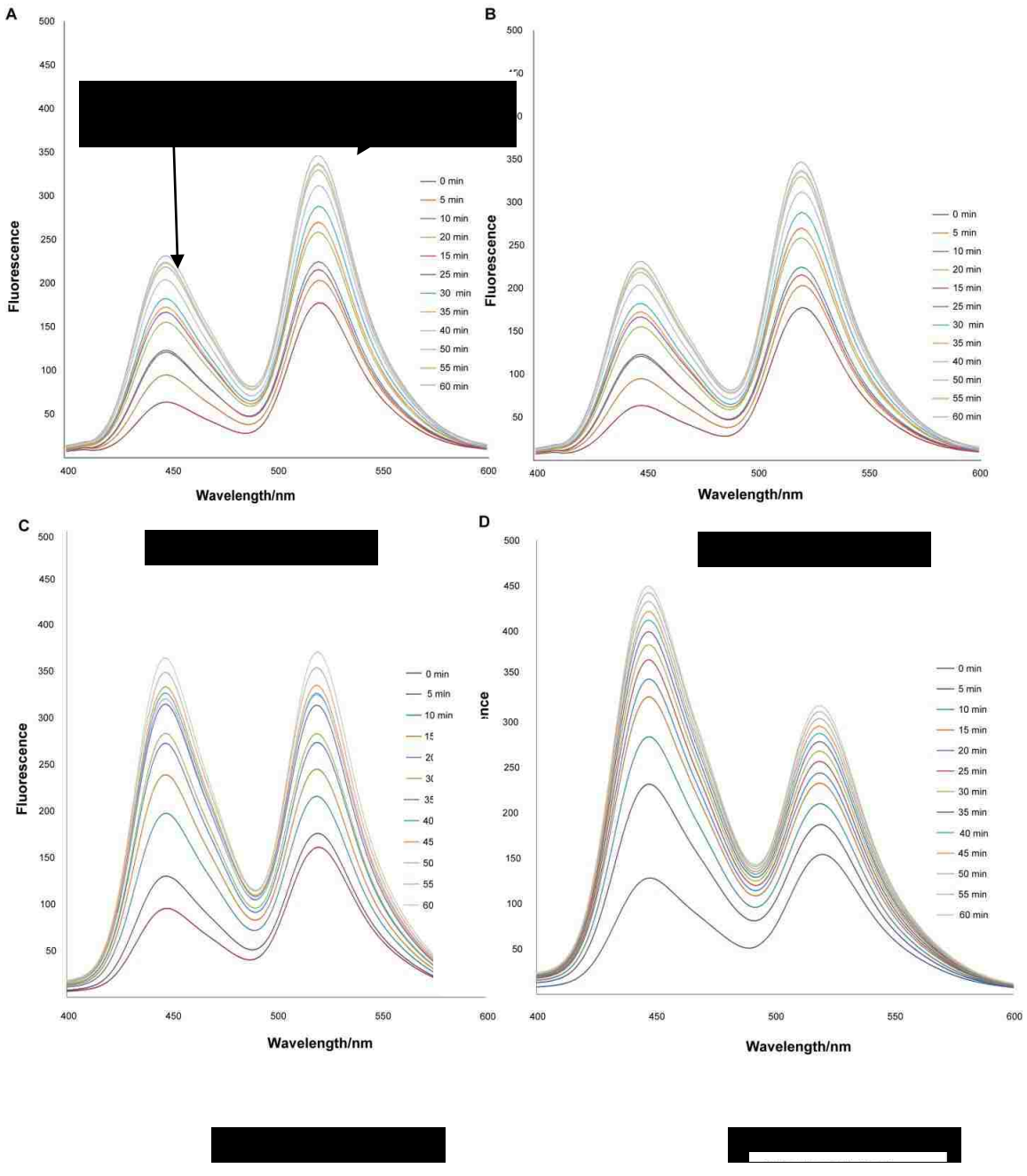
A
B
C
D
Fluorescence
Wavelength/nm
0 min
5 min
10 min
15 min
20 min
25 min
30 min
35 min
40 min
45 min
50 min
55 min
60 min

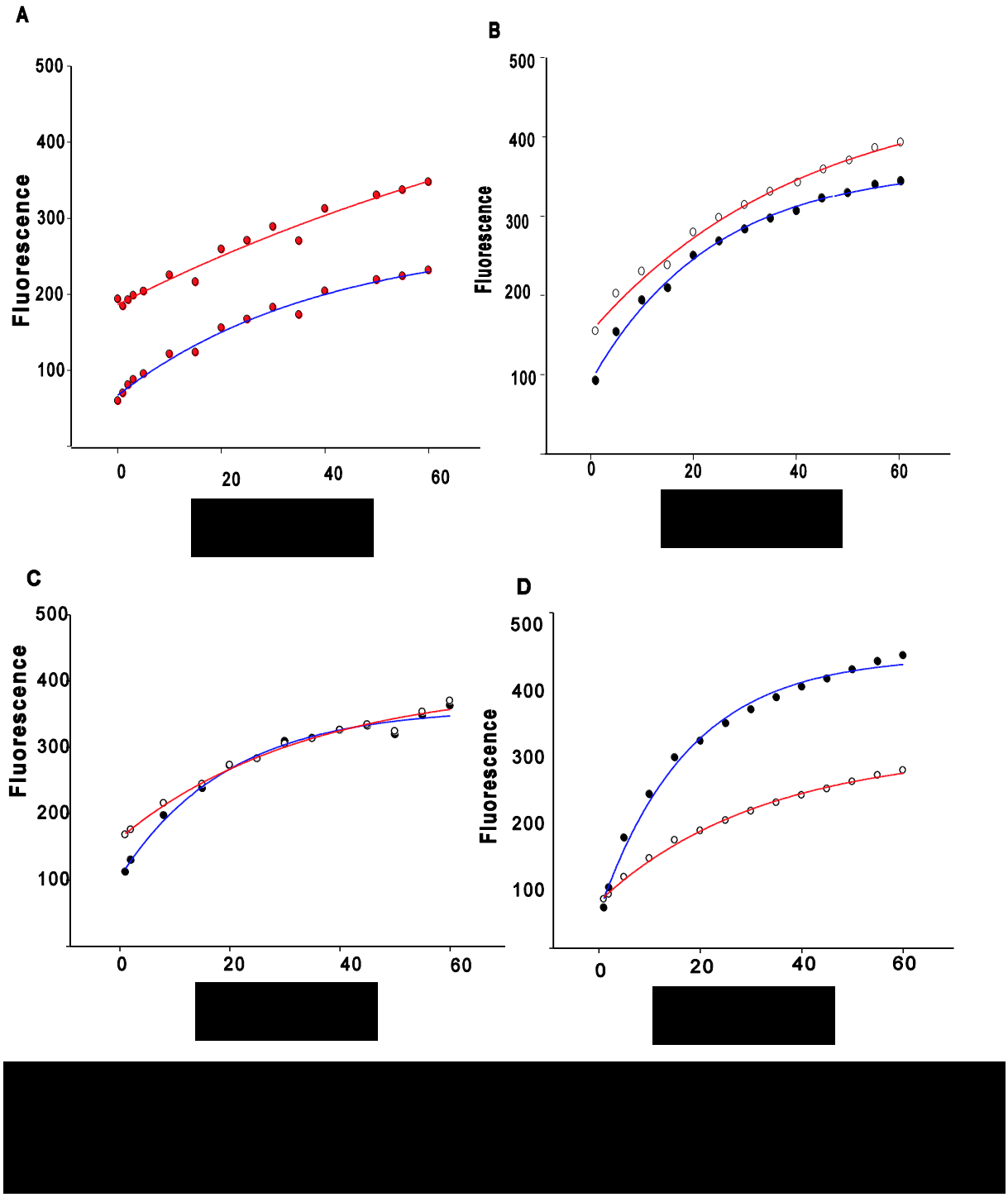
A
B
C
D
Fluorescence
500
400
300
200
100
0
20
40
60

| | A/B | $F_0$ | | a | | k | |
|---|---|---|---|---|---|---|---|
| | | **FITC** | **COUM** | **FITC** | **Coum** | **FITC** | **Coum** |
| **2 mM** | 0.48 | 186 | 67.3 | 398 | 207 | 0.0087 | 0.0254 |
| **8 mM** | 0.78 | 161 | 76.1 | 313 | 277.01 | 0.0223 | 0.0484 |
| **12 mM** | 0.90 | 174 | 85.5 | 244 | 266 | 0.0238 | 0.0596 |
| **16 mM** | 1.30 | 168 | 107 | 194 | 328 | 0.0224 | 0.0733 |

[redacted]

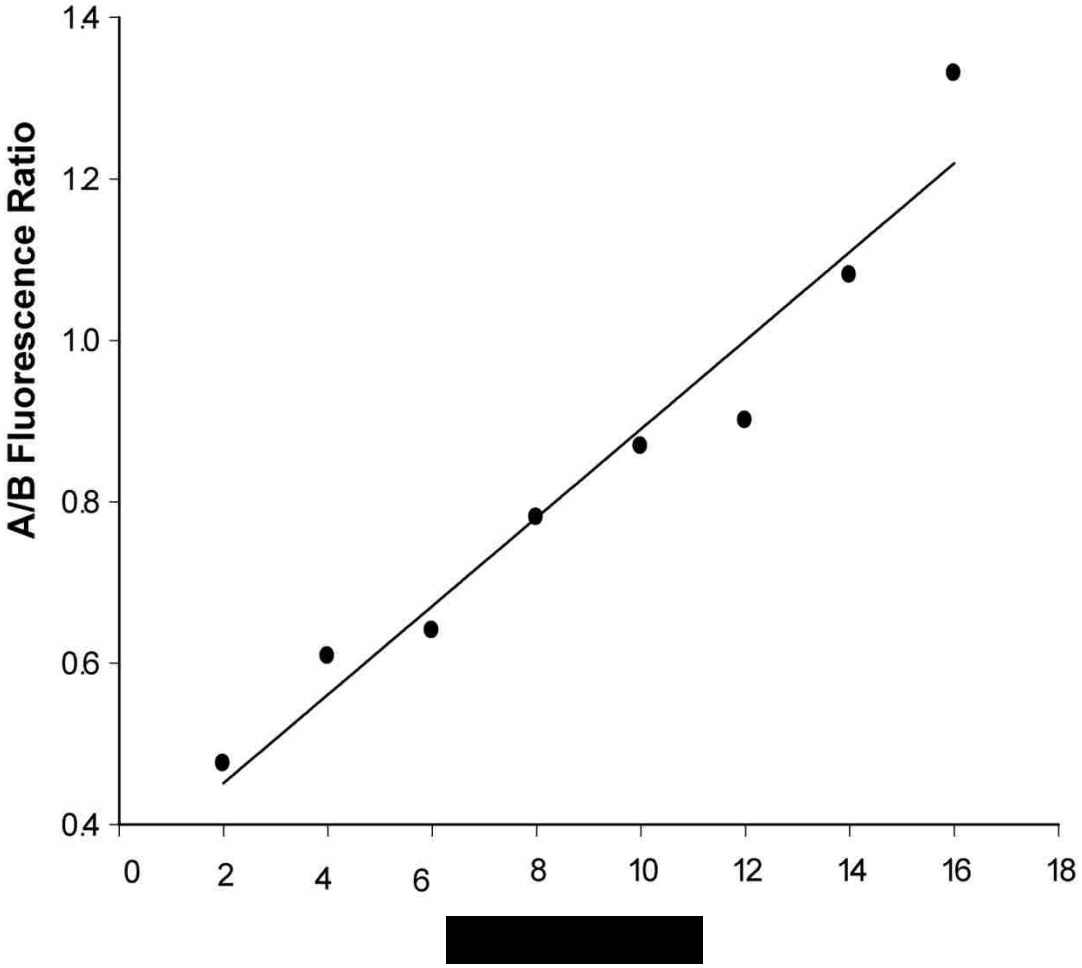
A/B Fluorescence Ratio
1.4
1.2
1.0
0.8
0.6
0.4
0
2
4
6
8
10
12
14
16
18

For ratiometric analysis, the kinetic data from **Fig 20** were analyzed by monitoring fluorescence bands for OH-coumarin and FITC versus reaction time (Fig. 19,20) and data fitted to an exponential equation:

$$\mathbf{F = F_0 + a( 1- e^{-kt})} \qquad (5)$$

where $a = F_{max}-F_0$, the fluorescence change due to reaction, and k is the rate constant for thiol reduction. Fitted constants for the plots in **Fig 20** and other GSH concentrations sumerized in **Fig 21**, with the final fluorescence after reaction goes to completion being given by $F_{max} = a + F_{0.}$ The ratios of maximum fluorescence ($F_{max}$), for OH-coum (A) to FITC (B), were determined at different glutathione concentrations and then plotted against their corresponding concentrations (**Fig 22**). The results show that the ratio of donor/acceptor emissions increases with both time (as is clear in **Figs 19** A-D) and concentration of GSH (as seen in **Figs 21** and **8**). These results are as expected and can be used in a ratiometric assay to determine concentrations of thiols such as GSH.

### 3.2 Reaction of DSSA with GSSG

**D**SSA (OH-coum-Cys-FITC) was reacted with oxidized glutathione (GSSG). Results from **Fig 23** suggest that there is no reaction between the two at different concentration of GSSG (2 mM to 16 mM, over a period of 60 minutes. The disappearance of the fluorescein absorption peak around 490 nm in **Fig. 24 c**, suggests that there might be some modification of the fluorescein ring to one of its several non-fluorescent forms.

Absorption spectra of a reaction of a mixture of GSSG/GSH (**Fig.24**d) show that fluorescein absorption band diminishes with increasing [GSSG] in a GSSG/GSH mixture.

[redacted]

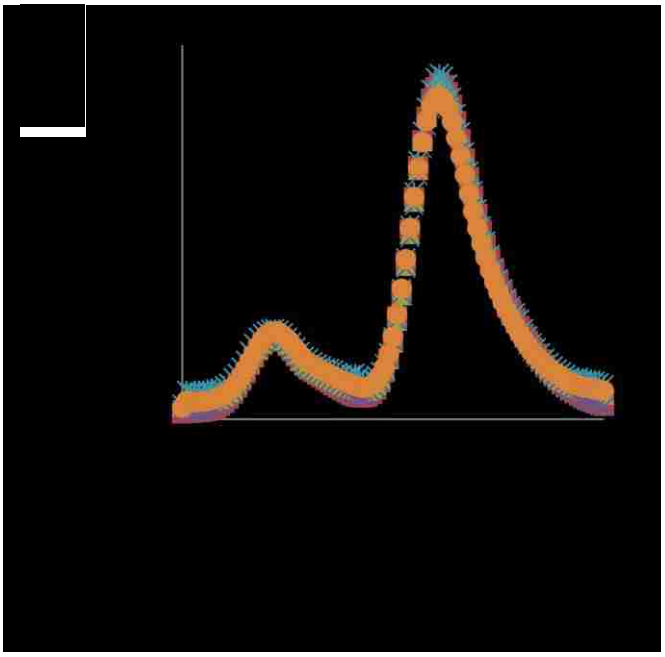

[redacted]

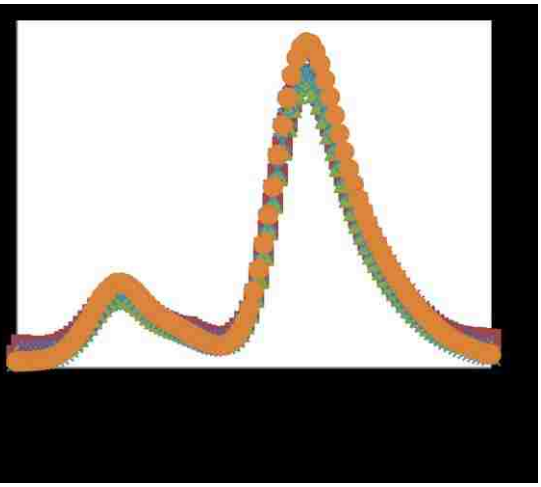

[redacted]

[redacted]

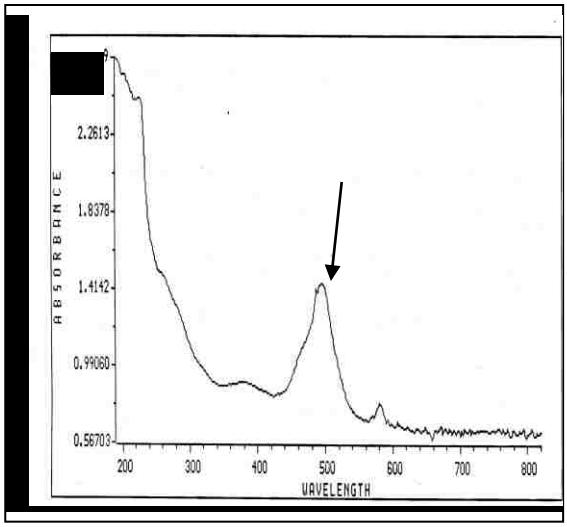
ABSORBANCE
2.2613
1.8378
1.4142
0.99060
0.56703
200
300
400
500
600
700
800
WAVELENGTH

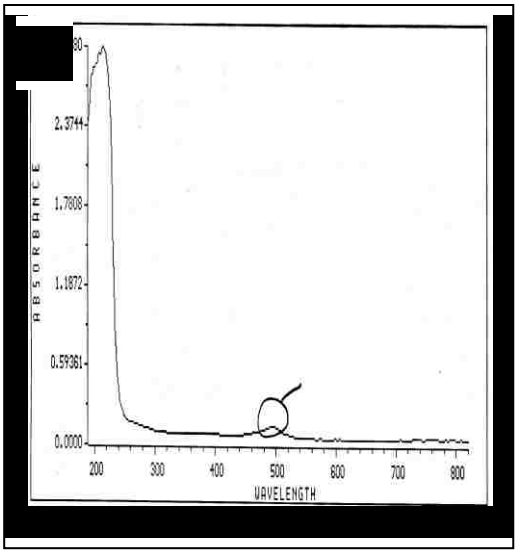
ABSORBANCE
2.3744
1.7808
1.1872
0.59361
0.0000
200
300
400
500
600
700
800
WAVELENGTH

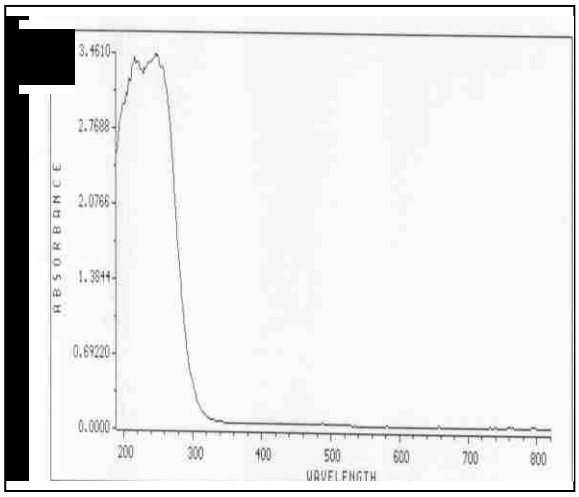
ABSORBANCE
3.4610
2.7688
2.0766
1.3844
0.69220
0.0000
200
300
400
500
600
700
800
WAVELENGTH

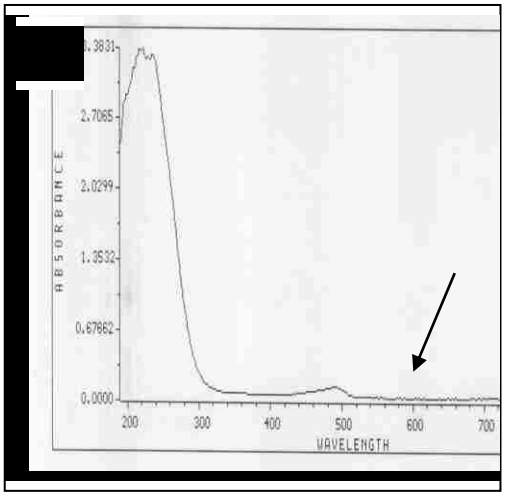
ABSORBANCE
2.7065
2.0299
1.3532
0.67662
0.0000
200
300
400
500
600
700
WAVELENGTH

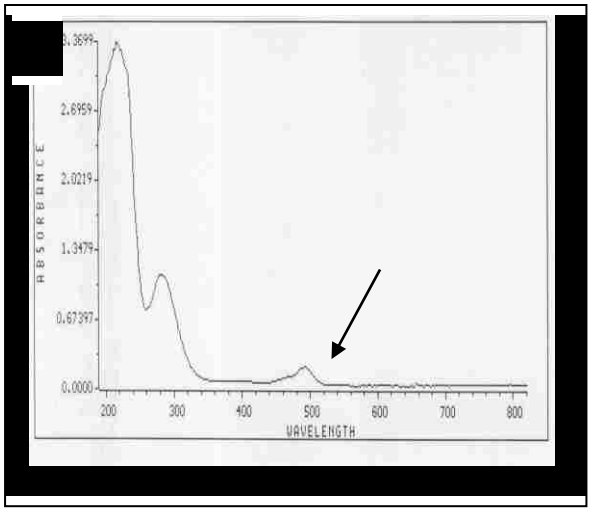
ABSORBANCE
2.6959
2.0219
1.3479
0.67397
0.0000
200
300
400
500
600
700
800
WAVELENGTH

[redacted]

## 3.9 **Control reaction of GS-Me with DSSA**

To demonstrate that it is the thiol of GSH that reacts with the disulfide in DSSA fluorescein, reaction of the thiol-blocked analog of GSH was studied. The reaction was carried out as described in **Fig.19**. GS-Methyl was used in place of GSH:

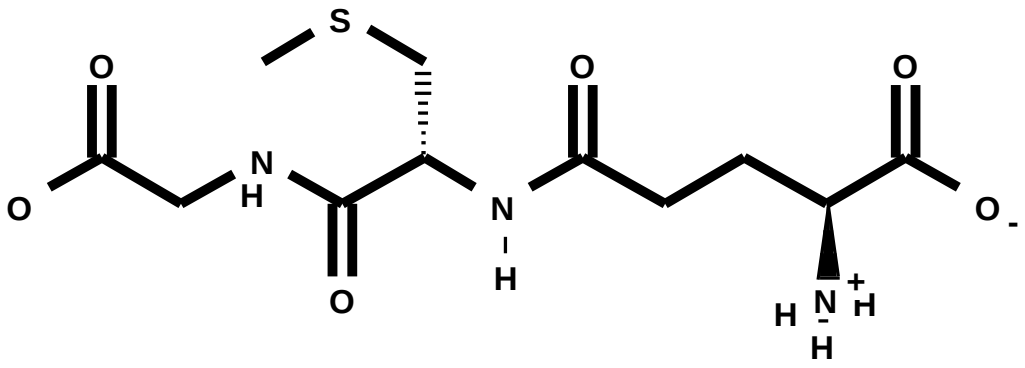


If spectral changes were due to reactions at some other functional groups in GSH, spectral changes analogous to results as in **Fig. 19** would be observed even with the blocked thiol. Results in **Fig.24** clearly show no significant change in peak intensities with time. Therefore, it can be concluded that spectral changes observed in Fig.19 were due to reaction with the thiol of GSH.

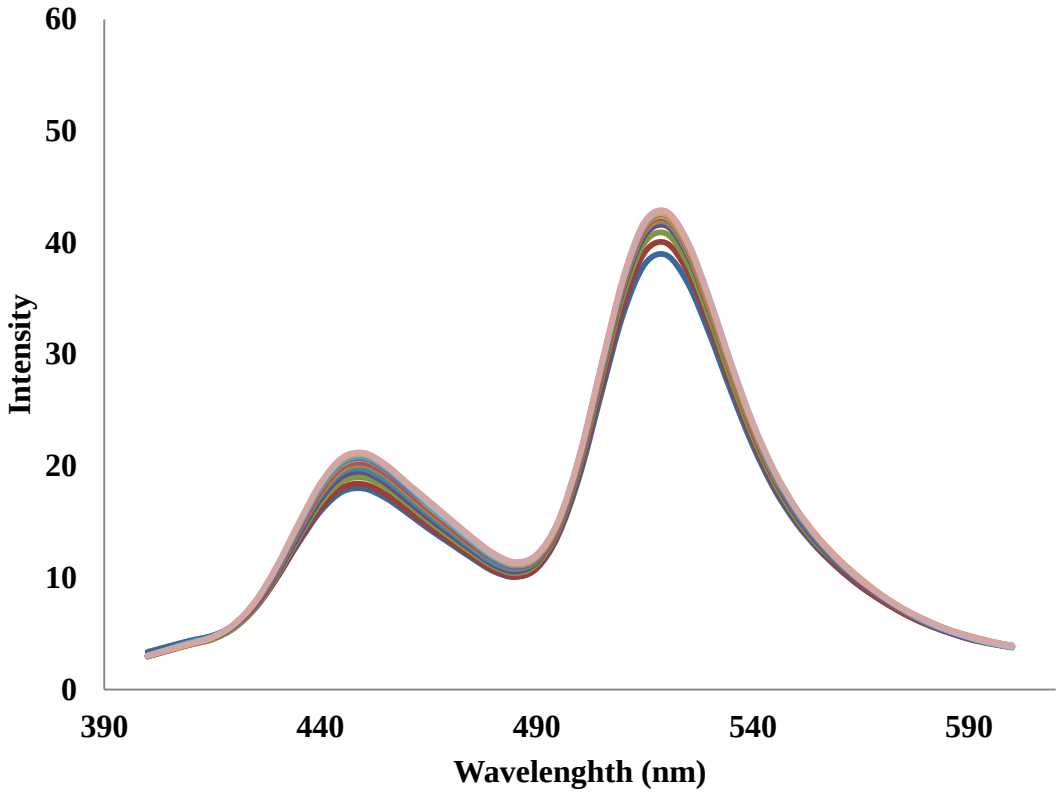
60
50
40
30
20
10
0
Intensity
390
440
490
540
590
Wavelenghth (nm)

## 3.10 **Control studies of fluorescein and coumarin**

As another control, experiments on the effects of GSH on the fragments that comprise OH-Coum-Cys-FITC (DSSA) probe were carried out. The results in **Fig.26** (fluoresceinamine) and **Fig. 27** (coumarin carboxylic acid) show that there are no spectral changes in these reactions, proving that DSSA fragments do not react directly with the fluors. Absorbance studies for coumarin (**Fig 28**) and fluorescein show no changes, indicating no reaction. (**Fig 29**) with various thiols also show no changes , indicating there is no reaction with GSH. Accordingly, previous spectral change observed when DSSA probe was exposed to either reduced (GSH) or oxidized (GSSG) glutathione must have involved reaction with the DSSA disulfide.

,

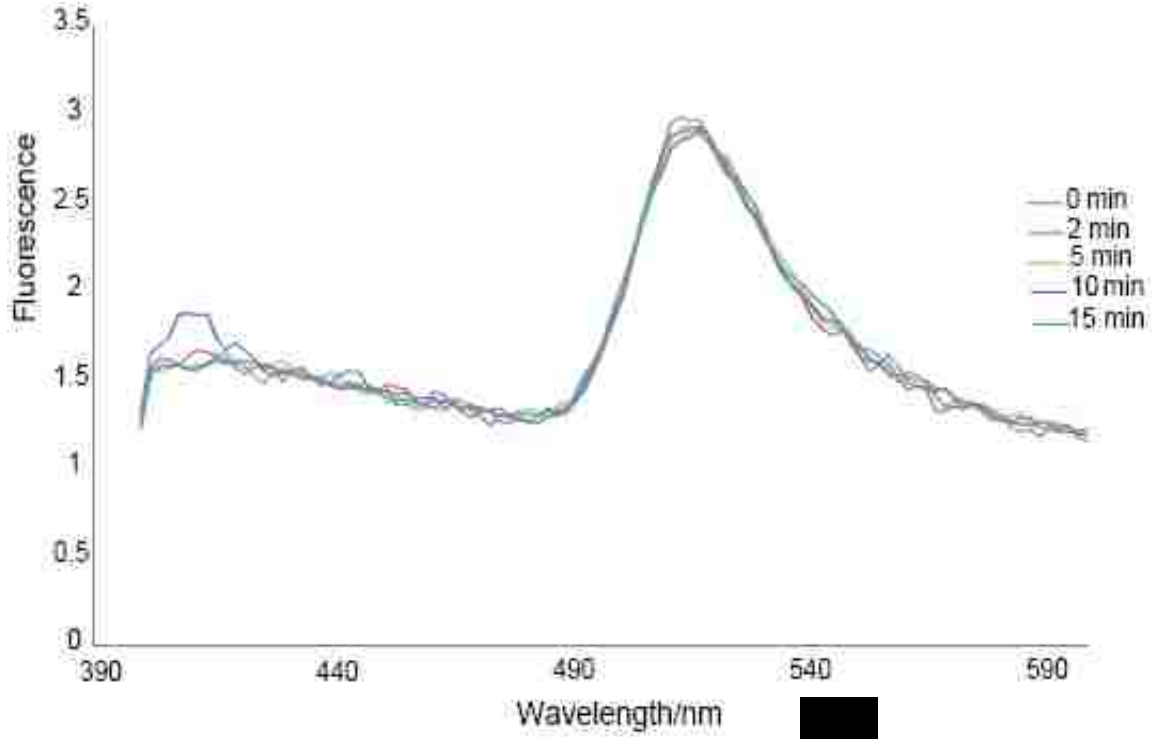
Fluorescence
3.5
3
2.5
2
1.5
1
0.5
0
390
440
490
540
590
Wavelength/nm
0 min
2 min
5 min
10 min
15 min

[redacted]

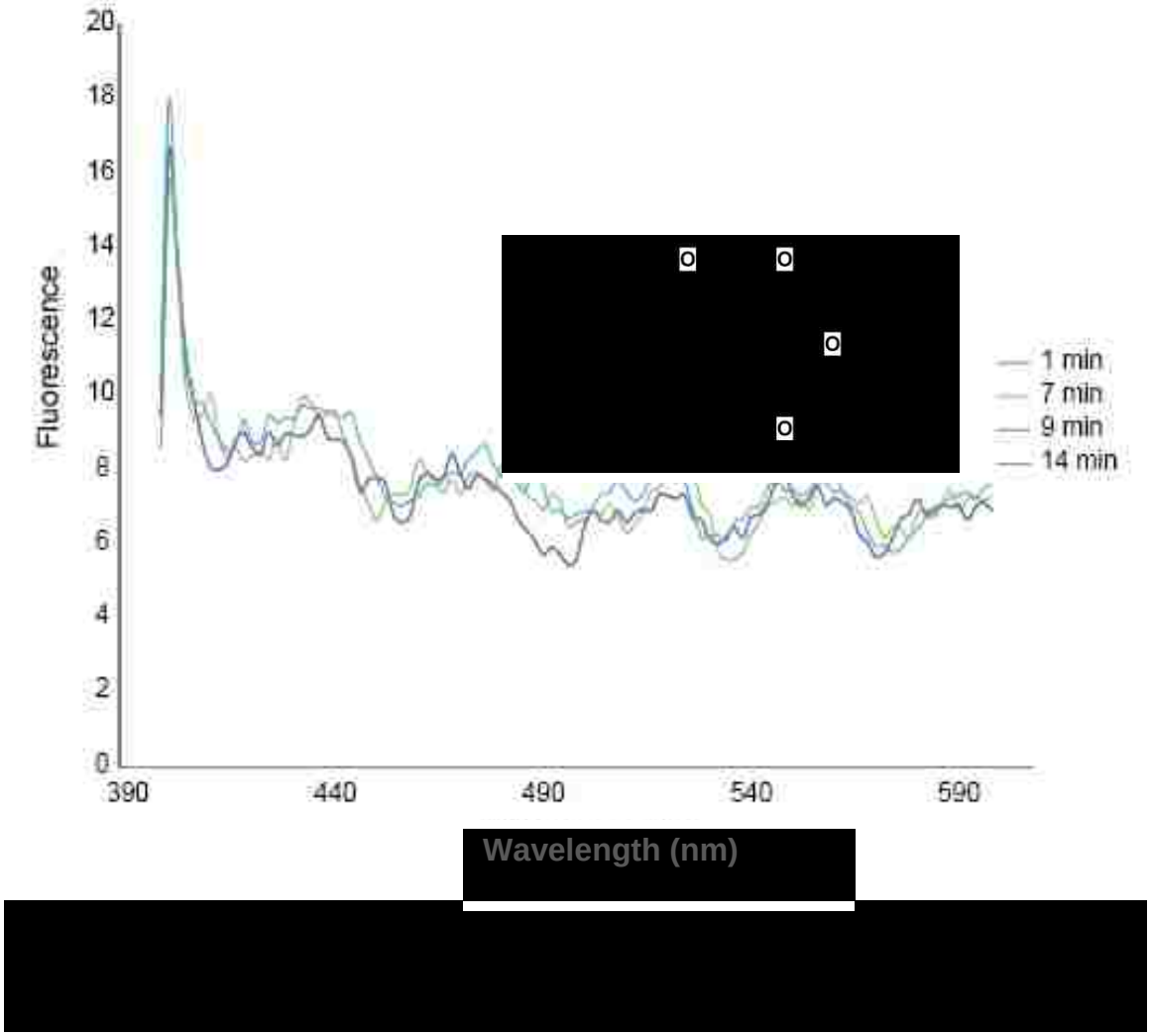
Fluorescence
20
18
16
14
12
10
8
6
4
2
0
390
440
490
540
590
Wavelength (nm)
1 min
7 min
9 min
14 min

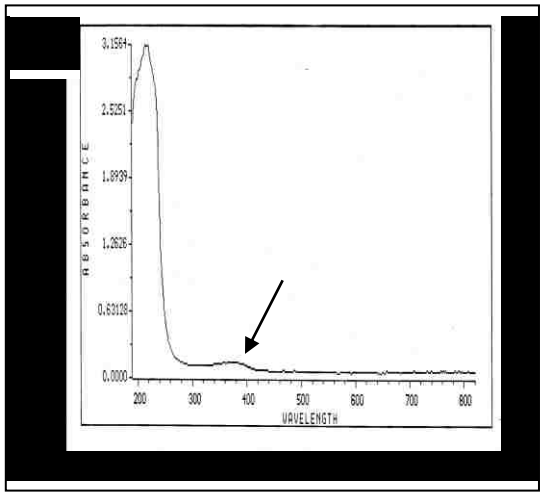
ABSORBANCE
3.1564
2.5251
1.8939
1.2626
0.63128
0.0000
200
300
400
500
600
700
800
WAVELENGTH

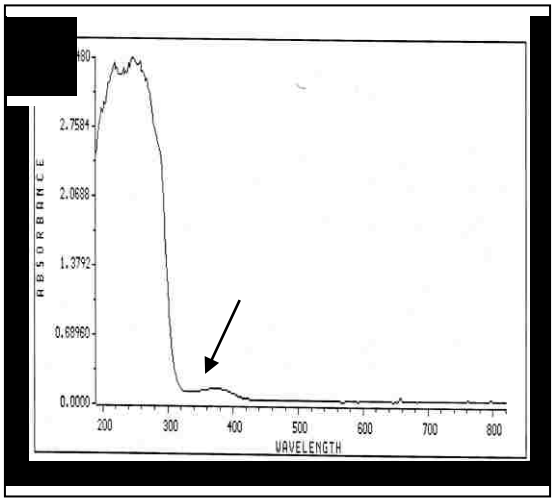
ABSORBANCE
2.7584
2.0688
1.3792
0.68960
0.0000
200
300
400
500
600
700
800
WAVELENGTH

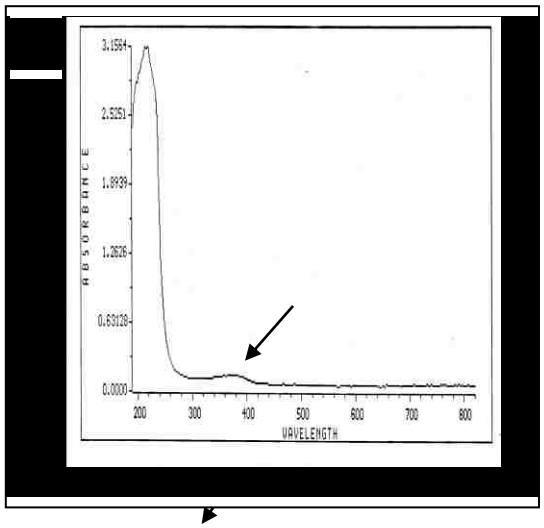
ABSORBANCE
3.1564
2.5251
1.8939
1.2626
0.63128
0.0000
200
300
400
500
600
700
800
WAVELENGTH

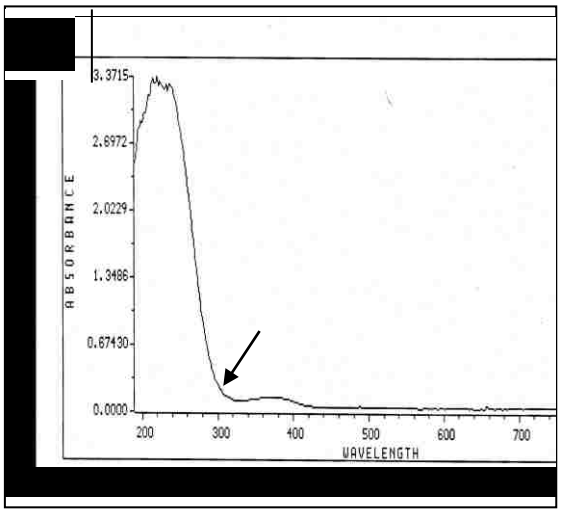
ABSORBANCE
3.3715
2.6972
2.0229
1.3486
0.67430
0.0000
200
300
400
500
600
700
WAVELENGTH

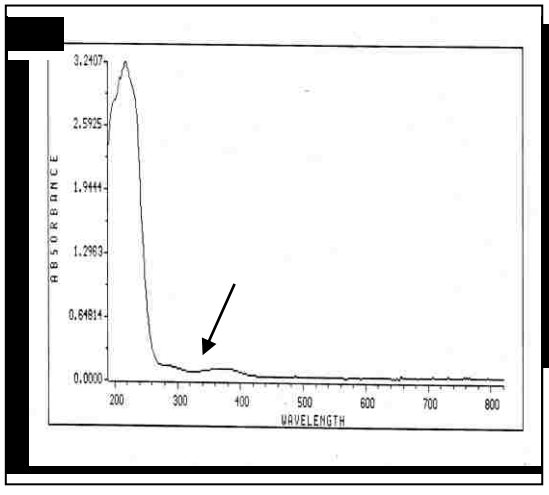
ABSORBANCE
3.2407
2.5925
1.9444
1.2963
0.64814
0.0000
200
300
400
500
600
700
800
WAVELENGTH

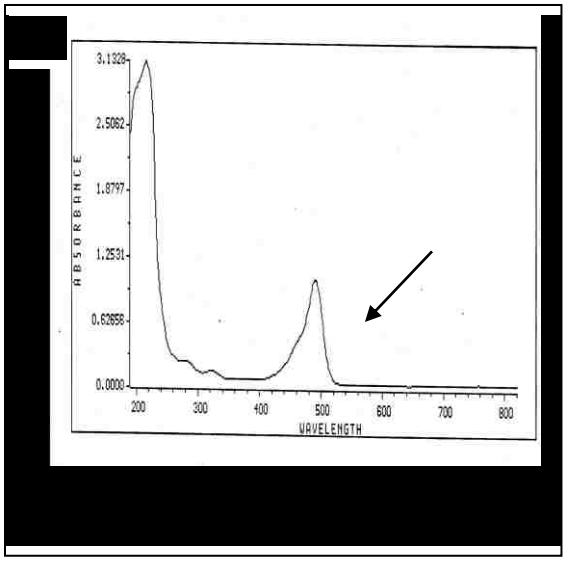
3.1328
2.5062
1.8797
1.2531
0.62658
0.0000
ABSORBANCE
200
300
400
500
600
700
800
WAVELENGTH

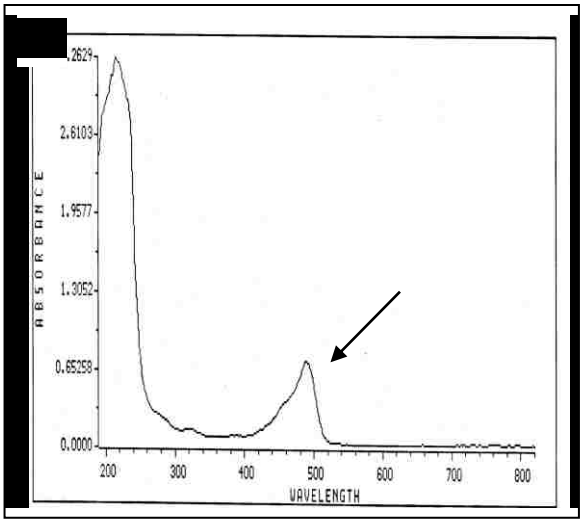
2629
2.6103
1.9577
1.3052
0.65258
0.0000
ABSORBANCE
200
300
400
500
600
700
800
WAVELENGTH

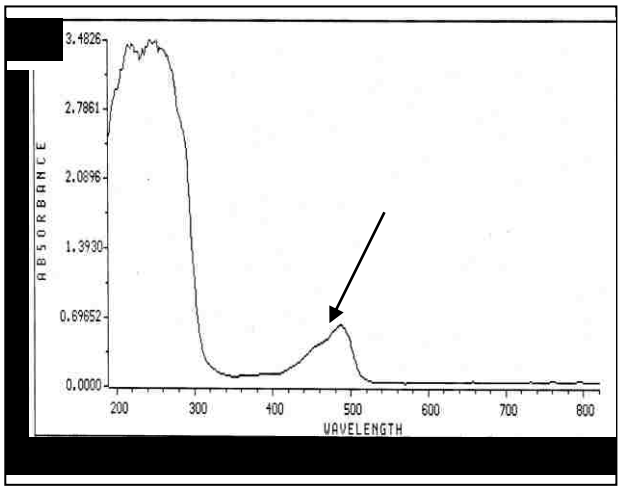
3.4826
2.7861
2.0896
1.3930
0.69652
0.0000
ABSORBANCE
200
300
400
500
600
700
800
WAVELENGTH

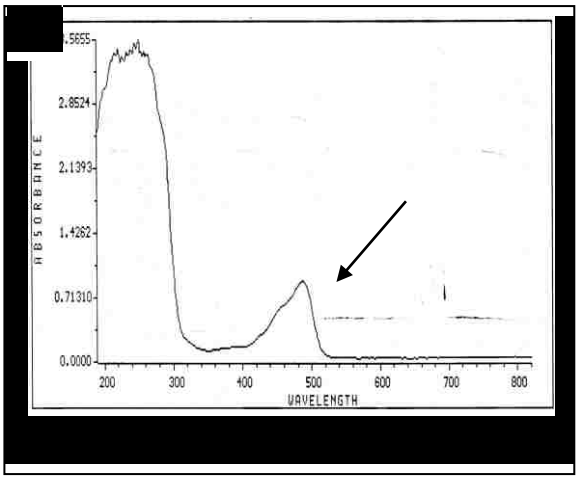
2.8524
2.1393
1.4262
0.71310
0.0000
ABSORBANCE
200
300
400
500
600
700
800
WAVELENGTH

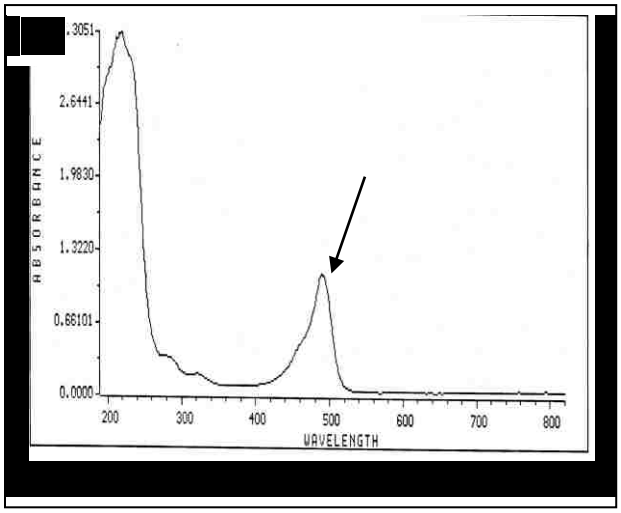
2.6441
1.9830
1.3220
0.66101
0.0000
ABSORBANCE
200
300
400
500
600
700
800
WAVELENGTH

[redacted]

**Preliminary in *vivo studies***

For our DSSA probe to be useful in determination of cellular thiol levels, it should be able to penetrate cells. **Fig 30** shows cell confocal fluorescence microscopy permeability studies done on bovine pulmonary artery endothelial cells (BPAEC). Results show that our DSSA probe can pass through the cell membrane. Interesting results were also obtained in fluorescent probe labeling of bovine lung cell proteins, with thiol-containing proteins characterized by fluorescence imaging of cell lysates separated using SDS PAGE gels (**Fig. 31**). Preliminary in cell studies of thiol redox state using OH-Coum-Cys-FITC were also performed on Origami *E. coli* cells and wild BL21DE3 *E. coli* cells[1]. **Fig.32** shows that much less fluorescence signal is observed in Origami cells as compared to wild type. This is because origami cells lack thioredoxin reductase and glutathione reductase and therefore maintain cellular thiols in a reduced state. Presence of more thiols in the disulfide (oxidized) form inside Origami cells caused the observed reduction in fluorescence. Similar Origami *E.coli* uptake studies were reported previously with a related probe, and have shown analogous results[1]. These preliminary results show that this DSSA probe can be used to monitor levels of reduced thiols in bacteria[1].

Our lab has also reported *in vivo* detection of thiol levels with DSSA probes in the zebra fish embryo[1]. Significant accumulation of the probe in the chorion was observed in those studies suggesting the presence of thiol-rich proteins, which have been reported to have a protective role in the developing embryo [46].

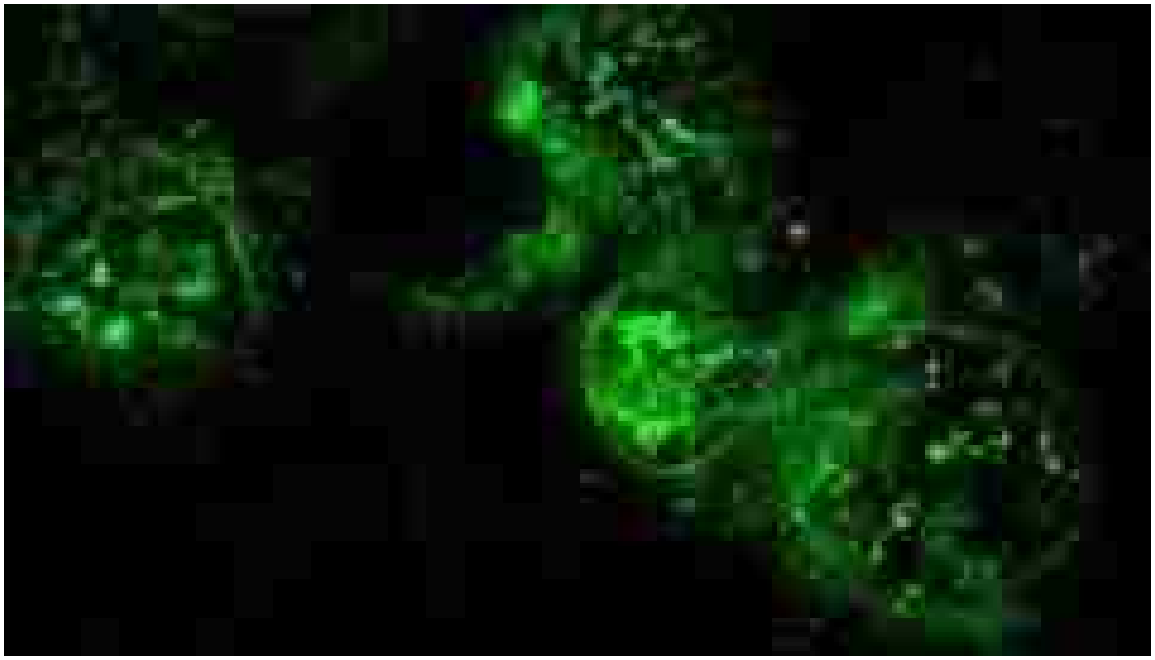

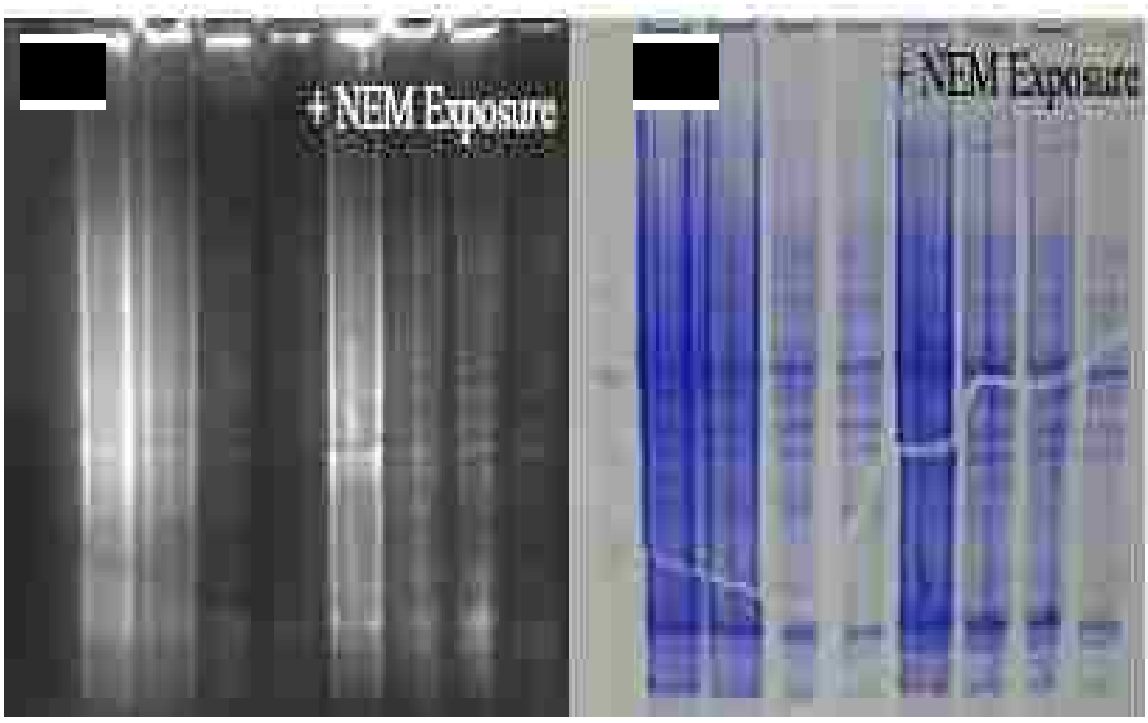


[redacted]

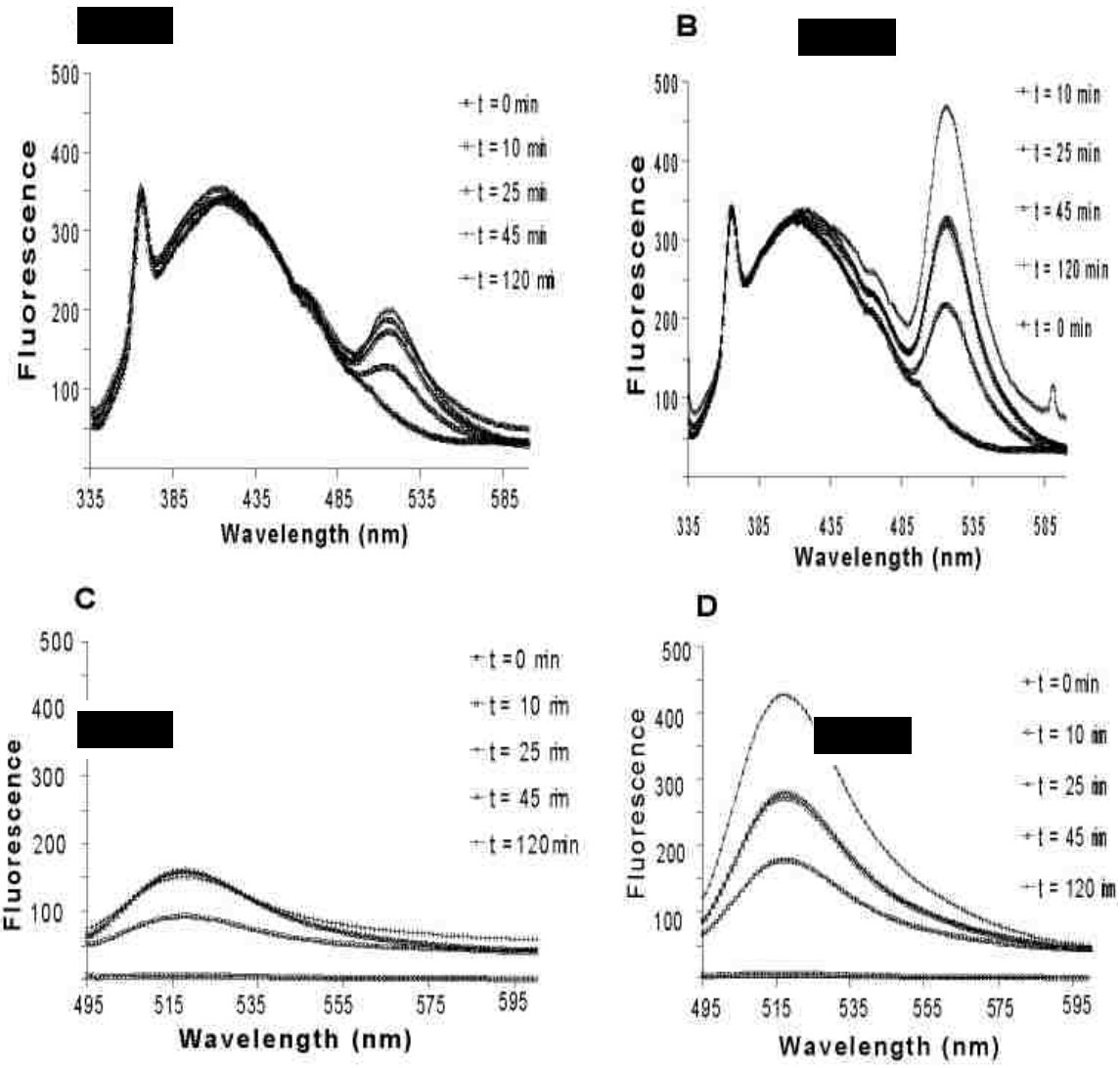
B
C
D
Fluorescence
Wavelength (nm)
t = 0 min
t = 10 min
t = 25 min
t = 45 min
t = 120 min
335
385
435
485
535
585
495
515
535
555
575
595
100
200
300
400
500

[redacted]

Oxidized and reduced glutathione were obtained from CALBIOCHEM. 7-hydroxycoumarin-3-carboxylic acid was obtained from INDOFINE. All other biochemical reagents were obtained from Sigma and all synthetic reagents were obtained from Aldrich.

**Synthesis of the DSSA probe**

The DSSA probe with an aliphatic cystamine linker (Fig 18, 33) was prepared in two steps. The first step involved synthesis of OH-coumarin cystamine (OH-Coum-cys), followed by reaction with fluorescein 5-isothiocyanate (FITC). OH-coumarin cystamine was prepared by dissolving 500 g of 7-OH-coumarin-3-carboxylic acid in a 4:1 acetonitrile/chloroform mixture. 1.5 equivalents of Cystamine dihydrochloride was slowly added. Cystamine dihydrochloride was added in excess to make sure the reaction went to completion and to minimize dimerization of coumarin to a dicoumaric product. Excess triethylamine (0.4 ml) was added, and the reaction was initiated by addition of 750 mg of BOP (benzotriazol-1(yloxy)tris(dimethylamino) phosphonium hexaxafluorophosphate) and the mixture was stirred for 2.5 hrs at room temperature. The precipitate that formed was then filtered off. TLC (9:1 $CHCl_3$:$CH_3OH$) was used to check for the product in both the supernatant and the precipitate. The precipitate was dried, turned into powder and washed with deionized water to remove the partially soluble unreacted cystamine dihydrochloride and left to dry in air. In the second step, coumarin cystamine was dissolved in a 1:1:1 mixture of acetone/MeOH/$CH_2Cl_2$, and was then reacted with FITC in the presence of triethylamine to form the product.

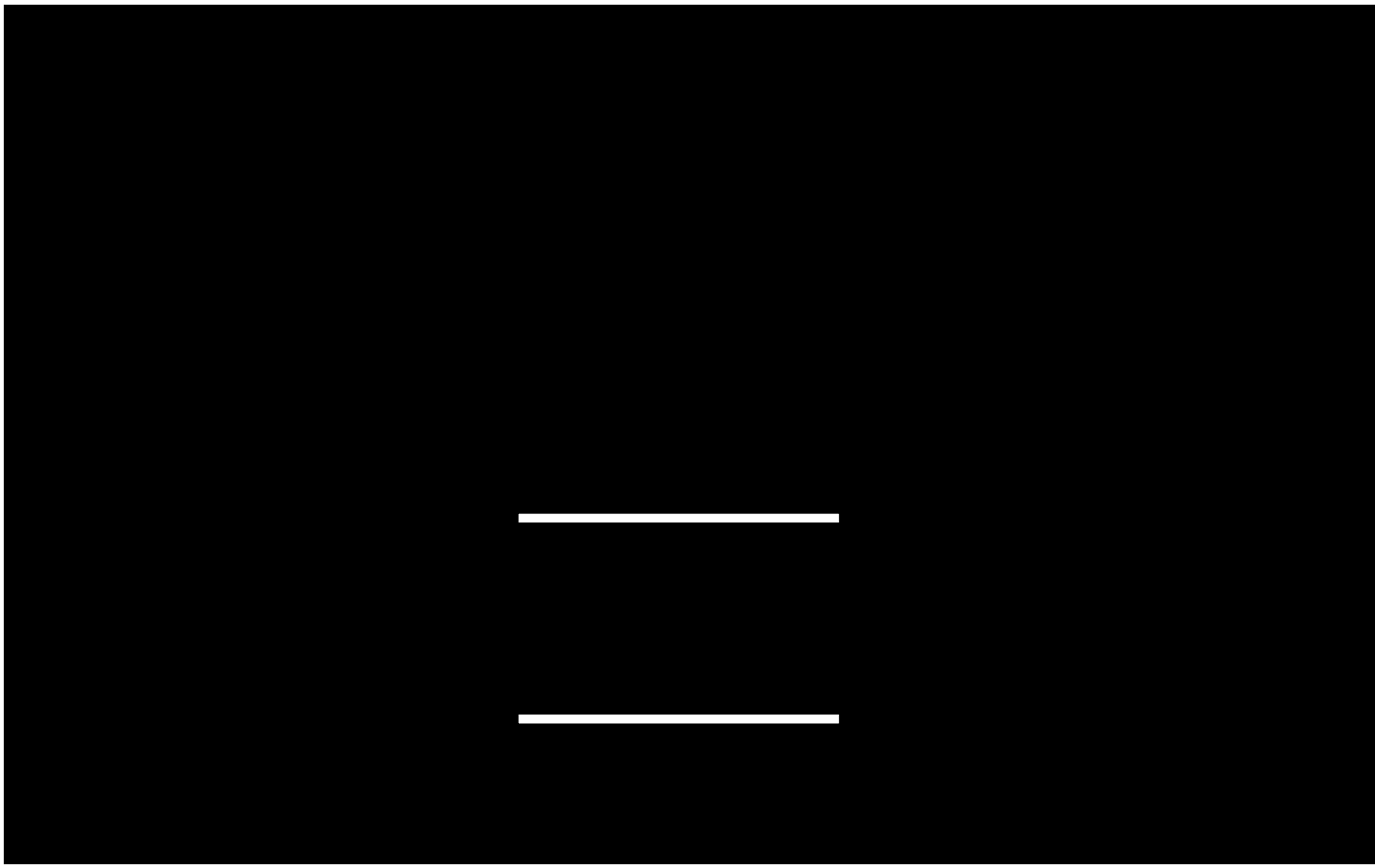

**Fig 33**: Synthesis of OH-Coum-Cys-FITC.

### *In vitro* fluorescence studies of thiol reactivity

The buffer used in this study was 100 mM HEPES, pH 7. Fluorescence studies were performed on a Jasco FP-6500 spectrofluorotometer. Reactivity with different thiols was quantified by measuring changes in fluorescence at 440 and 520 nm over time in a 3 ml cuvette using 5 μM DSSA probe (325 nm excitation). [1]

### Reduction of DSSA by reduced Glutathione (GSH)

OH-Coum-Cys-FITC is soluble in DMSO and partially soluble in water, so a stock solution was prepared by adding just enough DMSO to dissolve it, then deionized water (DI). A stock solution of 200 mM reduced GSH was prepared by dissolving GSH in DI water. The total volume in the cuvette was 3500 μL. Coumarin was excited at 325 nm and the emission was observed between 400 and 600 nm. The spectrum was blanked with air and sensitivity was turned to low, using 2 nm pitch and a band width of 5 nm for emission and 5 nm for excitation. Scanning speed was 1000 nm/min with a response time of 1 sec. For ratiometric analysis, and kinetic studies data at peak heights of OH-Coumarin and FITC were plotted versus reaction and data fitted to an exponential equation (eq. 5). The ratios of maximum fluorescence ($F_{max}$), for OH-coum and FITC emission bands, were determined at different glutathione concentrations.

**GSSG experiments**

All GSSG experiments were carried out as described for GSH experiments above. For GSSG/GSH experiments( see appendix), the total concentration was maintained at 16 mM.

**Absorbance studies**

All absorbance studies were were carried out under conditions described above. Wave length range was 190 nm to 820 nm. The instrument used was an HP 8452 diode array spectrophotometer.

***In vivo* E. coli studies**

In cell studies of thiol redox state using OH-Coum-Cys-FITC in *E. coli* bacteria were carried out under the following four conditions: BL21DE3 Origami *E. coli* cells treated with 10 μM OH-COUM-CYS-FITC-excited at 320 nm, BL21DE3 *E. coli* cells treated with 10 μM OH-COUM-CYS-FITC-excited at 320 nm, BL21DE3 Origami *E. coli* cells treated with 10 μM OH-COUM-CYS-FITC-excited at 485 nm and BL21DE3 *E. coli* cells treated with 10 μM OH-COUM-CYS-FITC-excited at 485 nm. Note that Origami *E.coli* cells are deficient in thioredoxin reductase and glutathione reductase and give less fluorescence compared to wild type BL21DE3 E.coli cells, due to the presence of more thiols in the disulfide (versus reduced) form inside Origami cells. Cells were grown to an absorbance at 600 nm of 0.6-0.7, then centrifuged and resuspended in a 100 mM Tris buffer of pH 8.2 with probe, and incubated for 60 minutes. Cells were washed 3 times with buffer then fluorescence read.

***In vivo* bovine lung pulmonary arterial endothelial cell studies**

Fluorescent probe labeling of bovine lung cell proteins was done using 50 µM coumarin-cys-FITC (DSSA). Labeling was done +/- 15 min. pre-exposure to 20 mM NEM (N-ethyl maleimide) to block surface exposed thiols first, in the native cell. Cells were then lysed by boiling in a non-reducing SDS loading buffer, centrifuged, and supernatants loaded and the gel run. Gels were fluorescently imaged (**Fig 31**) . Imaging was done using a Kodac easy share Z 730 camera. Cell permeability and proteomic studies of fluorescent dithio probes with bovine pulmonary artery endothelial cells (BPAEC) were performed by treating with 100 nM of OH-COUM-CYS-FITC (**Fig 30**). Fluorescence microscopy was performed using a Nicon A1 confocal microscope.

## 3.12 CONCLUSION

The evidence above gives rise to the conclusion that initial reaction between OH-Coum-FITC and thiols occurs at no other position than the cystamine –s-s- disulfide of the dye. As such, the DSSA probes react largely as expected. The studies presented herein give insight into how DSSA probes can be utilized for quantation of thiols. Reduced thiols (GSH) react with the DSSA probe (**Fig. 19**) as expected, and it appears that oxidized thiols (GSSG) do not react (**Fig. 23**), via disulfide exchange.

The reaction of DS-SA with a high concentration of thiols would not yield significant levels of an AS-SG intermediate, as reaction would be driven to completion in the following manner:


The OH-COUM-CYS-FITC reagent presented in this chapter is the first FRET version of a DSSA dithio probe, and has two characteristic emission bands at 448 nm and 520 nm, when excited at 325 nm. This probe could therefore be used to quantitate thiol levels using ratiometric measurements (**Fig 22**). The OH-Coum-Cys-FITC probe may even have utility for quantitation of cellular thiols, since it can cross the cell walls of *E. coli* and bovine pulmonary arterial endothelial cells(BPAEC), and is responsive to cellular thiol changes (**Figs 30** and **31**). This OH-COUM-CYS-FITC probe could serve as a prototype for the design of other DSSA probes for intracellular applications, using other donor-acceptor pairs (ex, red shifted). More work still needs to be done on the characterizing the mechanism of thiol exchange between the DSSA dye and thiols or disulfides, but the probe is responsive to total thiol level (**Fig 22**)and reacts at different rates (**Fig 20**)and in characteristic ways with GSH (**Fig 19**) and GSSG (**Fig 23**). Analogous successful FRET- based methods for thiol studies have also been reported elsewhere[44,45,49], but none have been reported that utilize small molecule probes that can penetrate cell walls-and rely on biological relevant disulfide chemistry, such as the probe reported herein.

## REFERENCES


**1.** Pullela,P.K., Chiku, T., Carvan, M. J.,3rd, & Sem, D.S. Fluorescence-based detection of thiols *in vitro* and *in vivo* using dithiol probes. *Anal. Biochem.* 352, 265-273 (2006).

**2.** Kondo,T. Yoshida,K. Urata,Y. S .Goto, S .Gasa and N .Taniguchi gamma-Glutamylcysteine synthetase and active transport of glutathione S- conjugate are responsive to heat shock in K562 erythroid cells *J. Biol. Chem*., 268, 20366-20372 (1993).

**3.** L. Canesi, A. Viarengo, C. Leonzio, M. Filippelli, G. Gallo,heavy metals and glutathione metabolism in mussel tissues *AquaticToxicology*. 46, 67-76 (1999).

**4.** Landar, A. Zmijewski, J.W., Dickinson, D. A. Le Goffe, C. Johnson, M.S., Milne G, L., Zanoni, G., Vidari, G., Morrow, J. D., & Darley-Usmar, V.M. Interaction of electrophilic lipid oxidation products with mitochondria in endothelial cells and formation of reactive oxygen species. *Am J Physiol Heart Circ Physiol.* 290, H1777-H1787 (2006).

**5.** Goligorsky M. S. Oxidative and nitrosative stress in acute renal ischemia *Am J Physiol Renal Physiol.* 281, F948-F957 (2001).

**6.** Yang, H., Huang, Z., Wang J.,&. Lu, S. C.The role of c-Myb and Sp1 in the up-regulation Noiri, E., Nakao, A., Uchida, K., Tsukahara, H., Ohno, M., Fujita, T., Brodsky, S. & of methionine adenosyltransferase 2A gene expression in human hepatocellular carcinoma *FASEB.*15,1507-1516 (2001).

**7.** Papadopulos-Eleopulos, E., Turner, V.F. & Papadimitriou, J.M. Oxidative Stress,HIV and AIDS, *Res. Immunol.*143,145-148 (1992).

**8.** Alexandrova, M. L., and Bochev, P. G. Oxidative Stress during the Chronic Phase After Stroke. *Free Radic. Biol. Med.* 39, 297-316 (2005).

**9.** Anderson, R. N., and Smith, B. L. Deaths: Leading Causes for 2002. *Natl. Vital Stat. Rep.* 53, 1-89 (2005).

**10.** Bandyopadhyay, D., Chattopadhyay, A., Ghosh, G., and Datta, A. G. (2004) Oxidative Stress-Induced Ischemic Heart Disease: Protection by Antioxidants. *Curr. Med. Chem.* 11, 369-387

**11.** Castellani, R., Smith, M. A., Richey, P. L., & Perry, G. Glycoxidation and Oxidative Stress in Parkinson Disease and Diffuse Lewy Body Disease. *Brain Res.* 737, 195-200 (1996).

**12.** Sereno, M., Garcia-Cabezas, M. A., Vara, J. A., Dominguez-Caceres, A., Perona, R., & Gonzalez-Baron, M. Implications of Oxidative Stress and Cell Membrane Li Cejas, P., Casado, E., Belda-Iniesta, C., De Castro, J., Espinosa, E., Redondo, A., pid Peroxidation in Human Cancer (Spain). *Cancer Causes Control.* 15, 707-719 (2004).

**13.** Perry, G., Cash, A. D., & Smith, M. A. (2002) Alzheimer Disease and Oxidative Stress. *J. Biomed. Biotechnol.* 2, 120-123.

**14.** Philip,E. Protein thiol oxidation in health and disease: Techniquues for measuring disulfides and related modifications in complex protein mixtures. Free rad bio & med 40, 1889-1899 (2006)

**15.** Fuchs, J., Podda M., & Packer L. R*edox-genome interactions in health and disease* Ch.1(Marcel Dekker Inc, New York,2004).

**16.** Hansen,R.E., Roth,D. & Withther,J.R. Quantifyfying the global cellular thiol-disulfide status. *PNAS* 106, 422-427 (2009).

**17.** Leonard,S.L. Reddie,K.G. & Carroll,K.S. Mining the proteomic for sulfenic acid modification reveals new targets for oxidation in cells. *ASC.Chem.bio*.4, no.9 (2009).

**18.** Michalek,R.D., Nelson,K.I., Holbrook,B.C., Yi,J.S., Strdiron,D., Daniel,L.W., Fetrow,J.S., King,S.B., Poole,L.B., & Grayson, J. M. The requirement of reversible cysteine sulfenic acid formation for T cell activation and function. *J. Immunol*. 179. 6456-6467 (2007).

**19.** Shenton,D. & Grant,C.M. Protein S-thiolation glycolysis and protein synthesis in response to oxidative stress in yeast *Saccharomyces cerevisiae* . *Biochem. J.* 374, 513-519 (2003)

**20.** Wrona,M., Patel,K.B. & Wardman,P. The roles of thiol-derived radicals in the use of 2',7'-dichlorodihydrofluorescein as a probe for oxidative stress. *Free.Rad. Biol & med*. 44, 56-62 (2008).

**21.** LeBel,C.P., Isciropouloos,H. & Bondy,S.C. Evaluation of probe 2',7'-dichlorodihydrofluorescein as an indicator of reactive oxygen species formation and oxidative stress. *Chem. Res. Toxicol*. 5, 227-231 (1992).

**22.** (a) Dickinson,B.C & Chang,C.J. Atargetable fluorescent probe for imagine hydrogen peroxide in the mitochondria of living cells. *J.AM.CHEM. SOC*. 130, 9638-9639 (2008).
(b) Leichet, L.I. & Jakob, U. Protein thiol modifications visualized in vivo. *PloS Biology* 2, 1723-737 (2004).

**23.** Tang, T., Xing, Y., Li, P., Zhang, N.,Yu, F., & Yang, G. A Rhodamine-Based Fluorescent Probe Containing a Se-N Bond for Detecting Thiols and its Application in Living Cells. *J.AM. CHEM. SOC*. 11666-11667 (2007).

**24.** Ahn, Y., Lee, J., & Chang, Y. Combinatorial Rosamine Library and Application to in Vivo glutathione Probe. *J.AM. CHEM. SOC*. 129, 4510-4511 (2007).

**25.** Shibata, A., Furakawa, K., Abe, H. Tsuneda, S., & Ito, Y. Rhodamine-based fluorogenic probe for imagine biological thiol. *Bioorg & Med Chem*. 18, 2246-2249 (2008).

**26.** Pires, M. M., and Chmielewski, J., Fluorescence Imaging of Cellular Glutathione Using a Latent Rhodamine. *Org. Lett*. 10, 837-840 (2007).

**27.** Yi, L., Li, H., Sun, Lu., Liu, L., Zhang, C., & Xi, Z*A* highly sensitive Fluorescence Probe for Fast Thiol-Quantification Assay of Glutathione Reductase. *Angew. Chem. Int. Ed*., 48, 4034-4037 (2009).

**28.** Le Moan, N., Clement, G., Le Maout, S., Tacnet, F., and Toledano, M. B. The *Saccharomyces cerevisiae* Proteome of Oxidized Protein Thiols. *J. BIio. Chem.* 281,10420–10430 (2006).

**29.** Yano, H & Kuroda, S. Introduction of the disulfide proteome: application of a techniques for the analysis of plant storage proteins as well as allergens. *J. Proteome. Res.* 7 3071-3079 (2008).

**30.** *Frand, A.R., J.W. Cuozzo, and C.A. Kaiser.* Pathways for protein disulphide bond formation. *Trends Cell Biol*. *10:203–210 (2000).*

**31.** Østergaard, H., Tachibana, C., and Winther, J. R. Monitoring disulfide bond formation in the eukaryotic cytosol *J. Cell Biol.* 166, 337–345 (2004).

**32.** Hwang, C., Sinskey,A.J. & Lodish, H.F. oxidized redox state of glutathione in the endoplasmic reticulum. Science. 257, 1496-1502 (1992).

**33.** Carmel-Harel, O., Stearman, R., Gasch, A. P., Botstein, D., Brown, P. O., and Storz, G. Role of thioredoxin reductase in the Yap1p-dependent response to oxidative stress in Saccharomyces cerevisiae. *Mol. Microbiol.39 595-605* (2001)

**34.** Kouwen, T.R.H.M & Van Dijl, J.M. interchangeable modules in bacterial thio-disulfide exchange pathways. *Trends in microbial*. 17, 6-12 (2008).

**35.** Vertommen, D. *et al.* The disulfide isomerase DsbC cooperates with the oxidase DsbA in a DsbD-indipendannt manner. *Mol.microbiol.* 67. 336-349 (2008).

**36.** Yoshimori, T., Semba, T., Takemoto, H., Akagi, S., Yamamoto, A. & Tashiro, Y. Protein disulfide-isomerase in rat exocrine pancreatic cells is exported from the endoplasmic reticulum despite possessing the retention signal. *J.Biol.Chem.* 265, 15984-15990 (1990).

**37.** Ryser,H.J.P., Levy, E.M. Mandel, R., DiSciullo, G.J. inhibition of human immunodeficiency virus infection by agents that interfere with thiol

interchange upon virus –receptor interaction. *Proc.Natl.Acad. Sci.* 91, 4559-4563 (1994).

**38.** Matthias, L.J., Yam, P.T.W., Jiang,X.M., Vandergraaff, N., Li, P., Poumbourios, P. Donoghue, N & Hogg, P.J. Disulfide exchange in domain 2 of CD4 is required for entry of HIV-1. *Nat. Immunol.* 3, 727-732 (2002).

**39.** Abou-Joude, G. & Sureau, C. entry of hepatitis delta virus requires the conserved cysteine residue of the hepatitis b virus envelop protein antigenic loop and is blocked by inhibitors of thiol-disulfide exchange. J. Virology. 81, 13057-13066 (2007)

**40.** Damont, J.N., & Brummelt, A.R. in developmental biology: a comprenhensive synthesis ( Browder,E.R.,ed, Plenum publishing corp, New York) 235-288 (1985).

**41.** a) manogaran, A. & Waring,G.L. N-terminal prodomain of sV23 is essential for the assembly of a functional vitelline membrane network in Drosophila.
b) Darie,C.C *et al.* Mass spectrometric evidence that proteolytic processing of rainbow trout egg vitelline envelop proteins takes place on the egg. *J.Biol.Chem.* 280, 37585-37598 (2005).
c) Jovine, L., Qi, H., Williams, Z., Litscher ,E. & Wassarman, P.M. *Nat.cell boil.* 4, 457-461 (2002).

**42.** Woycechowsky, K.J & Raines, R.T. Native disulfide bond formation in proteins. *Curr.Opinion.Chem.Biol.*4, 533-539 (2000).

**43.** Chivers, P.T., Prehoda, K.E., & Raines, R.T. The CXXC motif: A rheostat in the active site. *Biochem*. 36, 4061-4066 (1997).

**44.** Hennecke, J., Sillen,A., Huber-Wunderlich, M. Engelborghs, Y. & Glockshuber, R. Quenching of tryptophan fluorescence by the active-site disulfide bridge in the DsbA protein from E. coli. *Biochem.* 36. 6391-6400 (1997).

**45.** Iwamoto, H., Hiidaka Y., and Fukazawa Y. Conformational Control of Molecular tweezers containing a disulfide bond by redox reactions. *Tet. Lett*, 49, 277-280 (2007).

**46.** Lu, M. *et al*. Aromatic-participant interactions are essential for disulfide-bond ` trimerization in human heat shock transcription factor 1. *Biochem*. 48, 3795-3797 (2009).

**47.** Shrive,A.K. *et al*. three dimensional structure of human C-reactive protein. *Nat.Struct.Biol*. 3, 346-354 (1996).

**48.** Thompson, J.R., & Banaszak, L.J. Lipid –protein interaction in lipovitellin. *Biochem*. 41, 9398-9409 (2002).

**49.** Darrie,C.C et al. Structral Characterization of fish egg Vitelline envelope proteins by mass spectrometry. *Biochem*. 43, 7459-7478 (2004).

**50.** Li,A., Sadasivam,M. & Ding,J.L. receptor-ligand interaction between vitellogenin receptor (VtgR) and vitellogenin (Vtg), implications on loe density lipoprotein receptor and apolipoprotein B/E. *J.Biol.Chem.* 278, 2799-2806 (2003).

**51.** Opresko,L.K & Willey,H.L. Receptor-mediated endocytosis in *Xenopus* oocyte. I. Characterization of the vitellogenin receptor system.*J Biol Chem*. 262, 4109-4155 (1987).

**52.** Tillett, W.S. & Francis, T. Serological reactions in pneumonia with a non-protein somatic fraction of *pneumococcus*. *J. Exp. Med.* 52, 561−571 (1930).

**53.** Pepys, M.B. The acute phase response and C-reactive protein. In *Oxford Textbook of Medicine, 3rd Ed*. (D.J. Weatherall, J.G.G Ledingham & D.A. Warrell, eds.) 1527−1533 (Oxford University Press, Oxford; 1995).

**54.** Bujo, H., Hermann, M., Kaderli, M.O., Jacobsen, L., Sugawara, S., Nimpf, J.,Yamamoto, T., Schneider, W.J. Chicken oocyte growth is mediated by an eight ligand binding repeat member of the LDL receptor family. *EMBO J*. 13, 5165-5175, (1994).

**55.** Pepys, M.B. & Hirschfield, G.M. C-reactive protein: a critical update. *J.Clin. Invest.* 111, 1805-1812 (2003).

**56.** Danesh,J et al. C-reactive protein and other circulating markers of inflammation in the prediction of coronary heart disease. *New England J. Med*. 350, 1387-1397 (2004).

**57.** Ridker, P.M., Rifai, N., Pfeffer, M.A., Sacks, F. & Braunwald, E. Long-term effects of pravastatin on plasma concentration of C-reactive protein. *Circulation.* 100:230-235 (1999).

**58.** Pepys, M.B., Rowe, I.F. & Baltz, ML. C-reactive protein: binding to lipids and lipoproteins. *Int. Rev. Exp. Pathol.* 27, 83-111 (1985).

**59.** de Beer, F.C., et al. Low density and very low density lipoproteins are selectively bound by aggregated C-reactive protein. *J. Exp. Med.*. 156:230-242 (1982).

**60.** Chang, M.K., Binder, C.J., Torzewski, M. & Witztum, JL. C-reactive protein binds to both oxidized LDL and apoptotic cells through recognition of a common ligand: phosphorylcholine of oxidized phospholipids. *Proc. Natl. Acad. Sci. U. S. A.* 99:13043-13048 (2002).

# APPENDICES

## Appendix A

### Reaction of a mixture of reduced and oxidized glutathione (GSH/GSSG) with DSSA

In order to simulate cellular conditions, where both oxidized and reduced glutathione are present[44], samples of mixtures of these two interconvertible thiols were made. In trying to mimic cellular environments, where there are both reduced (GSH) and oxidized (GSSG) forms of glutathione present, mixtures of GSH/GSSG, in varying ratios were reacted with DSSA. Samples were made in such a way that [GSH] + [GSSG] = 16mM. The results in **Fig 34. a** show a rapid decrease in fluorescein emission (520 nm) upon addition of 16 mM GSSG. This surprising result might be attributed to a rapid disulfide exchange which results in the formation of a mixed disulfide.

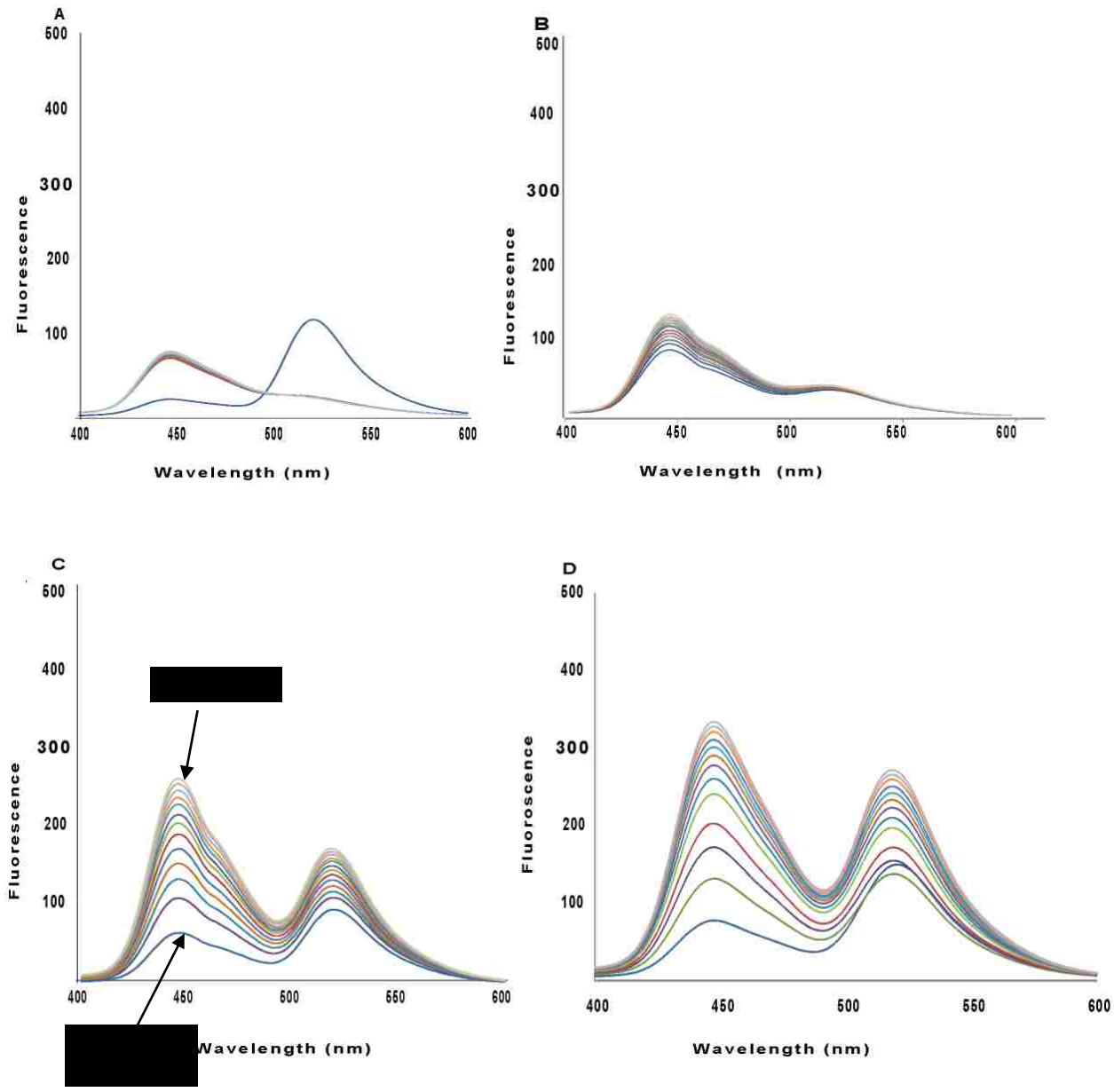


**Fig 34:** Fluorescence spectral changes for 5 µM DSSA, upon exposure to different concentrations of reduced glutathione (GSH)/GSSG at pH 7 (100 mM HEPES buffer). Spectra were acquired every 5 min and were overlaid: **a**) 2 mM GSH, **b**) 8 mM GSH, **c**) 12mM GSH and **d**) 16 mM GSH. Wavelength is in nm. Excitation was at 325 nm. Note: It is also possible that a decrease in pH, leading to fluorescien cyclization, could cause this effect

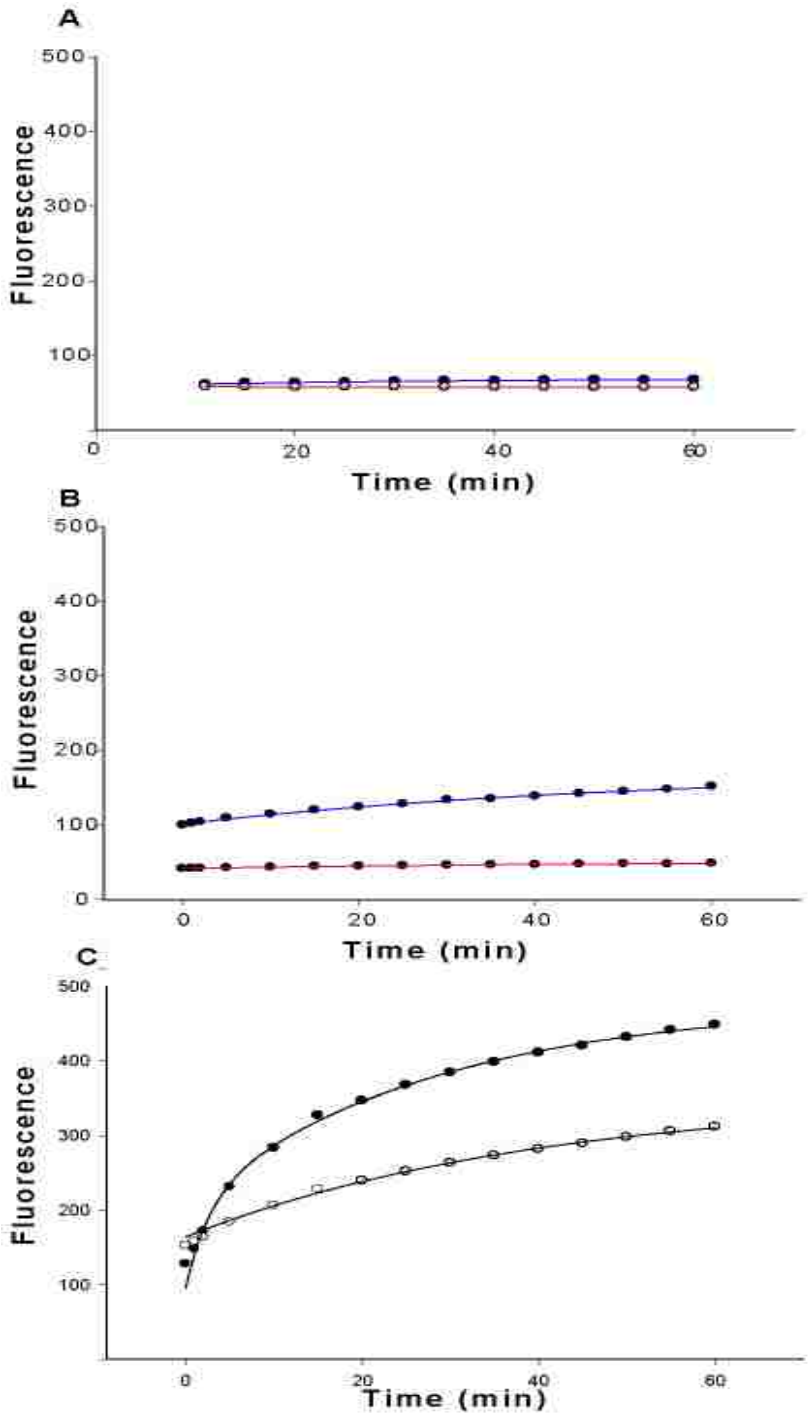
A
Fluorescence
500
400
300
200
100
0
20
40
60
Time (min)
B
Fluorescence
500
400
300
200
100
0
0
20
40
60
Time (min)
C
Fluorescence
500
400
300
200
100
0
20
40
60
Time (min)

[redacted]

GS-SA, and hence rapid loss of FRET It is also possible that a decerease in ph could cause a loss of the fluorescein fluorescence. Rapid increase in coumarin emission (450 nm) would be due to cleavage of the disulfide bond, and loss of quenching by fluorescein. **Figs. 34 a-d** shows the gradual increase in donor and acceptor emissions with increasing concentration of GSH and (decreasing [GSSG]). The increase in emission of the acceptor with increasing [GSH] is not fully understood, but could be attributed to the presence of the fluorescein absorption band around 320 nm, as suggested in chapter 2. It could also be due to some complex products which could be formed in the reaction, or the sum of all these effects. To further analyse these observations, the kinetic data were fitted to a first order exponential (**Fig. 35**).

**Fig 35. a-c** show changes in peak intensities of both the donor and acceptor. From the kinetic fitting results of **Fig. 35**, shown in **Fig. 36**, it can be seen that there is an increase in both rate constant and fluorescence intensity for the coumarin peak as [GSH] increases (as expected). For the fluorescein peak, fluorescence increases gradually with increasing in [GSH] and decreasing [GSSG], however the there is a general decrease in rate contant (**Fig' 36**).

By plotting ratios of donor/acceptor fluorescence as described in Fig 10, it can clearly be seen that generally there was no absolute change in peak intensities, as can be observed in **Fig. 37**. This can be attributed to disulfide exchange with the GSSG that was also present. O course, in a cell it is typically true that [GSH] is much greater than [GSSG].

| | $F_0$ | | a | | k | |
|---|---|---|---|---|---|---|
| | **Coum** | **FITC** | **Coum** | **FITC** | **Coum** | **FITC** |
| **0 mM GSH** | 58.43 | 98.29 | 10.82 | -40.19 | 0.00368 | 0.353 |
| **2 mM GSH** | 101.45 | 41.79 | 70.89 | 8.82 | 0.0195 | 0.0244 |
| **16 mM GSH** | 95.62 | 164.33 | 323.47 | 187.86 | 0.0701 | 0.0251 |

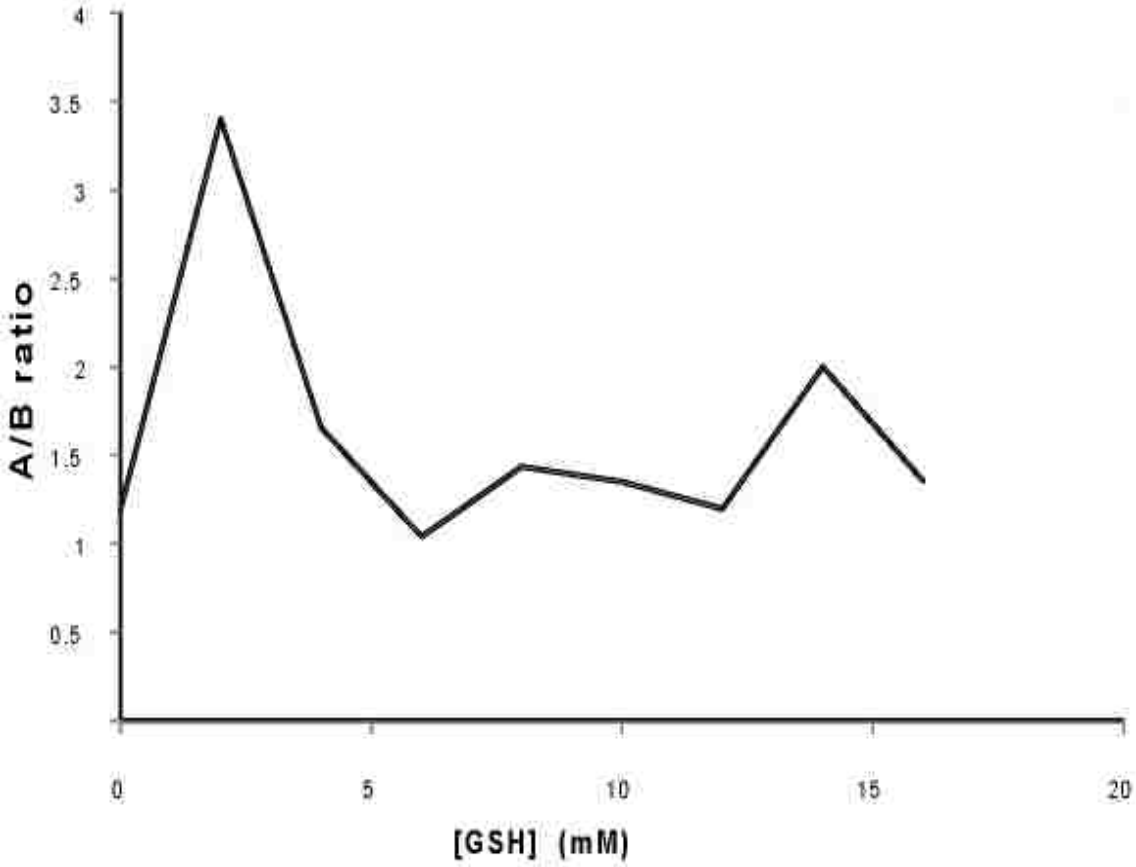
A/B ratio
4
3.5
3
2.5
2
1.5
1
0.5
0
5
10
15
20
[GSH] (mM)

# Appendix B

## Synthesis of rhodamine-cystamine- fluorescein 5-isothiocyanate (RH-Cys-FITC)

The DSSA probe with an aliphatic cystamine (Fig 1) was prepared in two steps following our lab established procedure[38]. The first step involved synthesis of rhodamine-cystamine (Rh-Cys), followed by reaction with fluorescein 5-isothiocyanate (FITC).

Rh-Cys was prepared by dissolving 1 equivalent of rhodamine B (RhB) in a 4:1 acetonitrile/chloroform mixture. 2 equivalents of Cystamine dihydrochloride was slowly added. Cystamine dihydrochloride was then added in excess to make sure the reaction goes to completion and to minimize dimerization of RhB. Excess trimethylamine (6-10 equivalents) was added, and the reaction was initiated by addition of 1 equivalent of BOP (benzotriazol-1 (yloxy)tris(dimethylamino) phosphonium hexaxafluorophosphate) and the mixture was stirred for 15 hrs at room temperature. The precipitate that formed was then filtered off and washed with chloroform. TLC (Hex:EtoAc 5:5) was used to check for the product in both the supernatant and the precipitate. The concentrated filtrate was then suspended in in 200 ml of 1N HCl and extracted with chloroform. The organic layer was washed with 1N NaOH and deionised water, and then dried over sodium sulfate and concentrated using the rotory evaporator vap and dried. Rh-cys was was dissolved in a 1:1:1 mixture of acetone/MeOH/$CH_2Cl_2$, and was then reacted with FITC in the presence of triethylamine. No Rh-CysFITC was formed. After NMR and MALDI analysis, it was discovered that the product was actually Rh-Cys-Rh and not Rh-Cys. Rh-Cys synthesis was attempted again and this time, instead of running the reaction for 16 hrs, it was

closely monitored from the moment the BOP reagent was added. Regular TLC checks were done and the product was detected in the first 2 hrs. Rh-Cys was then reacted with FITC as described above and 13% yield of the product was obtained.after silica column purification as described by Pullela et al[1]. This compund was well characterized with NMR and MALDI.

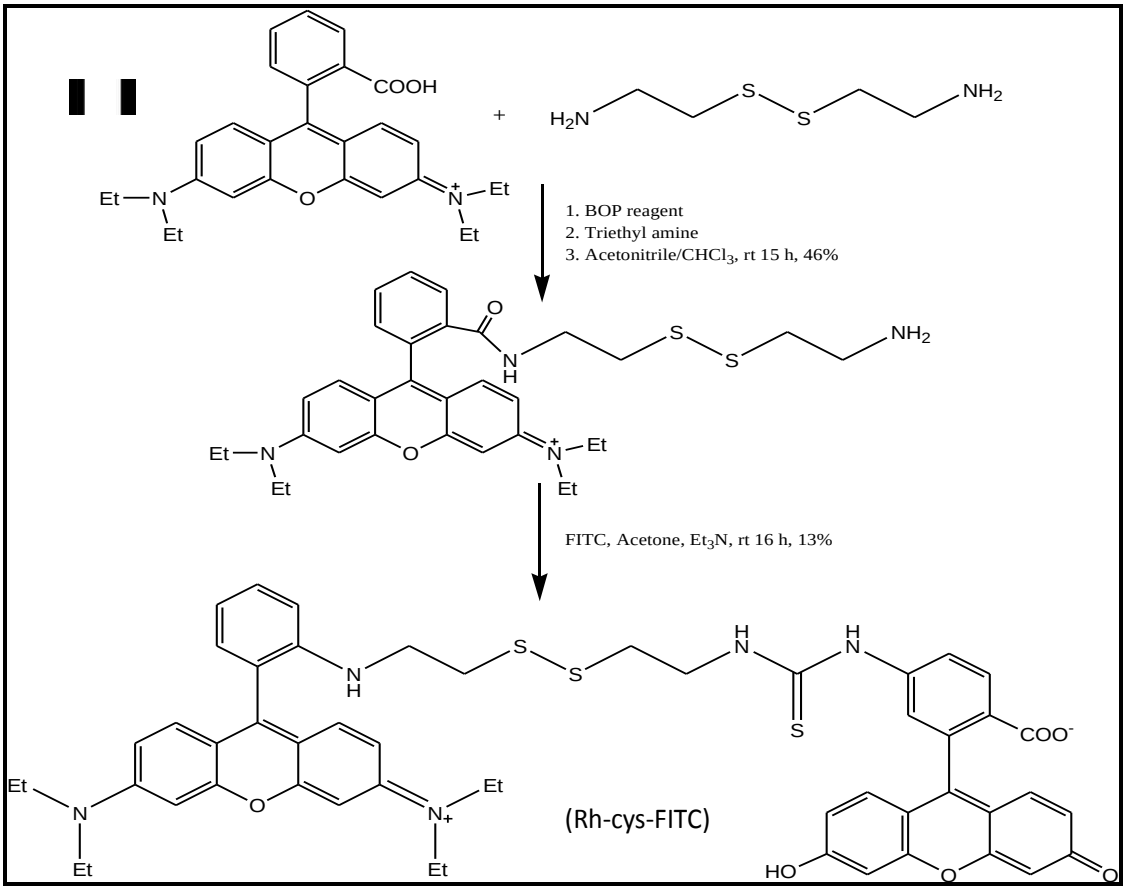

# Appendix C

## Fluorescence Quenching Studies on the Pmr-Cys-Fitc Probe

### a) General introduction

**Quenching efficiency**

An excited fluorescein (A*) can emit a photon and revert back to the ground state. The fluorescence decay process is first order:


The A* molecule can also lose its energy in the form of heat rather than light (non-radiative)

Assuming no photochemical reactions or phosphorescence, the quantum yield ,$\varphi^0$ is the rate at which excited fluorescence decays via fluorescence divided by the rate at which it decays via both fluorescence and non-radiative decay.

$$\phi = \frac{k_f[A*]}{k_f[A*]+k_{nr}[A*]} = \frac{k_f}{k_f + k_{nr}}$$

The fluorescent reagent we are studying is comprised of para-methyl-red tethered to fluorescein via a disulfide bond. To better understand how para-methy-red interacts with fluorescein, via intramolecular interactions in this molecule, we are first studying intermolecular interactions between para-methyl-red tethered to fluorescein. If para

methyl red is present in solution with fluorescein (A*), quenching of fluorescein can occur :

$$A^* + \text{p-methyl red} \longrightarrow \text{quenching of } A^*$$

Assuming a second-order rate constant, $k_q$, the net effect of the presence of p-MR (para methyl red) is reduction in the quantum yield of fluorescein:

$$\phi = \frac{k_f\,[A*]}{k_f\,[A*] + k_{nr}[A*] + k_q[A*][p-MR]} = \frac{k_f}{k_f + k_{nr} + k_q[p-MR]}$$

Dividing $\phi^0$ by $\phi$, relative radiative quantum yield can be obtained, giving rise to the Stern- Volmer expression:

$$\frac{\phi 0}{\phi} = 1 + \frac{k_q}{k_f + k_{nr}}[p - MR]$$

Replacing $\frac{\phi 0}{\phi}$ with fluorescence intensity ratios ($I^0/I$), which can be easily measured for fluorescein in the absence or presence of p-MR, a plot of $I^0/I$ against [p-MR] should yield a straight line with slope $k_q/ (k_f + k_{nr})$.

By first determining $(k_f + k_q)$, independantly, $k_q$ can be determined. In the absence of p-MR, rate of disappearance of excited fluorescein is given by :

$$\frac{d[A*]}{dt} = -(k_f + k_{nr})$$

By integration, the following linear relationship can be obtained:

$$\ln [A_t^*] = \ln[A_0^*] - (k_f + k_{nr})t$$

Since [A*] is proportional to fluorescence intensity, the latter can replace [A*] in the above equation. A plot of intensity against lifetime data can be used to obtain ($k_f + k_{nr}$), and therefore quenching efficiency of p-MR on fluorescein.

### i. Types of quenching

**Collissional (dynamic) and Static quenching**

Collisional quenching results from diffusive encounters between the fluorophore and quencher during the lifetime of the excited state and is described by the following S-V equation,

$$\frac{F_0}{F} = 1 + k_q \tau_0 [Q] = 1 + K_D\,[Q],$$

where $k_q$ is the bimolecular quenching constant , $\tau_0$ is the lifetime of the fluorophore in the absence of a quencher and Q is the quencher concentration. A linear S-V does not indicate dynamic quenching, as static quenching also shows this characteristic.

Static quenching result from formation of a non-fluorescent complex between fluorophore and the quencher. Quenching depends on the concentration of the quencher as illustrated by the S-V equation below:

$$\frac{F_0}{F} = 1 + K_S[Q]$$

Dynamic and static quenching can be distinguished mostly by their differing dependency on temperature and lifetimes. For example higher temperatures increase molecular collisions, hence increasing dynamic quenching, while at the same time increasing chances of dissociation, hence lowering quenching due to complex formation.

Collision quenching is an additional rate process that depopulates the excited state without emission and hence is accompanied by decrease in lifetimes and hence fluorescent yields:

$$\frac{F_0}{F} = \frac{\tau_0}{\tau}$$

While static quenching does not decrease as only fluorescent molecules are observed and the unquenched complex has $\tau_0$.

$$\frac{\tau_0}{\tau} = 1$$

As collisional quenching only affects the excited state of the fluorophore, it does not affect the absorption spectra of the fluorophore. But, ground state complex formation will result in perturbation of the aborption spectrum of the fluorophore.

Deviations from S-V linearity may be due to, among other things, combined effects of dynamic and static quenching, quenching sphere of action and effects of steric shielding and charge.

## b) EXPERIMENTS AND RESULTS

### i) To determine which is more fluorescent, fluoresceinamine or fluorescein

5µM of fluoresceinamine and fluorescein sodium salt in 100 mM, pH 7 hepes buffer were prepared. The dyes were excited at 490nm and emission was observed between 500 and 650 nm. Fluorescence was too high, so the dyes were diluted by transferring 300 µL of the 5000 µM stock solutions to 1200 µL of the buffer. The PMT (gain) was manually set to 225 V. As shown in fig 39 below, on the same scale, fluoresceinamine was found to be almost non-fluorescent relative to fluorescein. Non-fluorescence of fluoresceinamine could be due to its existence in the cyclized Form. In all further experiments fluorescein and not fluoresceinamine is going to be used.

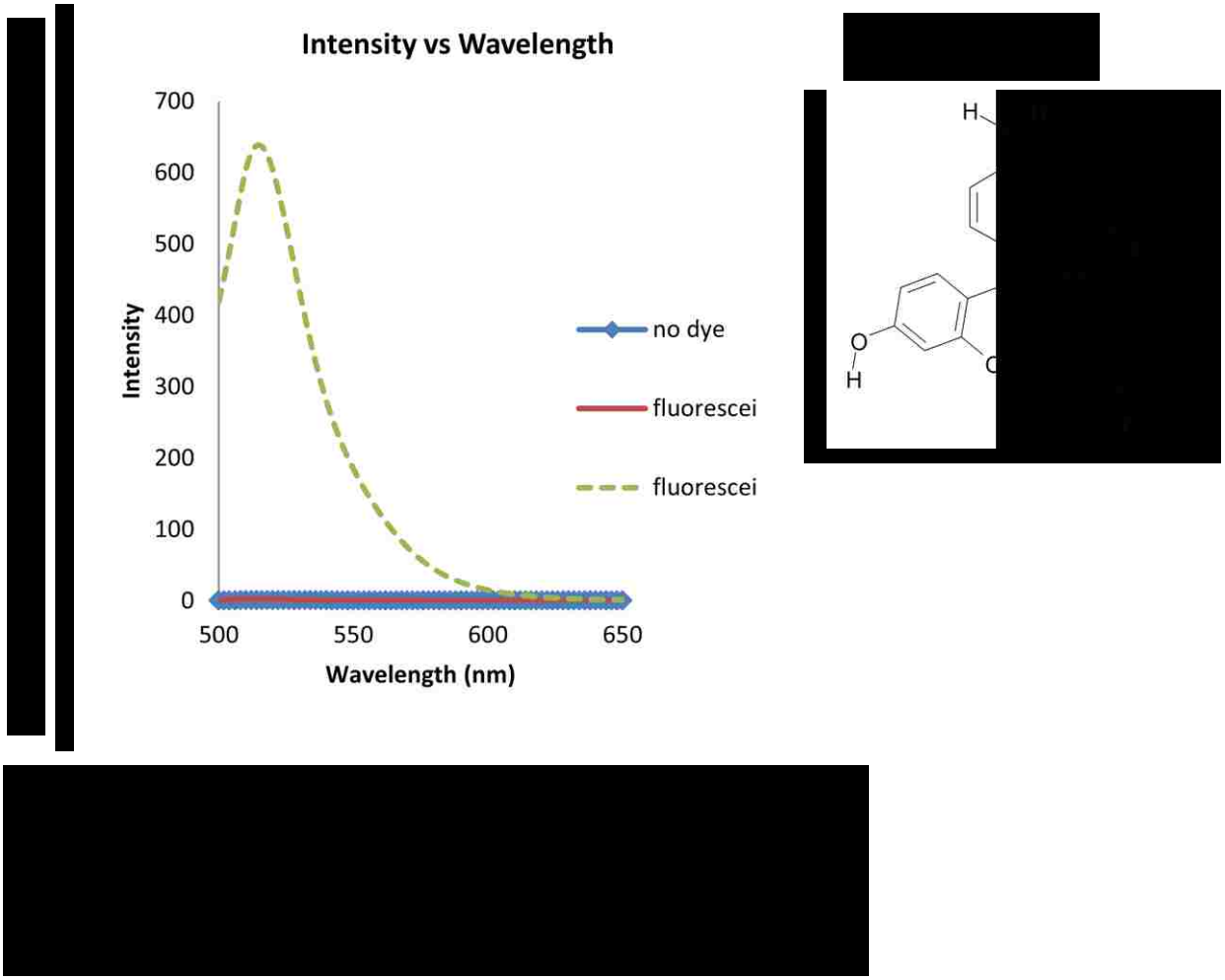

### ii) Molecular quenching of fluorescein by p-Methyl red (PMR)

Varied concentrations of PMR (1-245 µM) were added to a constant concentration of fluorescein (5 µM) and fluorescent changes were monitored. The data obtained were used to genereate the S-V plot.

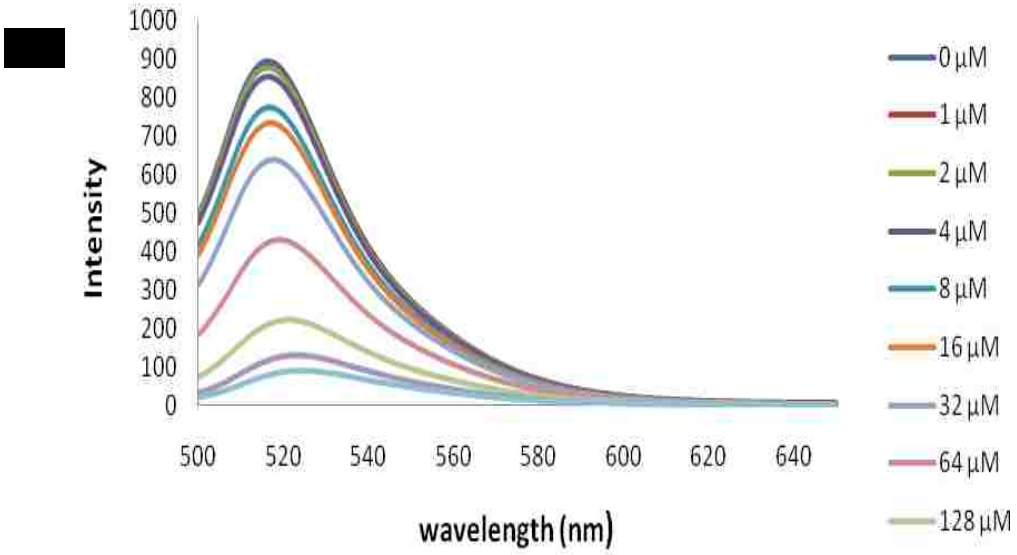


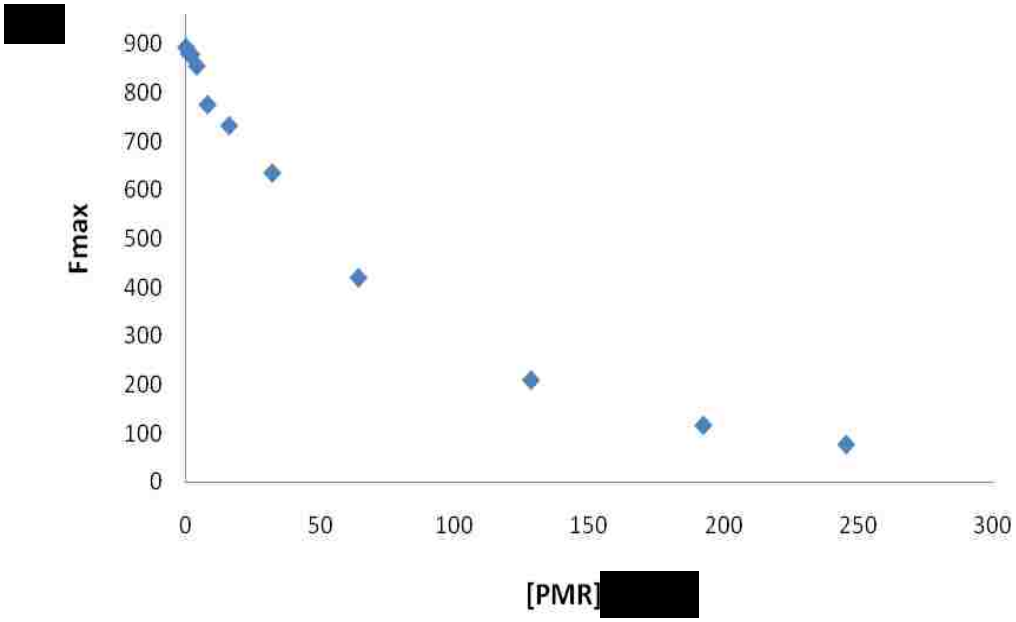

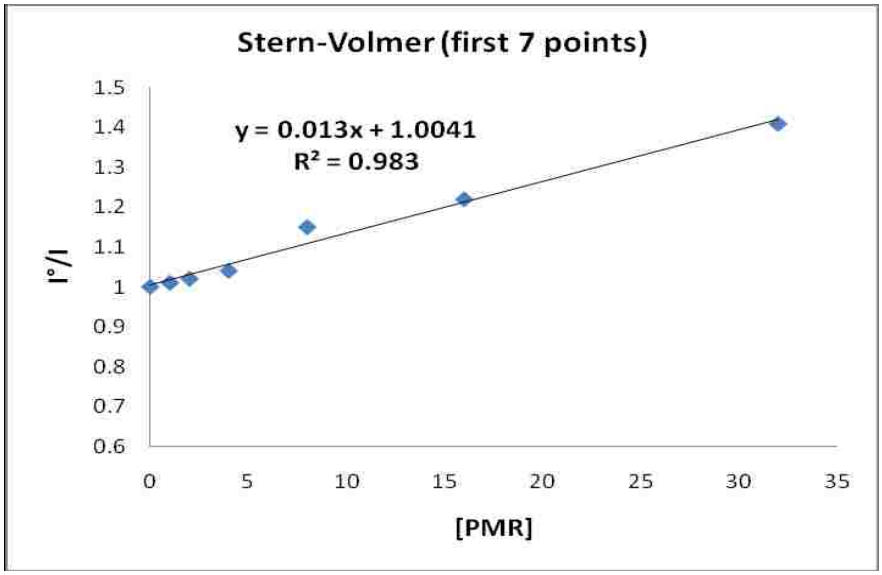


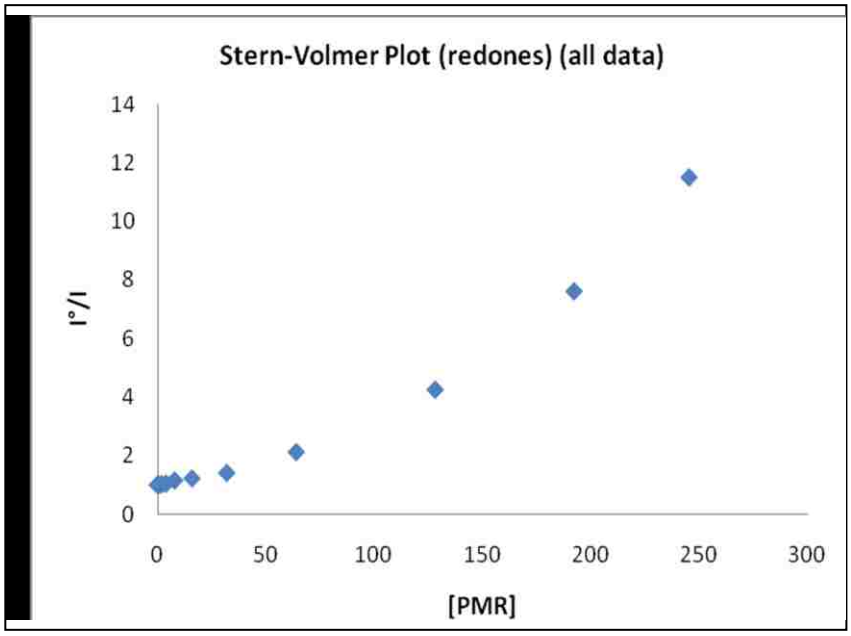


**Fig. 41**: Stern-Volmer plots, **a**) showing all points, **b**) first 7 points. All conditions are as mentioned in **Fig.** 2.

**Fig. 41a** show that at low [PMR], there is a linear relationship between fluorescence intensity ratios and [PMR], suggesting that dynamic quenching is predominant. Deviation from from Stern-Volmer behavior is however observed at higher [PMR], suggesting that not a single type of quenching is involved.

One way of distinguishing static quenching from dynamic quenching is to do absorbance studies as explained in the introduction. Dynamic quenching does not affect the absorbance of the fluorophore, while formation of a ground state complex in static quenching can perturb the absorbance. Absorbance studies were done at [PMR] between 0 µM and 8 µM and the results are as shown in figs 42 and 45 below.

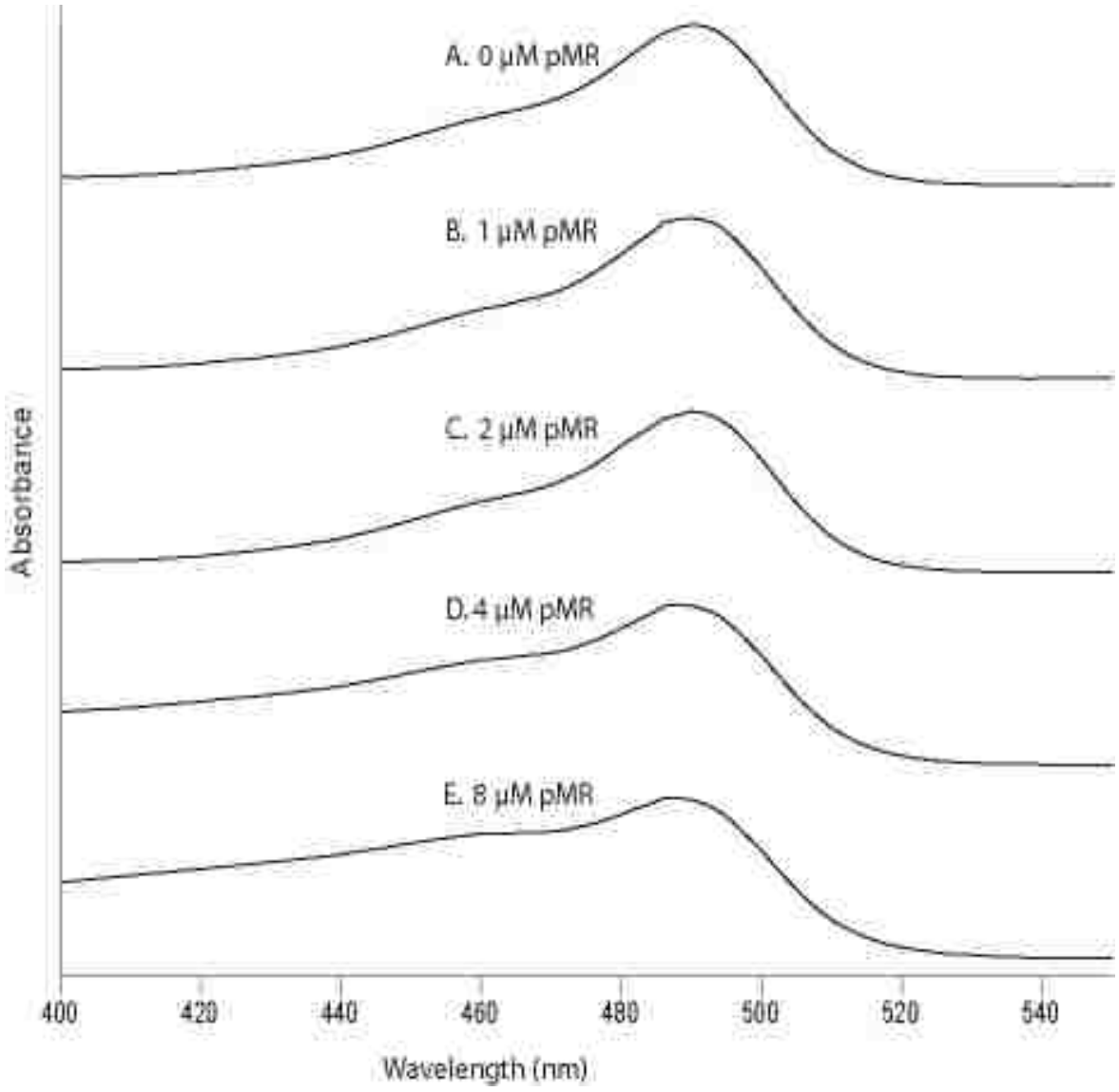


**Fig. 42:** Stacked absorbance peaks for fluorescein showing changes due to quenching at different [PMR]. The reaction was done in 100 mM Hepes buffer, at room temperature. The buffer was used as a blank.

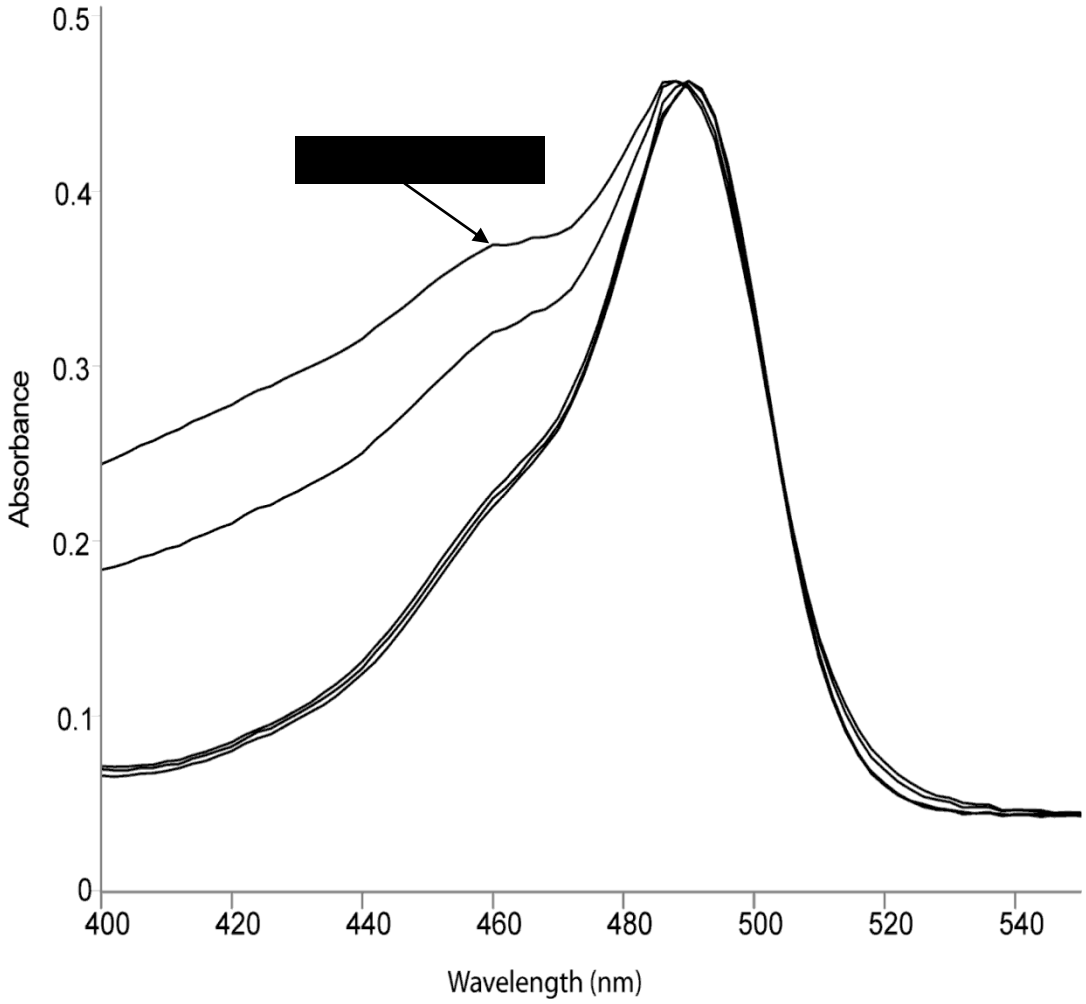


The results indicate no significant changes in absorbance at low [PMR] indicating that dynamic quenching is predominant. However at high [PMR] a new peak at around 450

nm begins to appear. The experiment was repeated several times at more regulated temperature and the results are shown below.

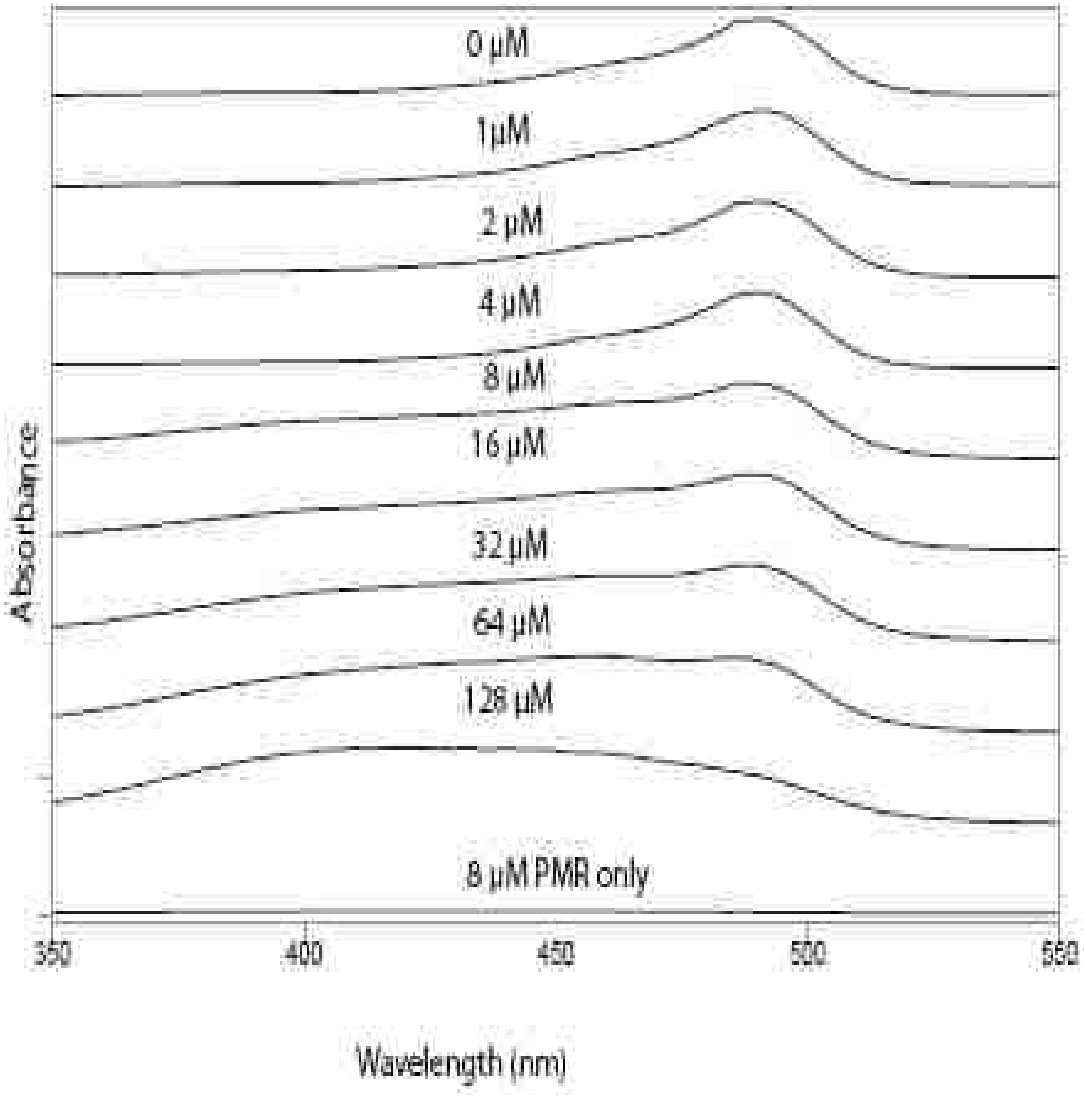


**Fig. 44:** Stacked absorbance peaks for fluorescein showing changes due to quenching at different [PMR]. The reaction was done in 100 mM Hepes buffer, pH 7, at 25 $^{0}$ C. Temperature was controlled by carrying out the reaction in a Precission 180 series water bath. The cuvettes were pre-incubated in the water bath for 5 mins. The spectrophotometer was blanked with the corresponding [PMR] inHEPES buffer each time a reading was taken.

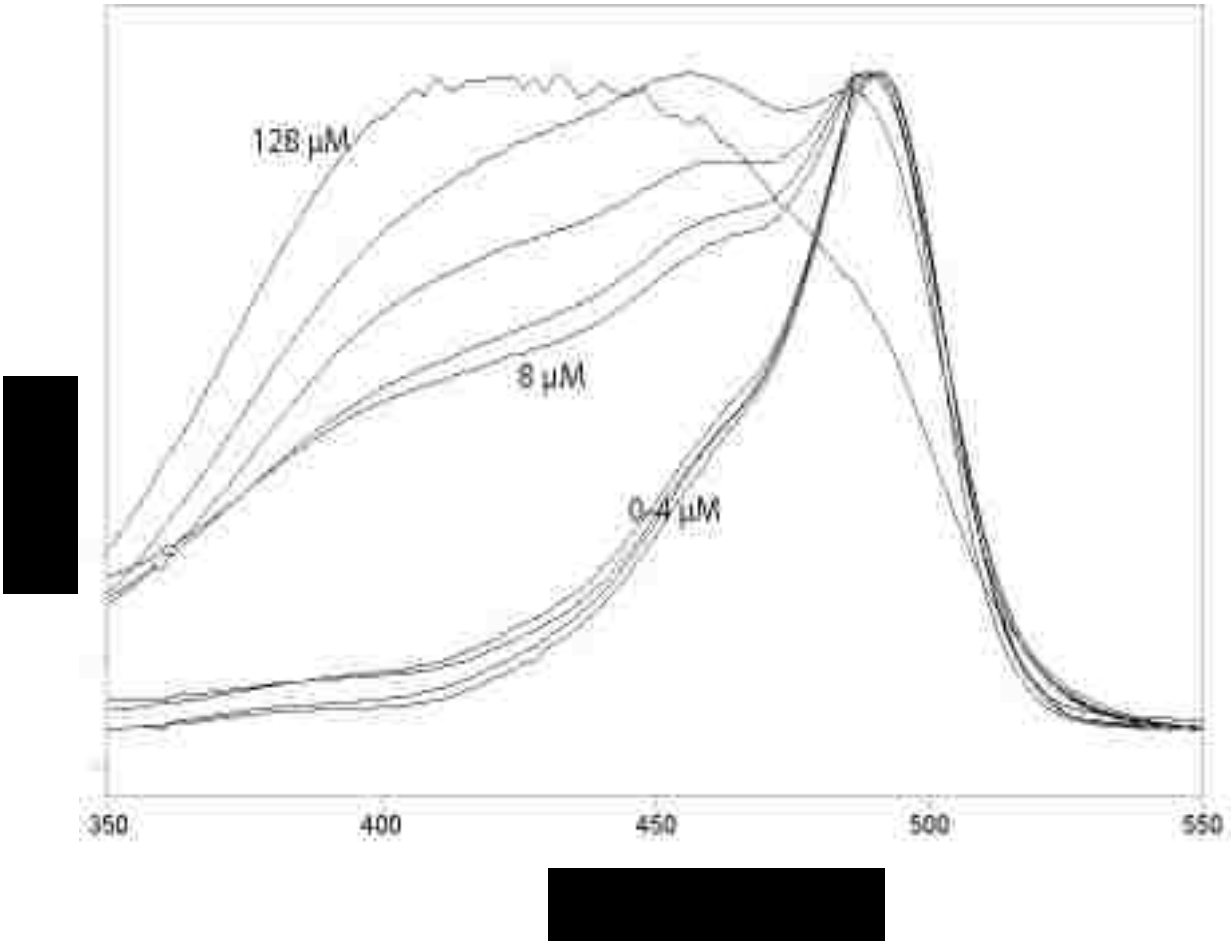


**Fig.45:** Overlays of fluorescein absorbance spectra showing changes due to addition of different [PMR]. The reaction was performed in 100 mM Hepes buffer, pH 7. Temperature was controlled by carrying out the reaction in a Precission 180 series water bath. The cuvettes were pre-incubated in the water bath for about 5 mins. The spectrophotometer was blanked with the corresponding [PMR] in hepes buffer each time a reading was taken. The peak intensities are normalized to the most intense absorbance peak.

Absolute maximum peak intensities at 490 nm were then plotted against increasing [PMR] to observe if there is any significant change (**Fig. 46**). Significant peak changes

indicate perturbation of the excited state and therefore formation of a complex. Complex formation results in static quenching.

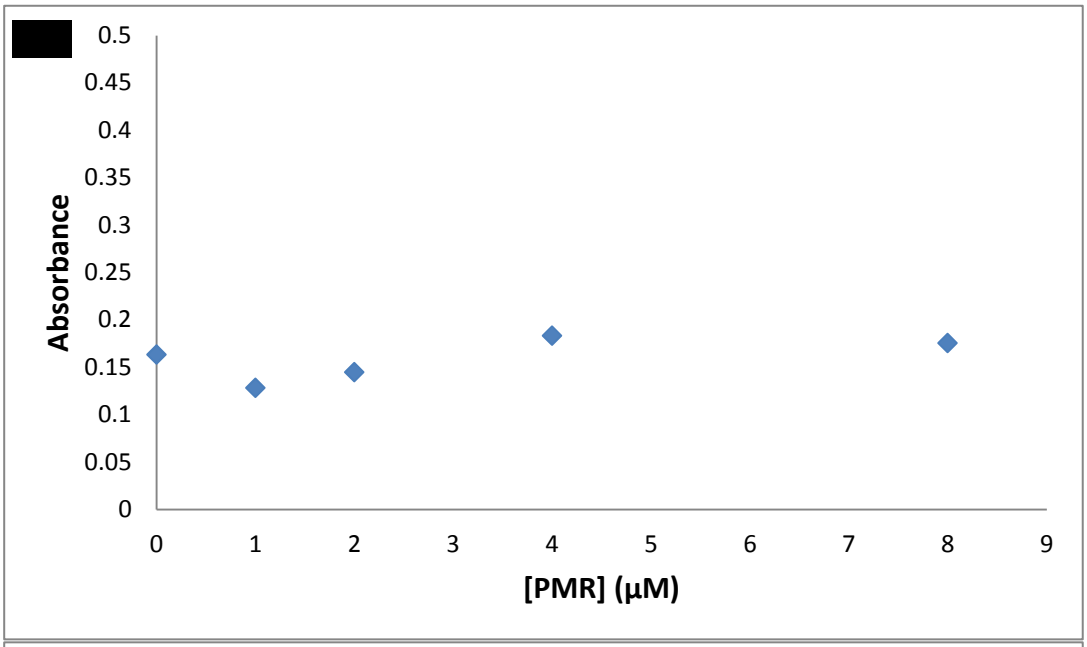


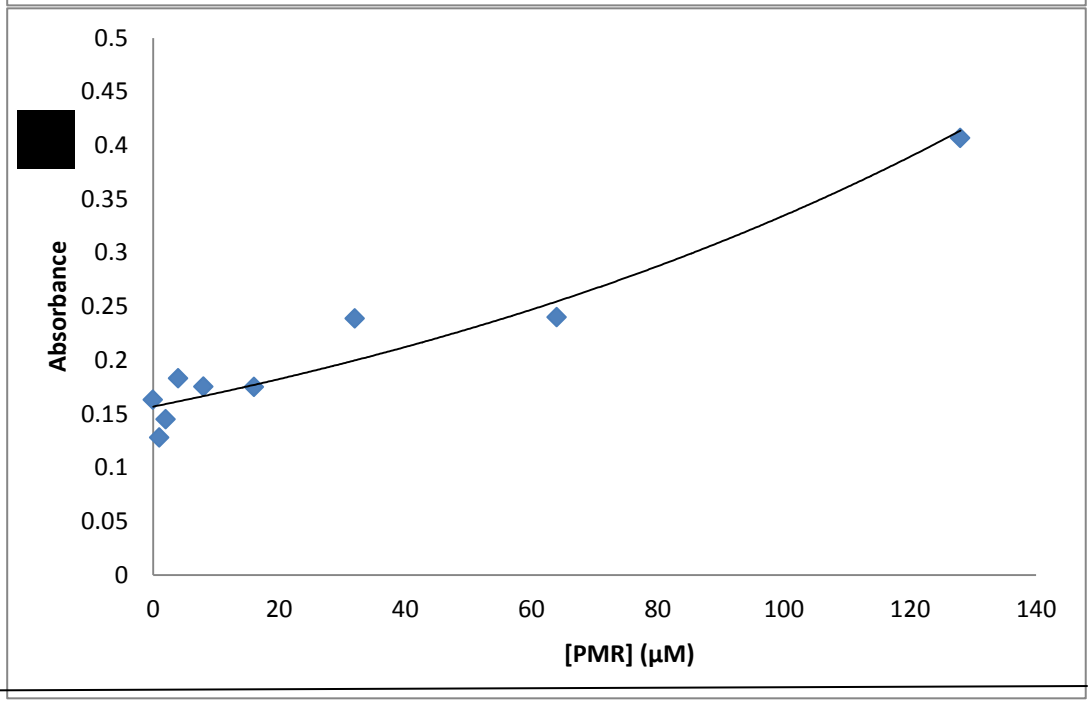

Evidence from figs 3 to 8 shows that at high [PMR], quenching is not only due to collissional factors, but may also be due to formation of a PMR/fluorescein complex. The upwards curvature in the S-V plot in fig 3a above may be due to combined dynamic and static quenching[1] **.** The following equation can be used to account for these deviations to the S-V plots;

$$\frac{F_0}{F} = (1 + K_D[Q])(1 + K_S[Q])$$

This equation is second order in Q and accounts for the upward curvature observed when both dynamic and static quenching occurs.

Modification of the above equation can be used to allow graphical separation of $K_S$ and $K_D$. This equation can be simplified to:

$$\frac{F_0}{F} = 1 + (K_D + K_S)[Q] + (1 + K_S)[Q]^2$$

And then re-written as:

$$\frac{F_0}{F} = 1 + K_{app}$$

Where the apparent quenching constant ($K_{app}$) is given by:

$$K_{app} = \left[\frac{F_0}{F} - 1\right]\frac{1}{[Q]} = (K_S + K_D) + (K_D K_S)[Q]$$

By calculating $K_{app}$ at each quencher concentration [PMR], a plot of $K_{app}$ versus [PMR] should yield a straight line with the intercept of $K_D + K_S$ and a gradient $K_D \times K_S$.

$K_{app}$ was calculated for [PMR] between 0 µM and 245 µM and the results are as shown in **Fig 47** below.

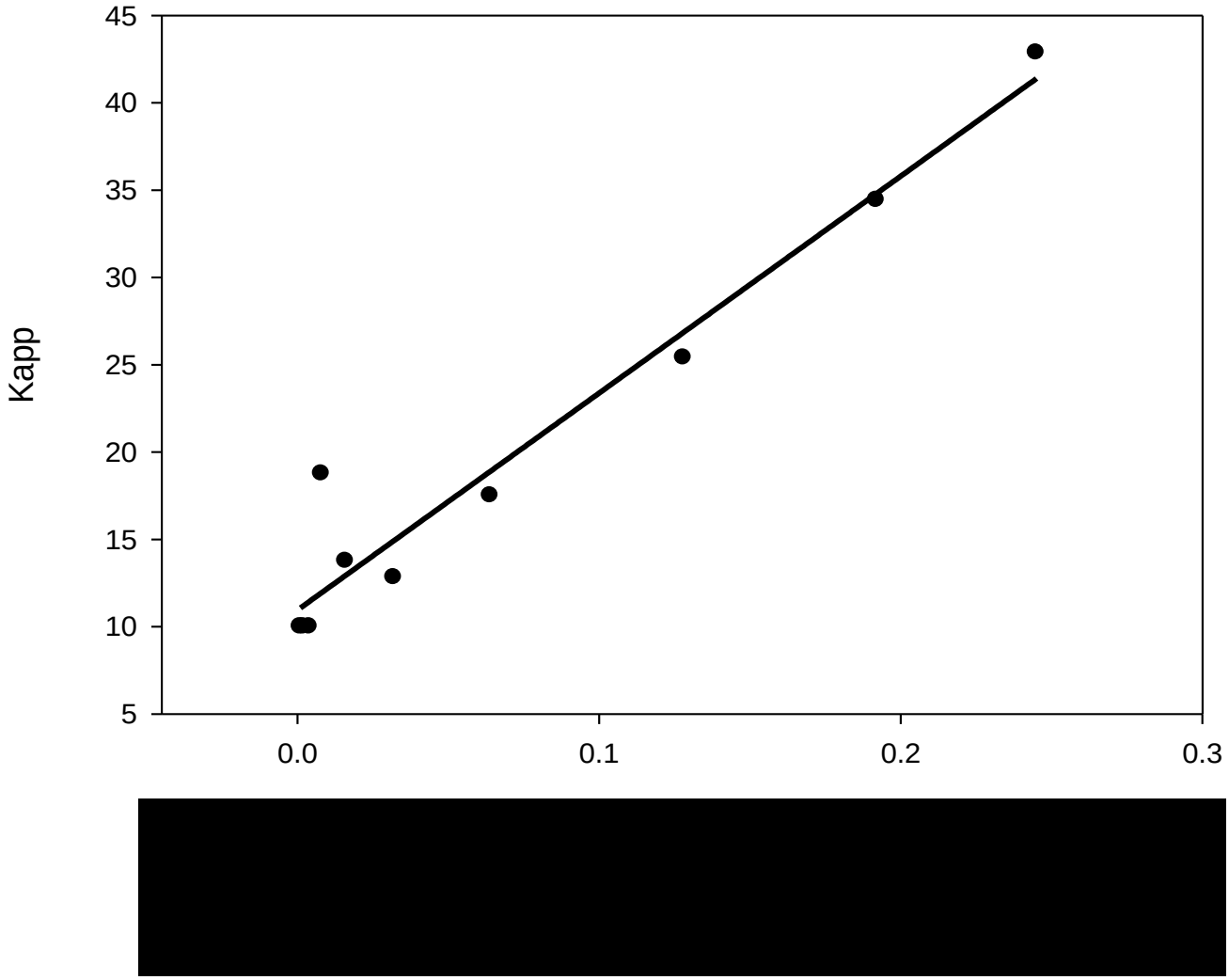

From both intercept and slope values, the following equations can be written:

$$K_D \times K_S = 11.0$$

$$K_D + K_S = 124$$

Solving these two equations gives:

$$K_S^2 - 11.0*K_S + 124 = 0.0$$

The quadratic equation resulting from these two equations gives no real solutions, meaning that at high quencher concentration, complex activities beyond simply static and dynamic quenching are at play.

## c) CONCLUSION

Intermolecular quenching of fluorescein by PMR at low [PMR] is mainly due to collissional effects. However at higher [PMR] quenching is not attributed to a particular single form of quenching, but rather to the combinations of both forms and possibly other factors. Failure to separate collissional from static quenching as evidenced by lack of real solutions to the quadratic equation above indicates that not only static and dynamic quenching are at play, but other factors as well, such as quenching sphere of influence, steric shielding and effects charge. Appearance of a new peak at 450 nm at high [PMR] may indicate a shift of equilibrium between the monoionic and diionic forms of fluorescein.

# Appendix C

## AM 1 calculations calculations on pmr-cys-fitc

Computational calculations were done on the Pmr-Cys-FITC as described in chapter 2. Below are the results obtained.

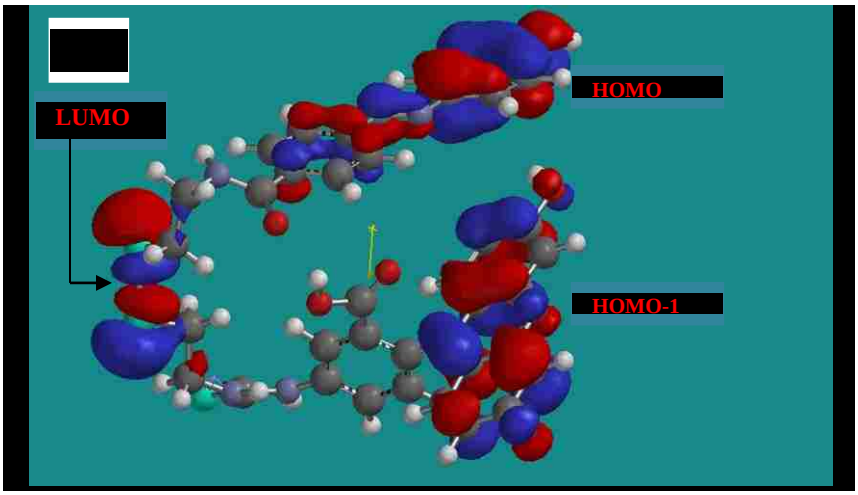


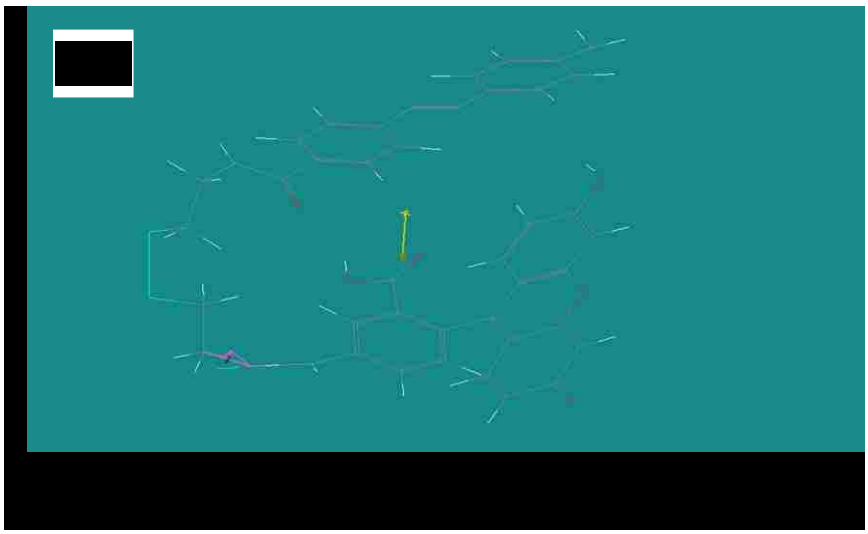

[redacted]

| | |
|---|---|
| Energy | 17.0212251 kcal/mol |
| Energy (HOMO) | -8.36877290 eV |
| Energy (LUMO) | -2.19641569 eV |
| Dipole | 6.135 debye |
| Total charge | neutral |
| Multiplicity | single |
| Pt. group | C1 |